

Mapping magnetic fields around super massive black holes

Eduardo Ros, J. Anton Zensus,
A.P. Lobanov, M. Janßen, T.P. Krichbaum, M.L. Lisakov, A.K. Baczko, M. Wielgus, et al.

Kraków, November 7, 2022

M₂FINDERS



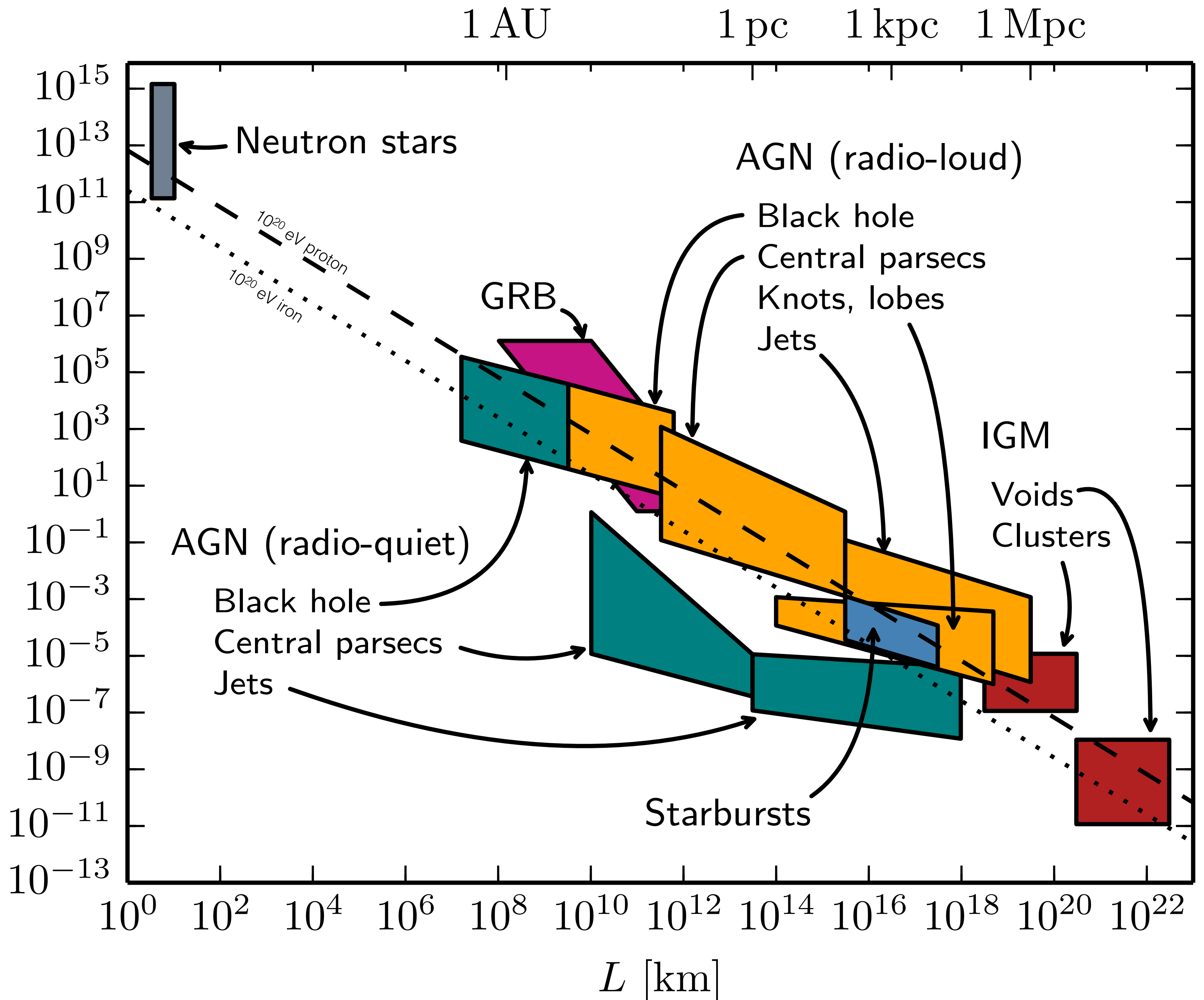
MAX-PLANCK-INSTITUT
FÜR RADIOASTRONOMIE



Magnetic field scales

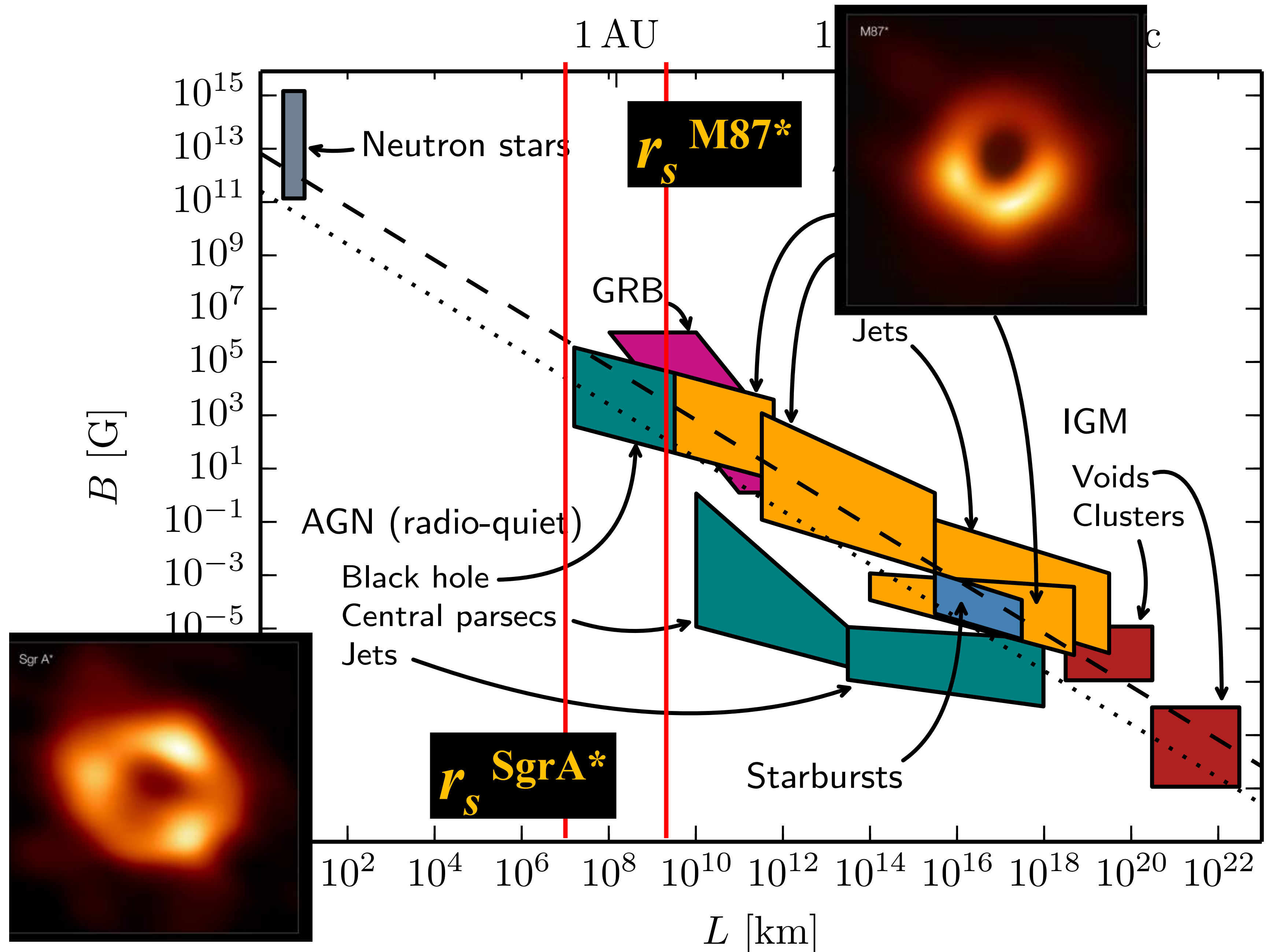
Physical extent vs magnetic field strength

Proposed by Hillas ARA&A 22 (1984)
Version by Ptitsyna & Troitski,
Physics-Uspekhi 53 691 (2010)

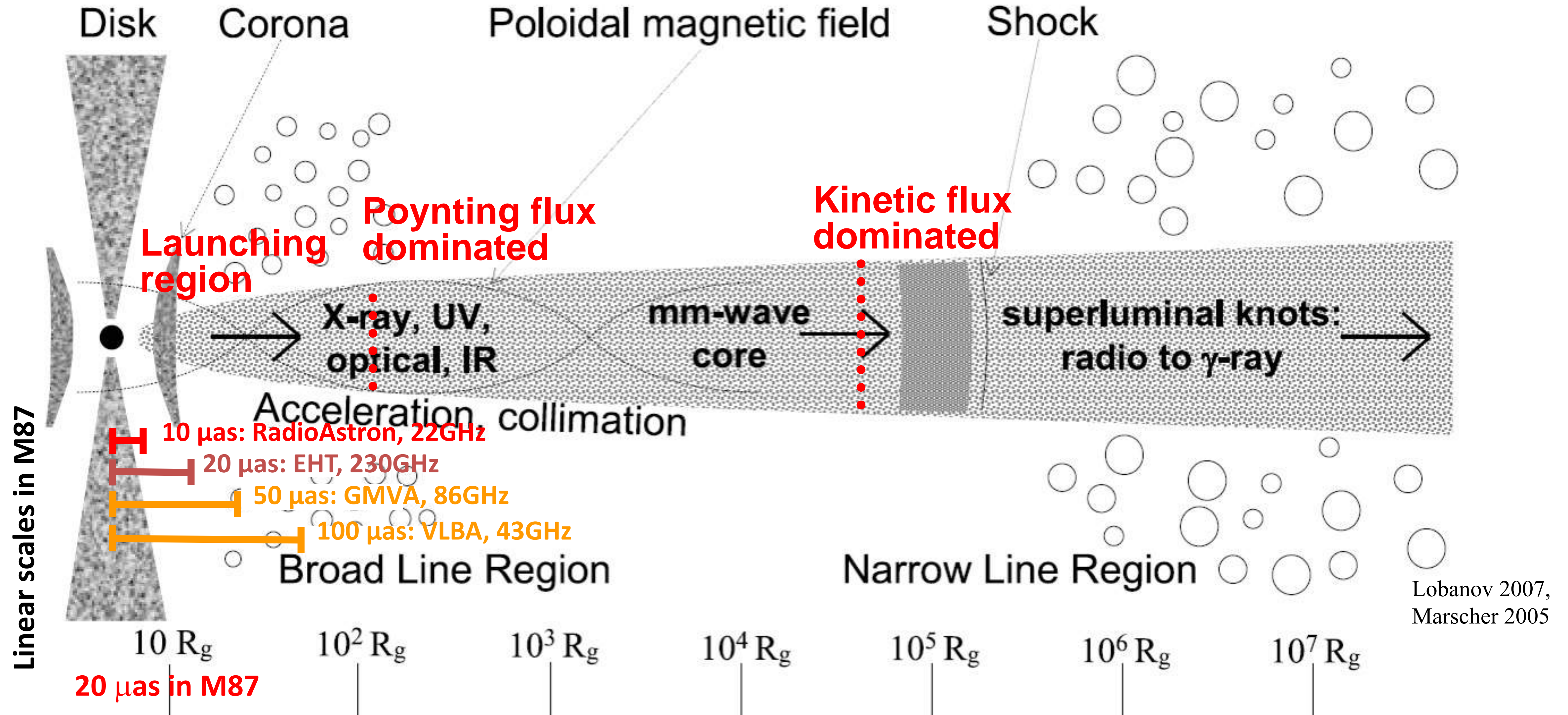


Magnetic field scales

$$r_s = 2GM/c^2 = 2.95 \text{ km} \left(\frac{M}{M_\odot} \right)$$



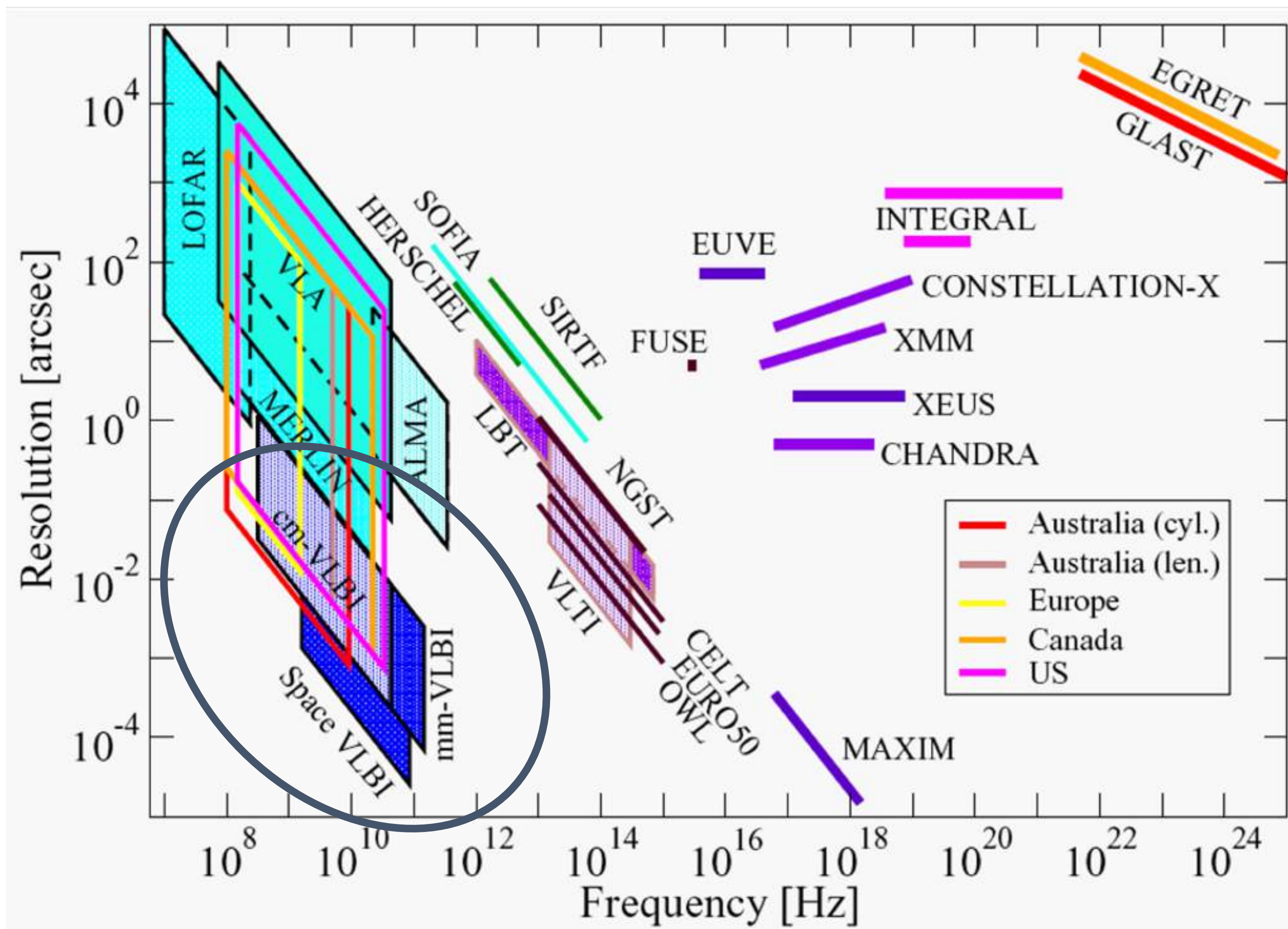
VLBI View on Central Regions in AGN



Lobanov 2007,
Marscher 2005

Brightness temperature: plasma/emission diagnostics, with inverse Compton (IC) and equipartition limits.
Jet structure and B-field: launching mechanism: disk (Blandford-Payne, BP) or BH (Blandford-Znajek, BZ).⁸

The quest for resolution



Gravitational radius:

- 1 nas in AGN
($M_{\text{bh}} = 10^8 M_{\text{sun}}$ at 1 Gpc)
- 0.1 nas in X-ray binaries
($M_{\text{bh}} = 10 M_{\text{sun}}$ at 1 kpc)

→ 5 μas in Sgr A*

→ 2 μas in Messier 87

Resolution limits at present

Millimetre VLBI

- Continental and global arrays
- D up to Earth size (10^7 m)
- Recent boost in sensitivity by phased ALMA, offered both for GMVA at 3.5 mm and EHT at 1.3/0.8 mm

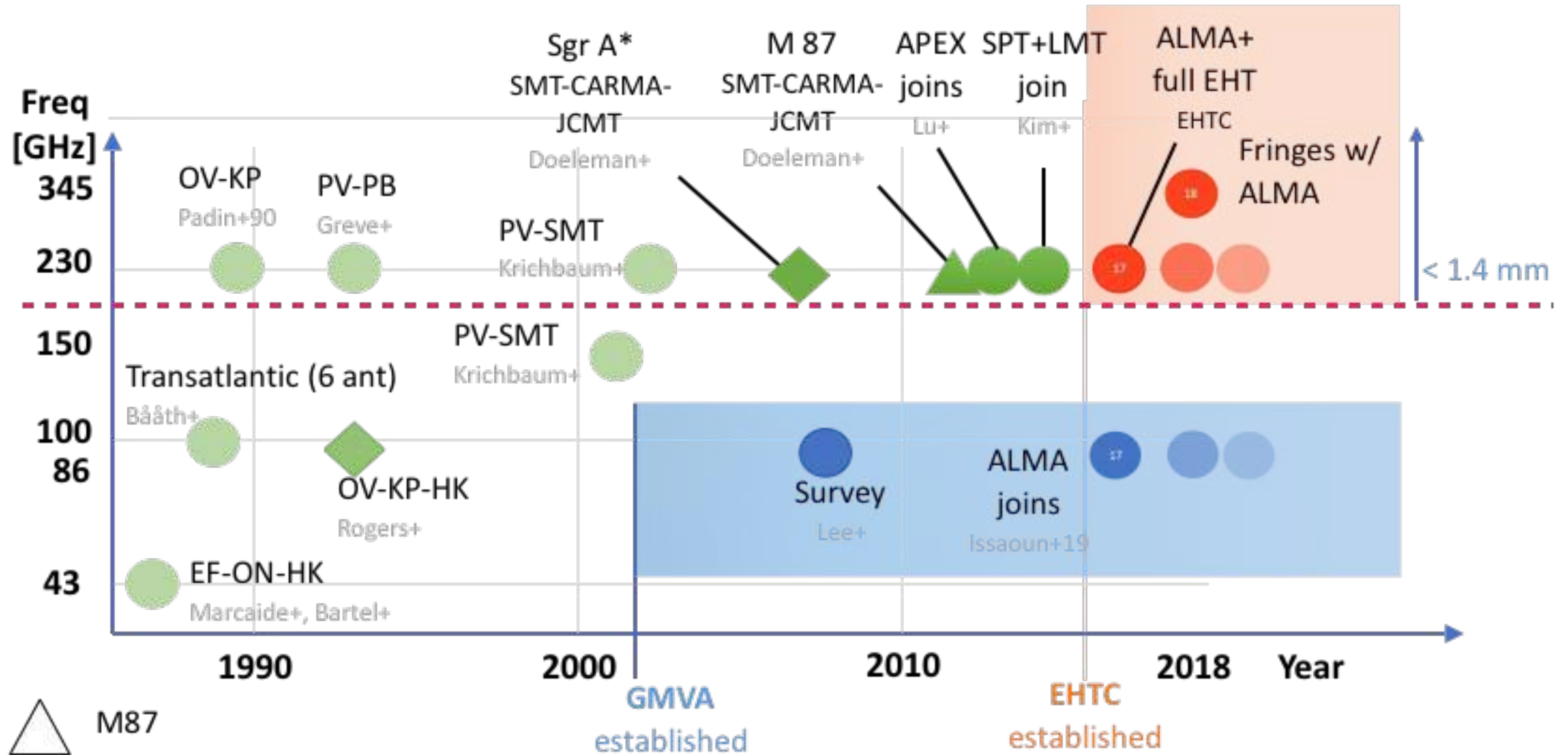
Space VLBI

- Ground array supporting space baselines
- D up to 3x or 10x Earth size (10^7 m)
- High resolution for Tb determination, not necessarily for imaging

| Array | ν [GHz] | D [km] | D [$M\lambda$] | θ [mas] |
|---------------|----------------------|----------|---------------------------|-----------------------------|
| VSOP | 1.65/4.8/22.1 | 33000 | 175/528/2432 | 1.17/0.39/0.085 |
| Ground global | 22 | 11600 | 893 | 0.231 |
| RadioAstron | 0.33/1.66/ 4.8/22 | 350000 | 7230/8500/ 24230/99600 | 0.540/0.106/ 0.037/0.009 |
| Ground global | 43 | 11600 | 1660 | 0.124 |
| GMVA | 86 | 11045 | 3680 | 0.056 |
| EHT | 230/345 | 11045 | 8500/12300 | 0.024/0.017 |

$$\theta = 1.22 \frac{c}{\nu D}$$

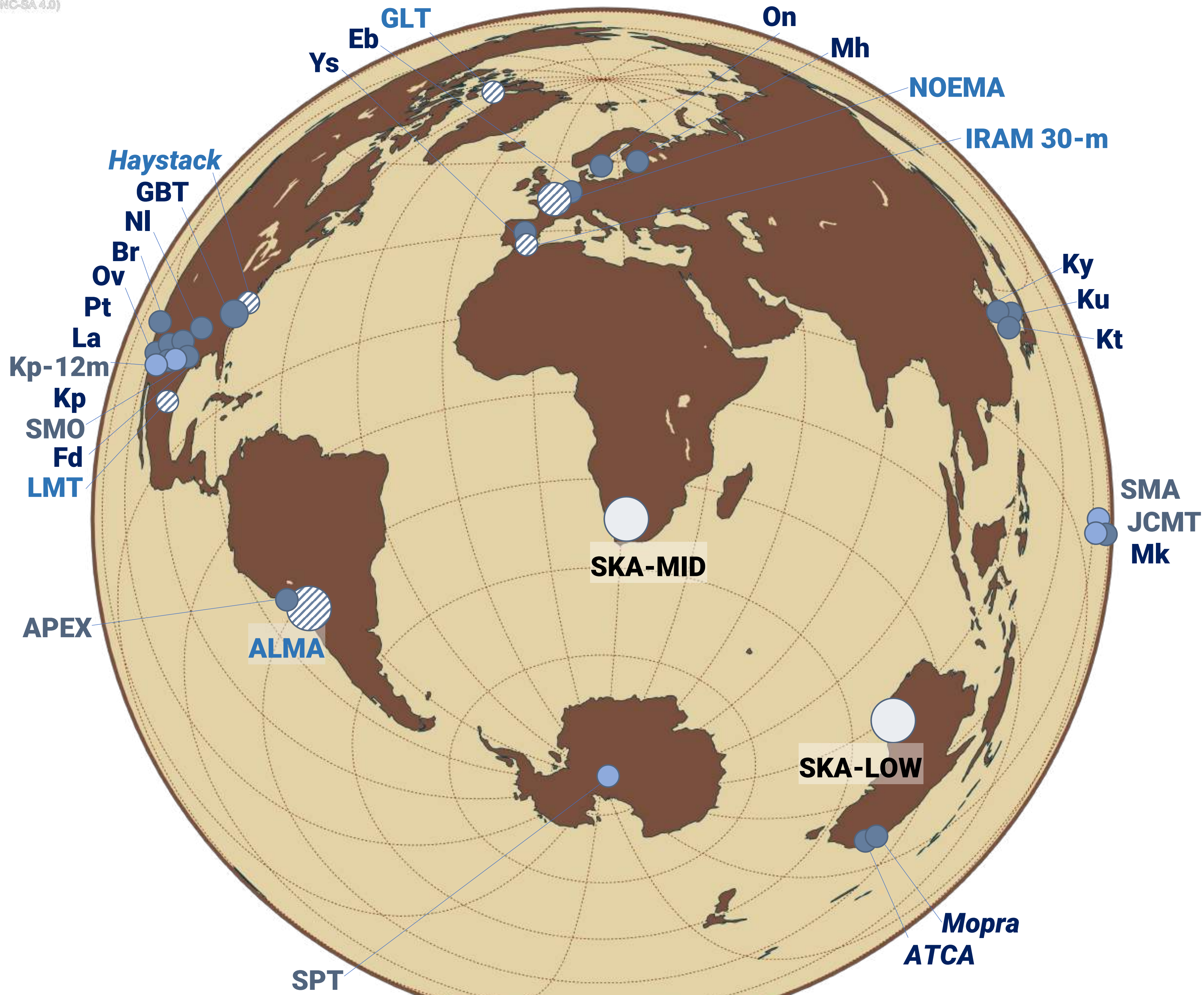
mm-VLBI developed over 35 yr

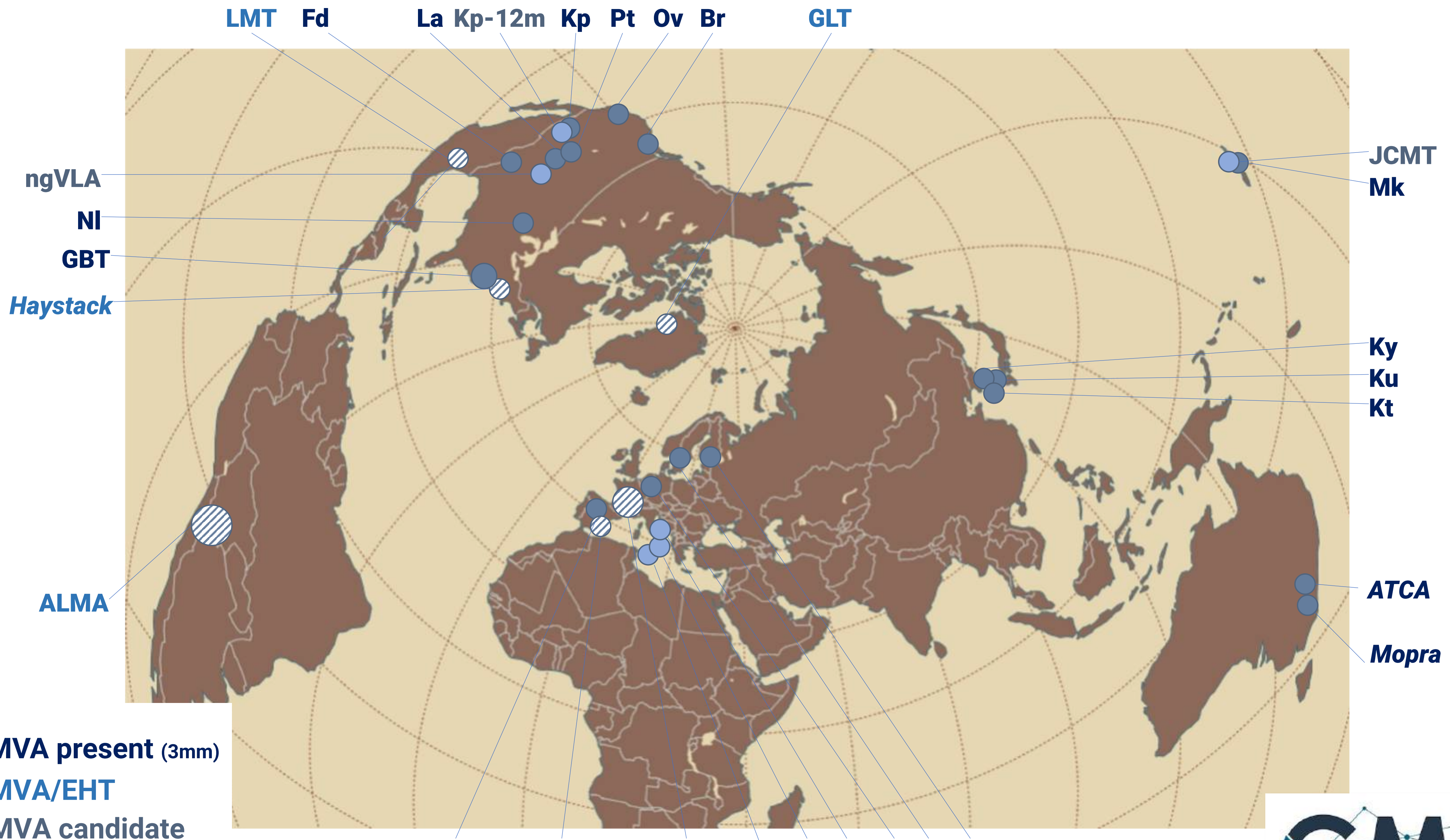


Observatories:

APEX: Atacama Pathfinder Experiment (North Chile) **CARMA:** Combined Array for mm Astronomy (California) **EF:** Effelsberg (MPIfR Bonn) **HK:** Haystack (Massachusetts) **JCMT:** James Clerk Maxwell Telescope (Hawaii) **KP:** Kit Peak (Arizona) **LMT:** Large mm Telescope (Mexico) **ON:** Onsala (Sweden) **OV:** Owens Valley (California) **PB:** Plateau de Bure (France) **PV:** Pico Veleta (Spain) **SMT:** Submm Telescope (Arizona) **SPT:** South Pole Telescope

- GMVA (3mm)
- EHT (1.3/0.8 mm)
- ◌ GMVA/EHT
- SKA





- **GMVA present (3mm)**
- ▨ **GMVA/EHT**
- **GMVA candidate**



Magnetic field from core-shift



Core position offset measure

Core-shift measure

Luminosity distance

$$\Omega_{rv} = 4.85 \times 10^{-9} \frac{\Delta r_{\text{mas}} D_L}{(1+z)^2} \left(\frac{\nu_1^{1/k_r} \nu_2^{1/k_r}}{\nu_2^{1/k_r} - \nu_1^{1/k_r}} \right) \text{ pc GHz},$$

Lobanov (1998)

For a conical jet with spectral index

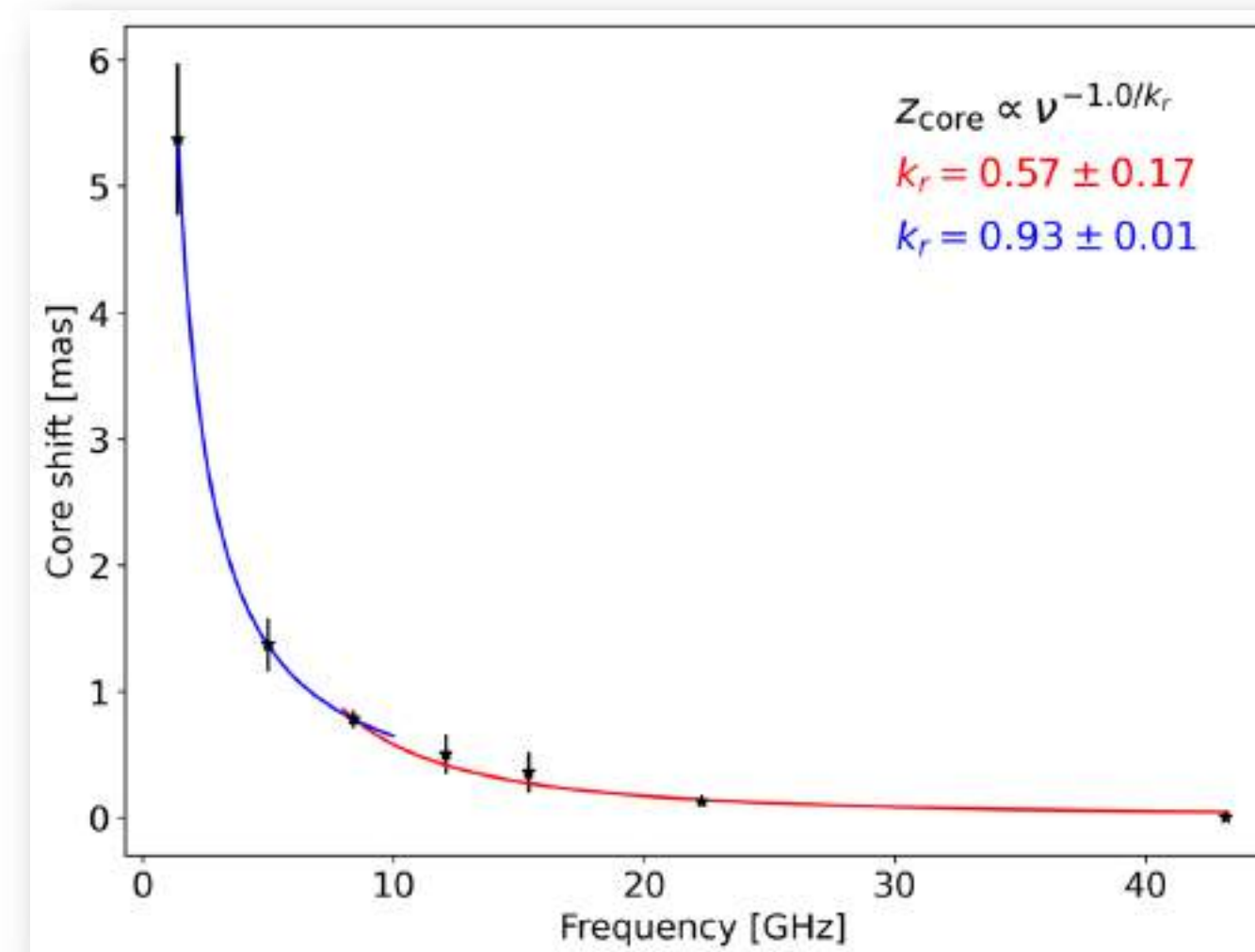
$$\alpha = -0.5$$

$$B_1 = 0.025 \left(\frac{\Omega_{rv}^3 (1+z)^2}{\delta^2 \phi \sin^2 \theta} \right)^{1/4} \text{ G},$$

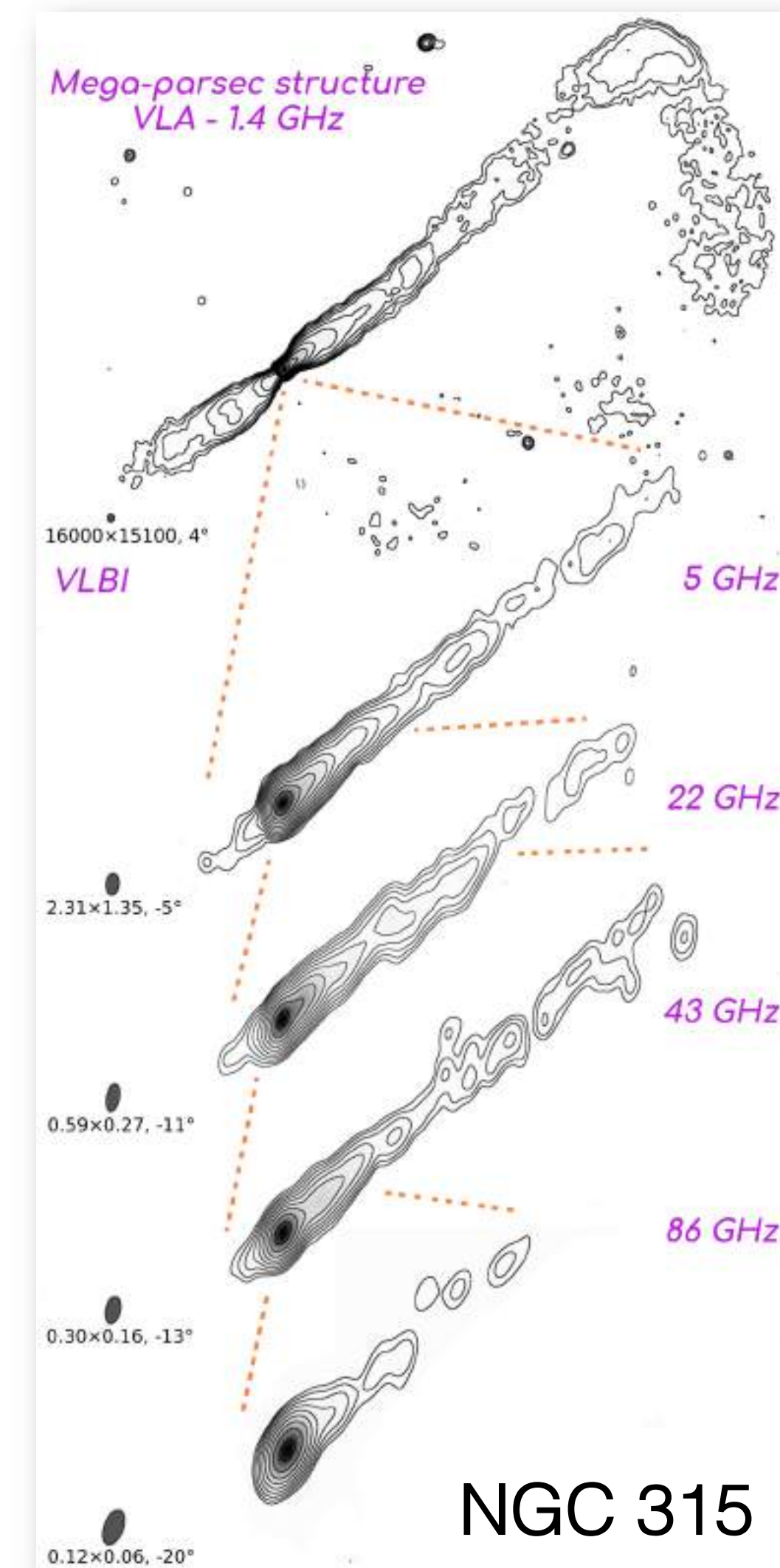
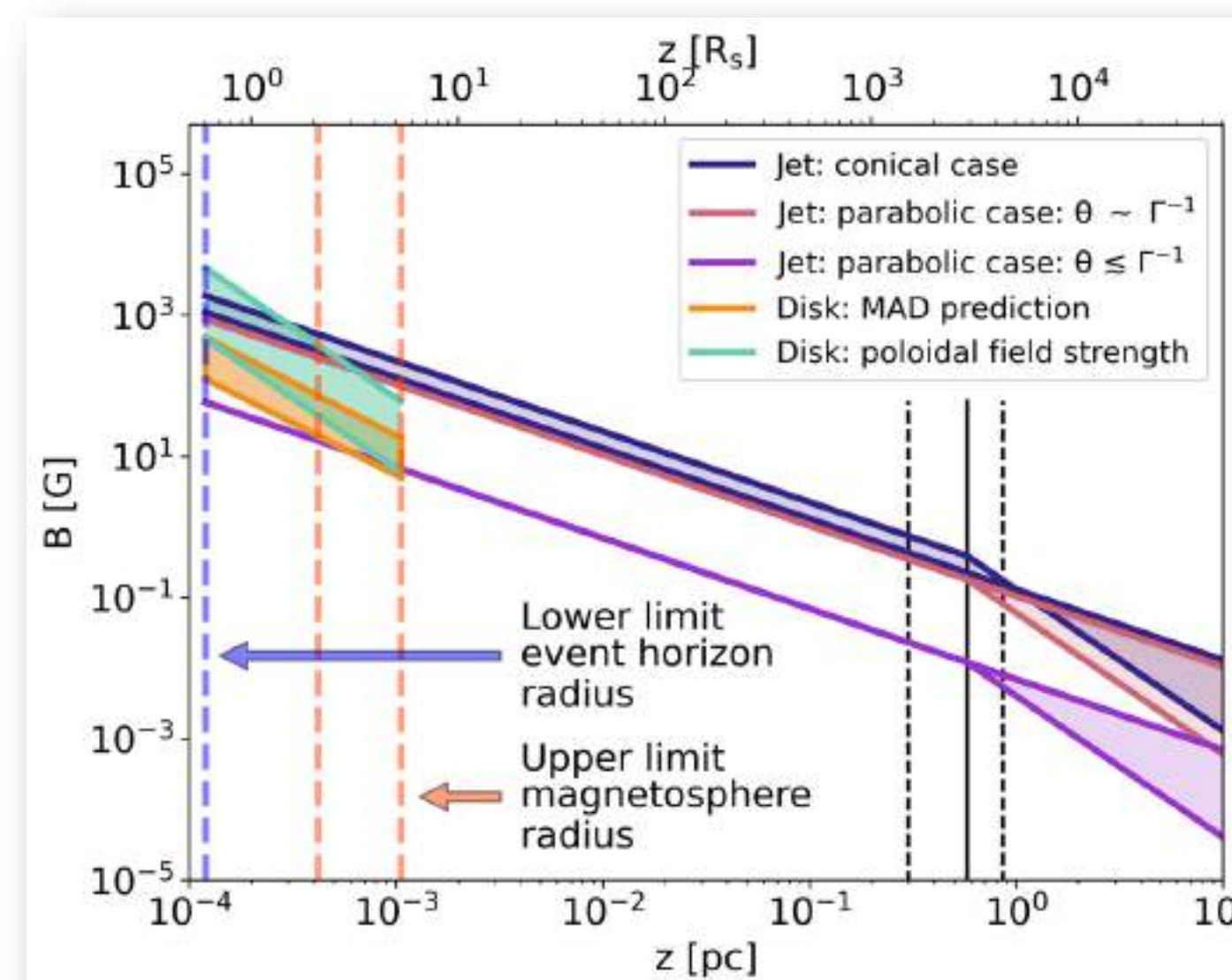
Accretion rate

$$\dot{M}_B = 0.012 \left(\frac{k_B T}{\text{keV}} \right)^{-3/2} \left(\frac{n_e}{\text{cm}^{-3}} \right) \left(\frac{M_{\text{BH}}}{10^9 M_\odot} \right)^2 M_\odot \text{ yr}^{-1},$$

Russell et al. (2015)

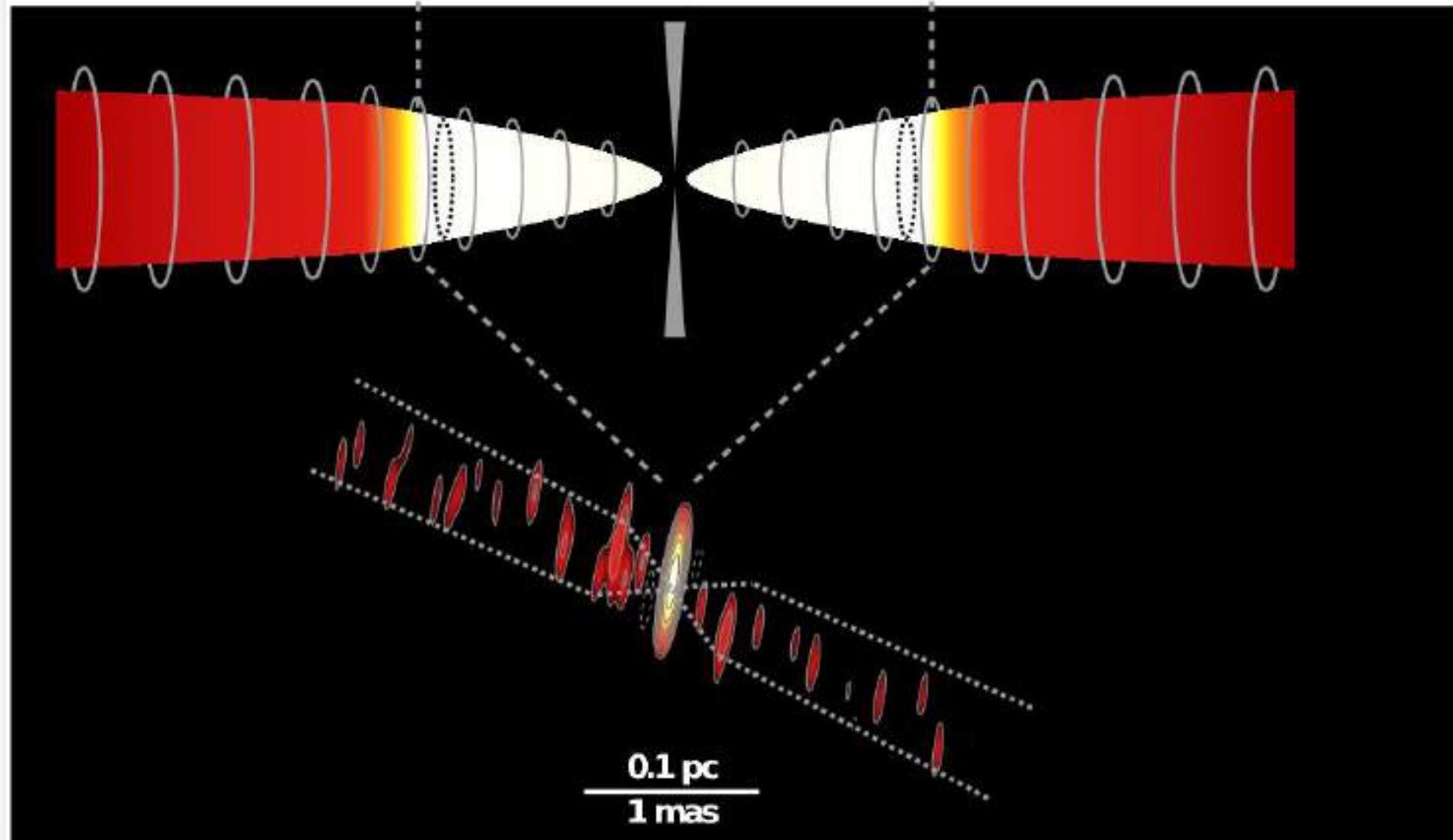
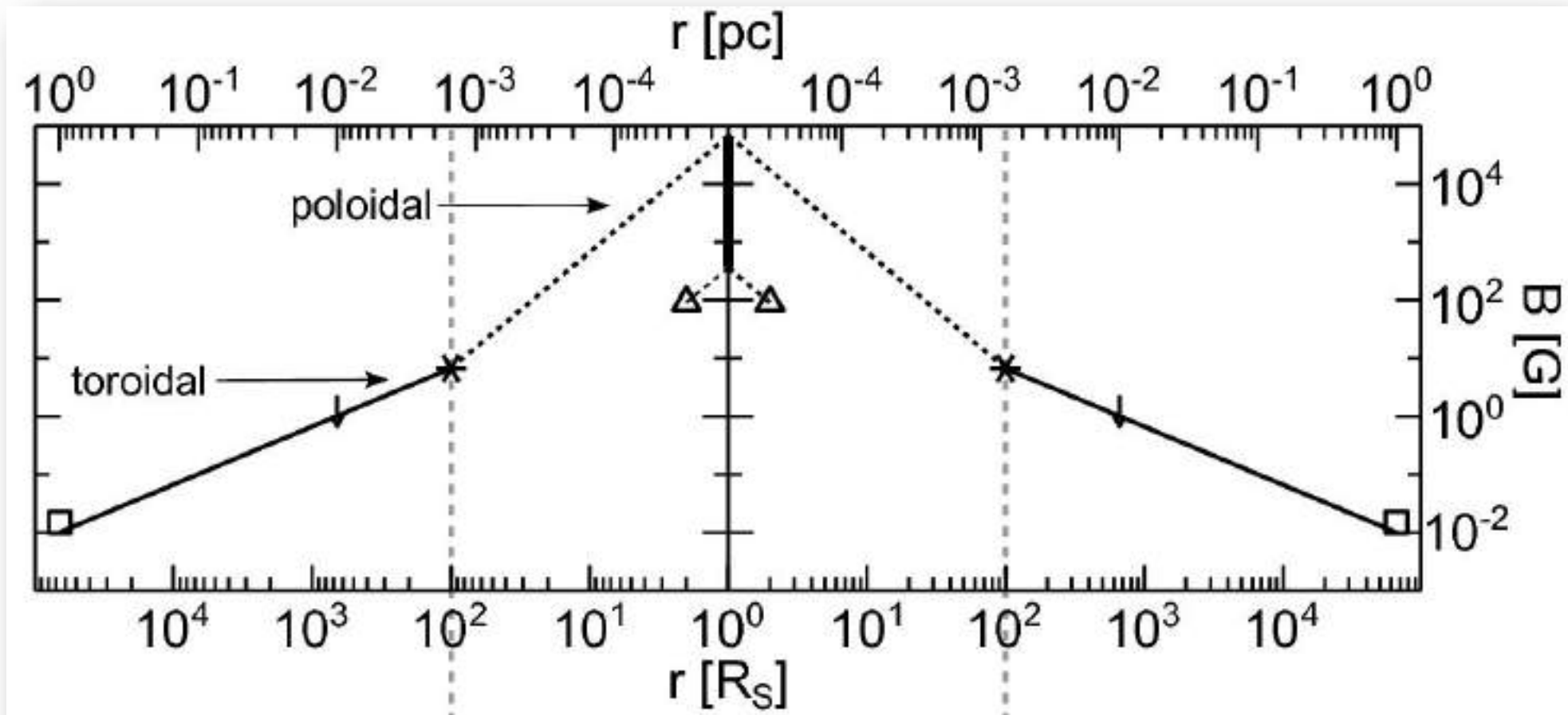


Radio galaxy NGC 315,
Ricci et al. (2022)

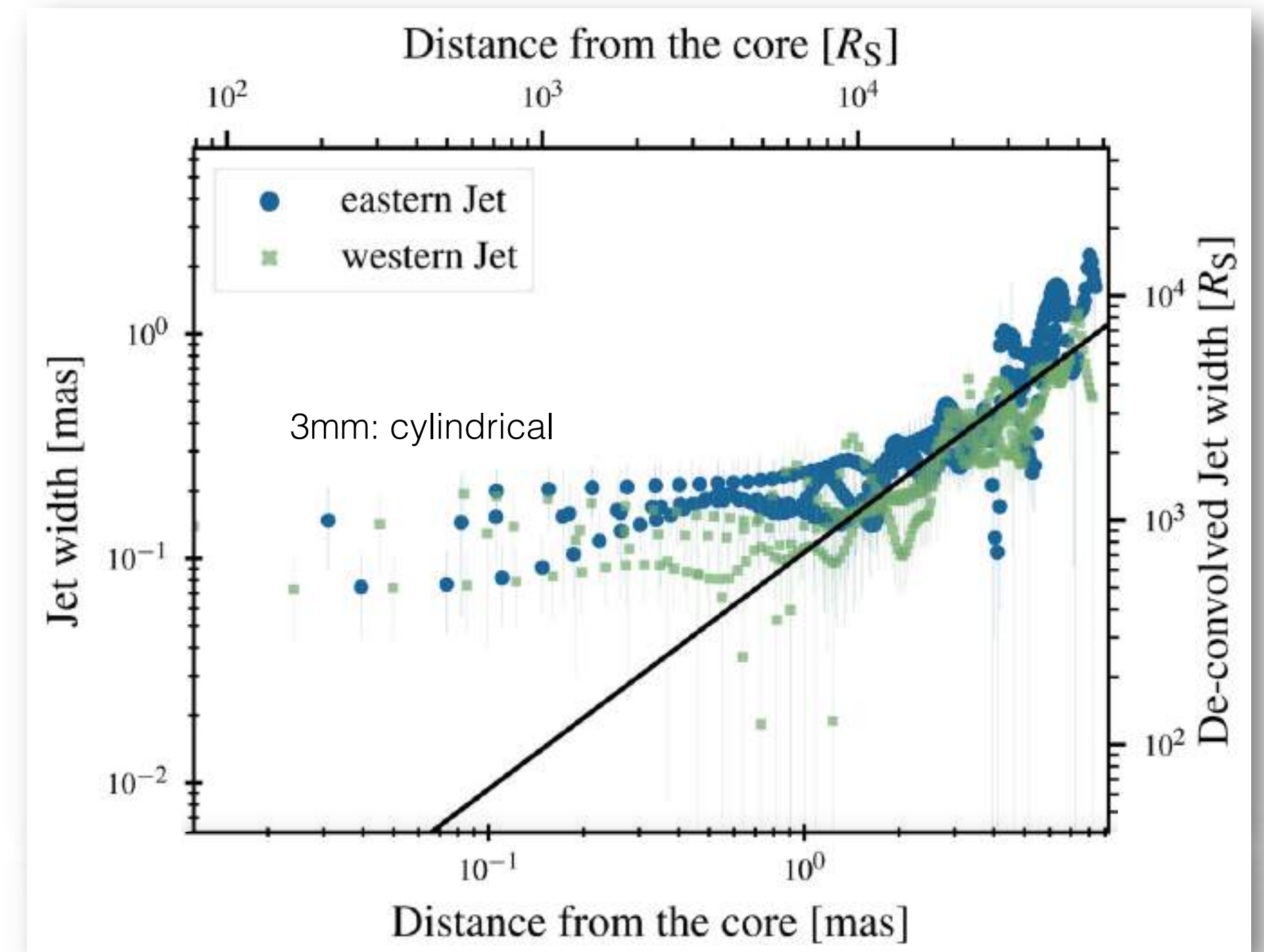


Boccardi et al. (2021)

Magnetic field from emission compactness: NGC 1052



$B \sim 10^4$ G near the EH,
 extrapolated from GMVA data
 Break in the collimation profile at $\sim 10^4 R_S$



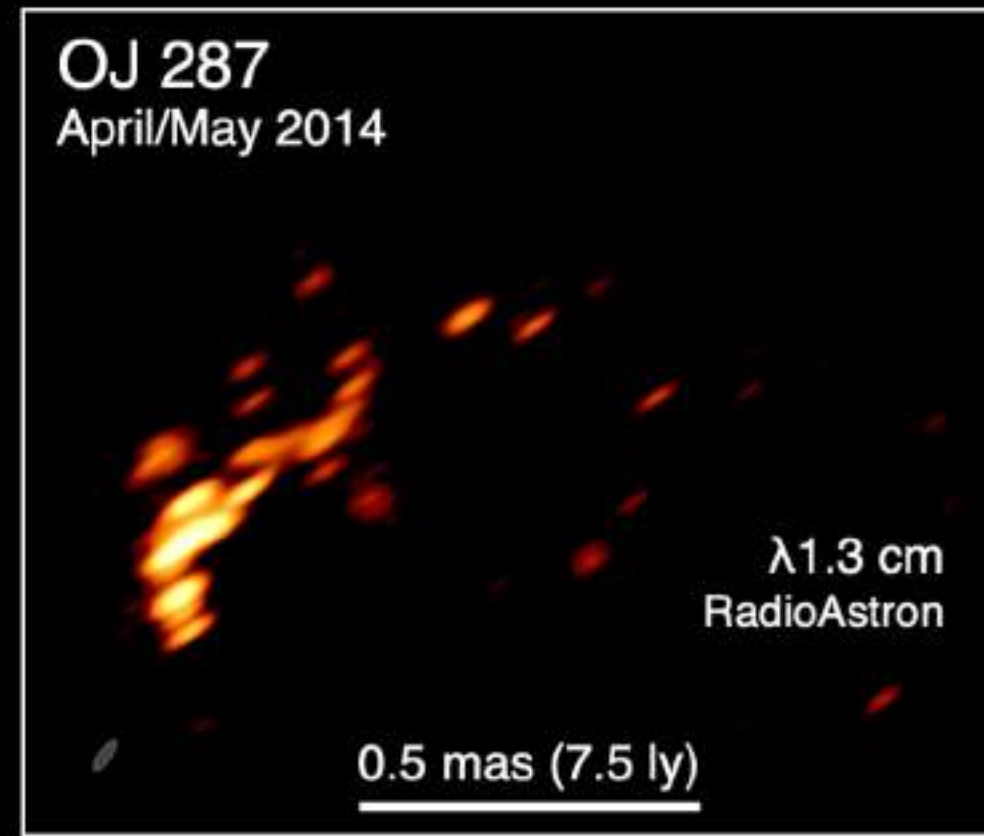
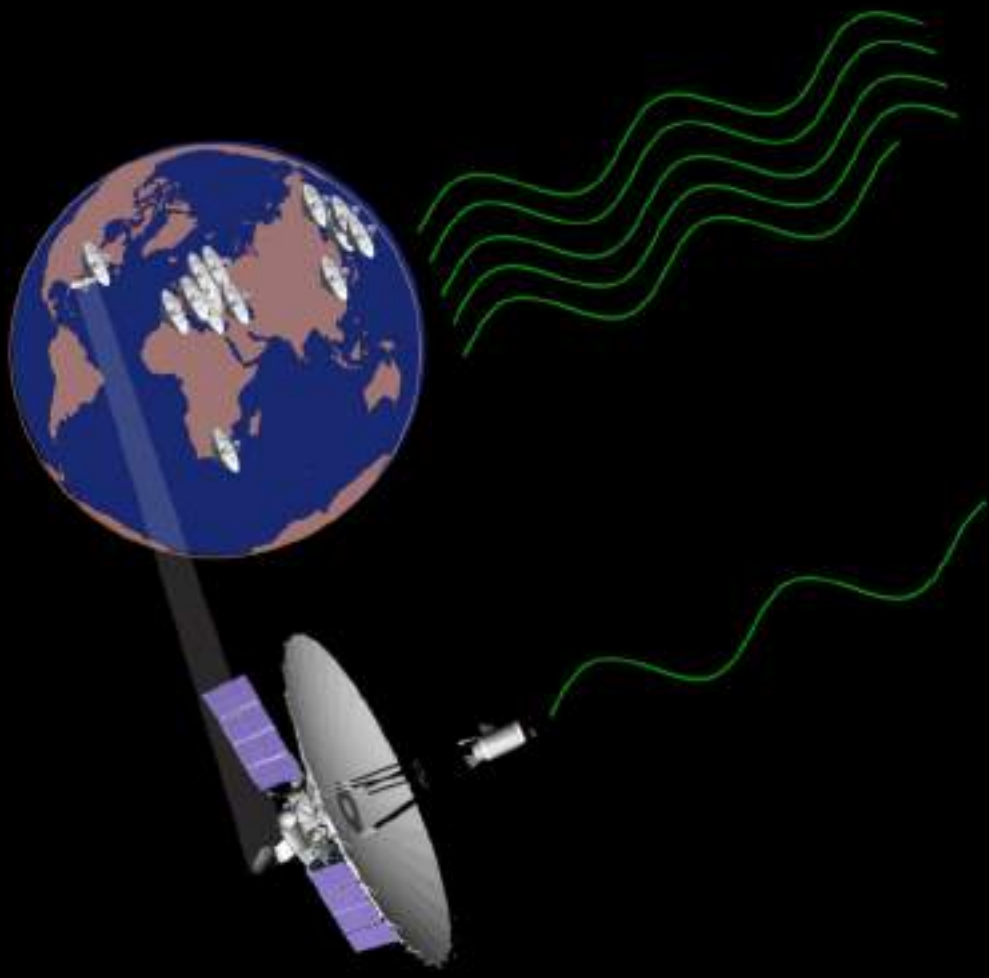
Baczko et al. A&A 593, A47 (2016)

Baczko et al. A&A 658, A119 (2022)

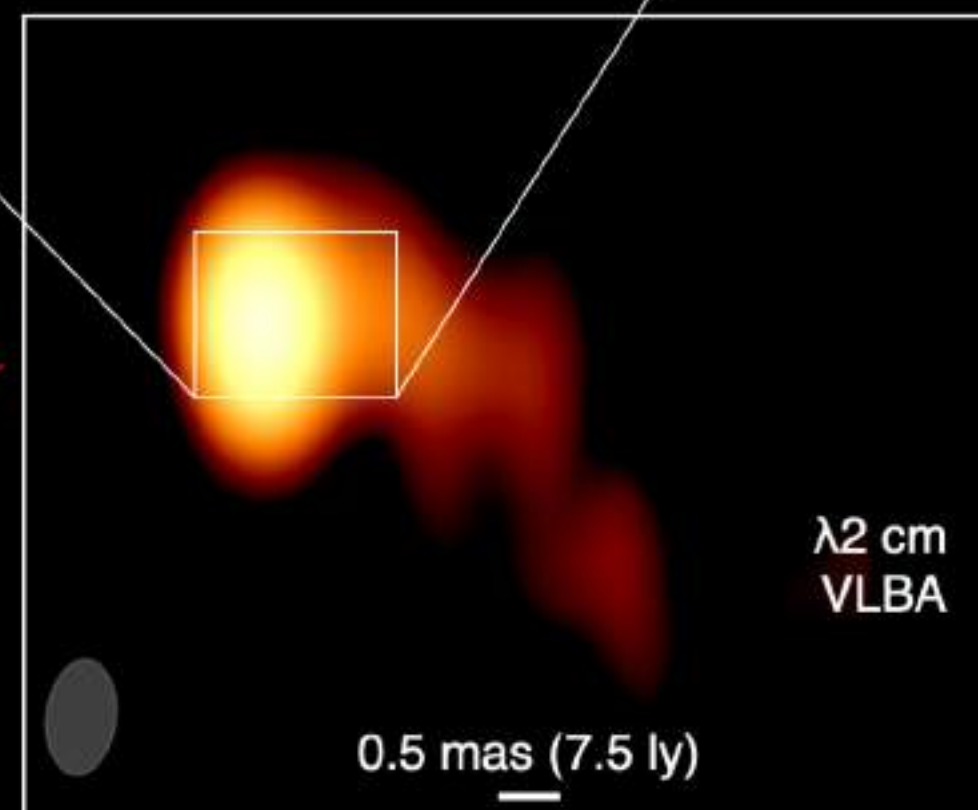
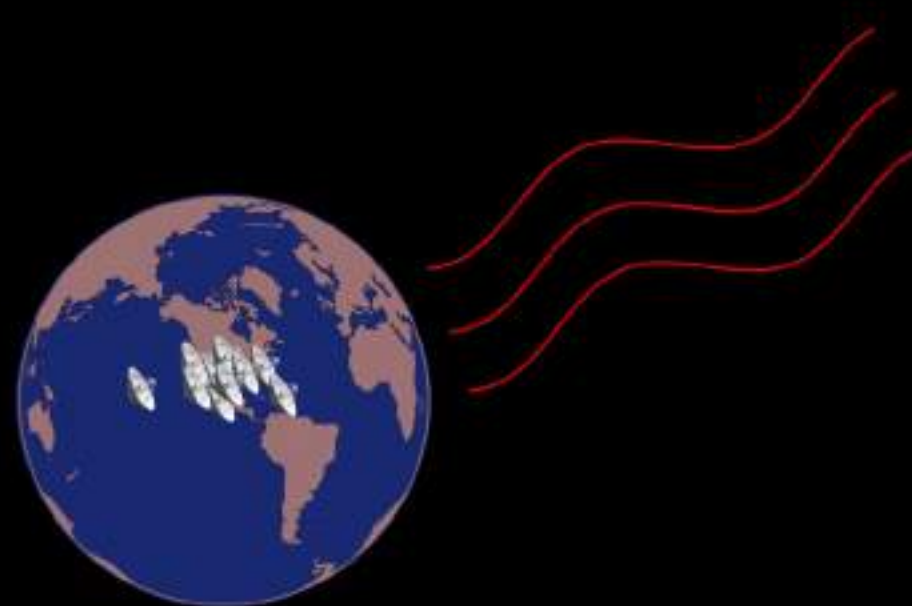
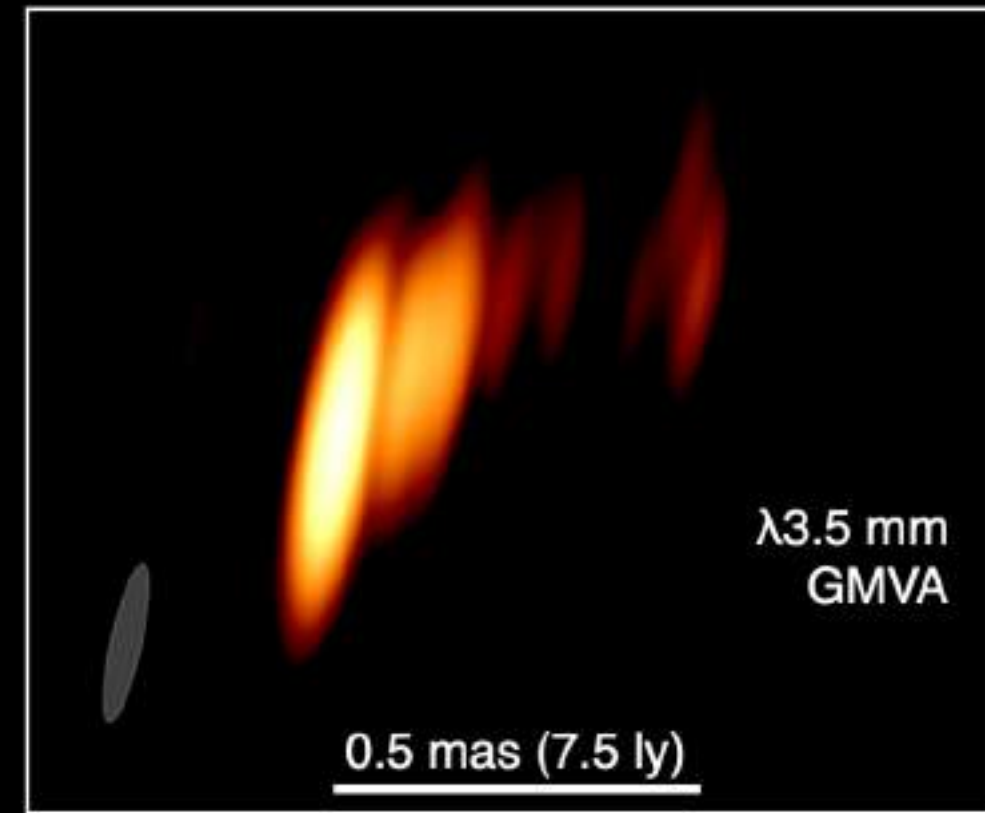
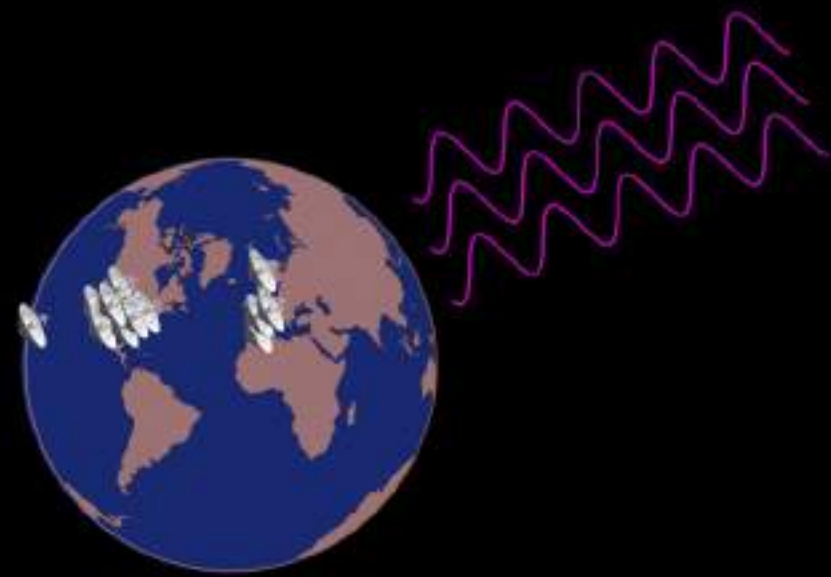


OJ 287, space-VLBI and GMVA

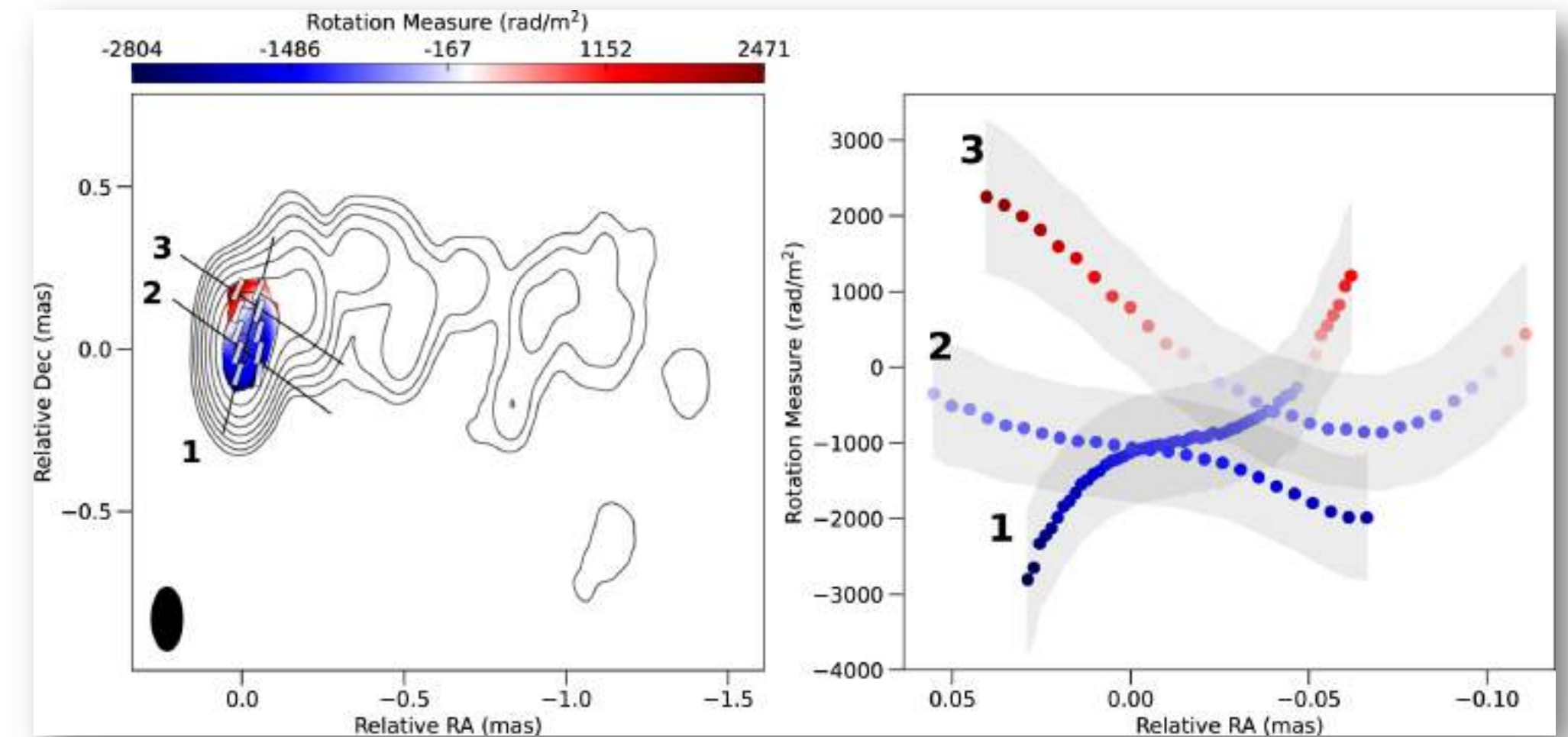
RadioAstron, GMVA and VLBA imaging



Collage: Eduardo Ros (MPIST)



© Gómez, Traianou, Krichbaum, et al., The Astrophysical Journal (2022)

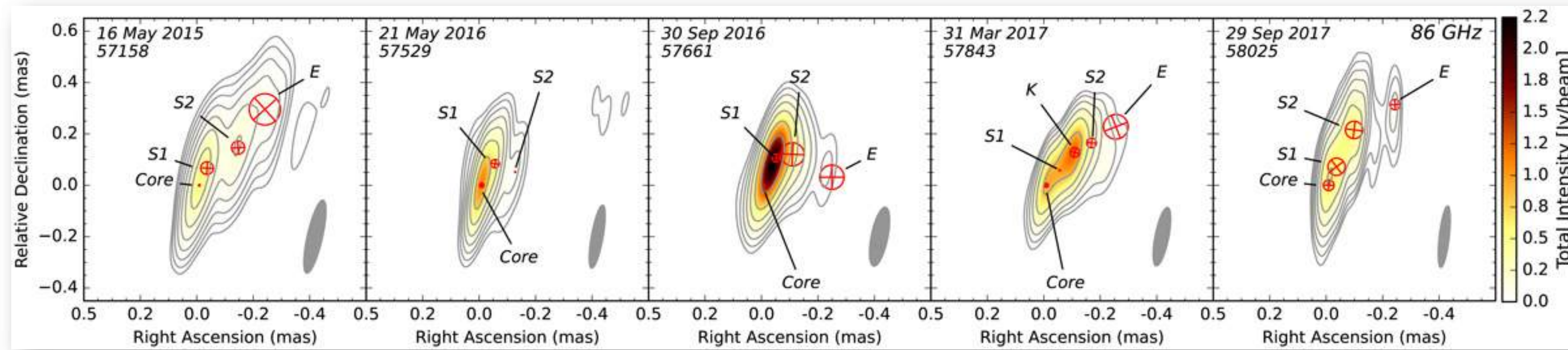


Magnetic field and Faraday Rotation Measure (RM)

Gómez et al. ApJ 924 122 (2022)

Eduardo Ros, 7 November 2022

OJ 287 GMVA – B from polarimetric imaging

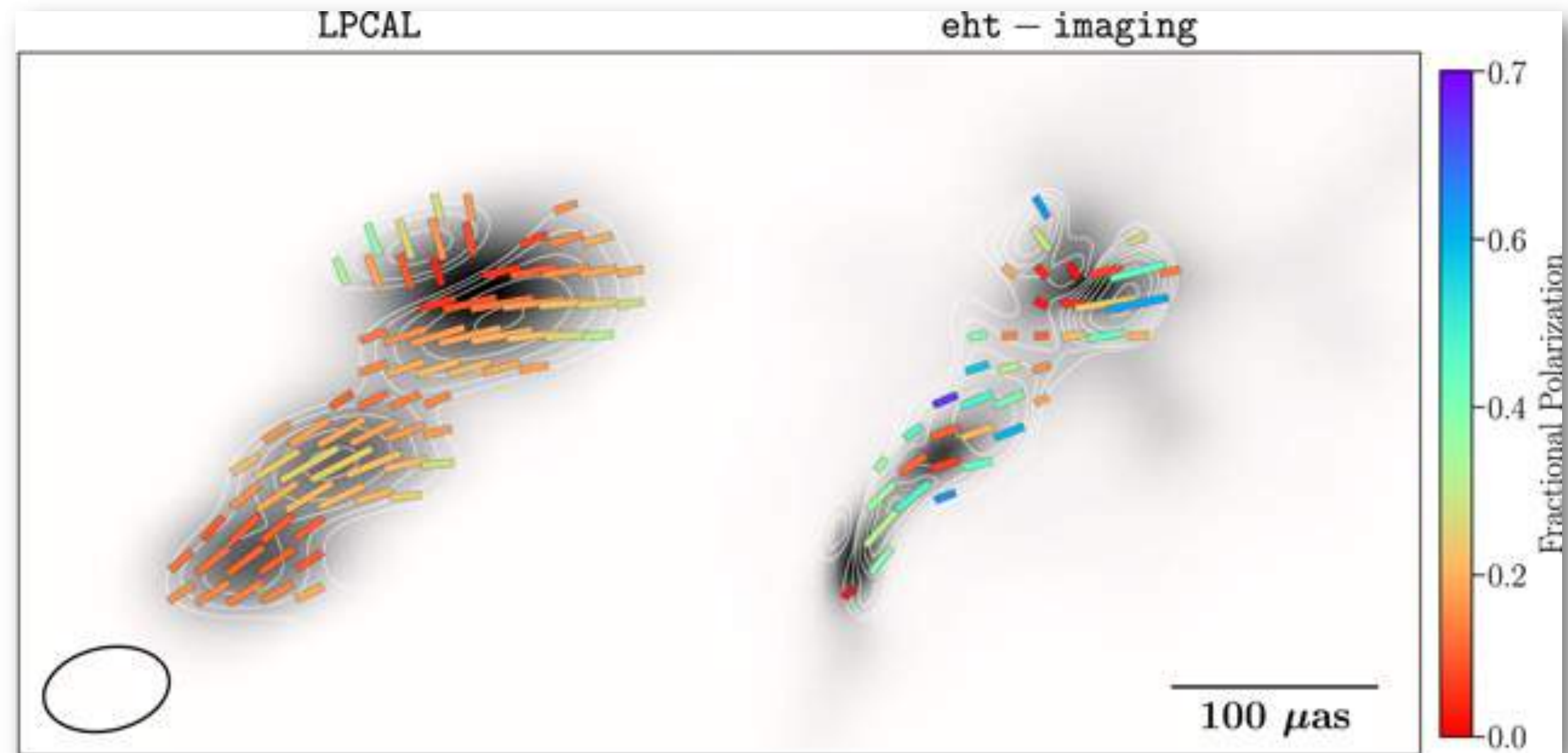


GMVA imaging
Jet feature associated
to TeV flare

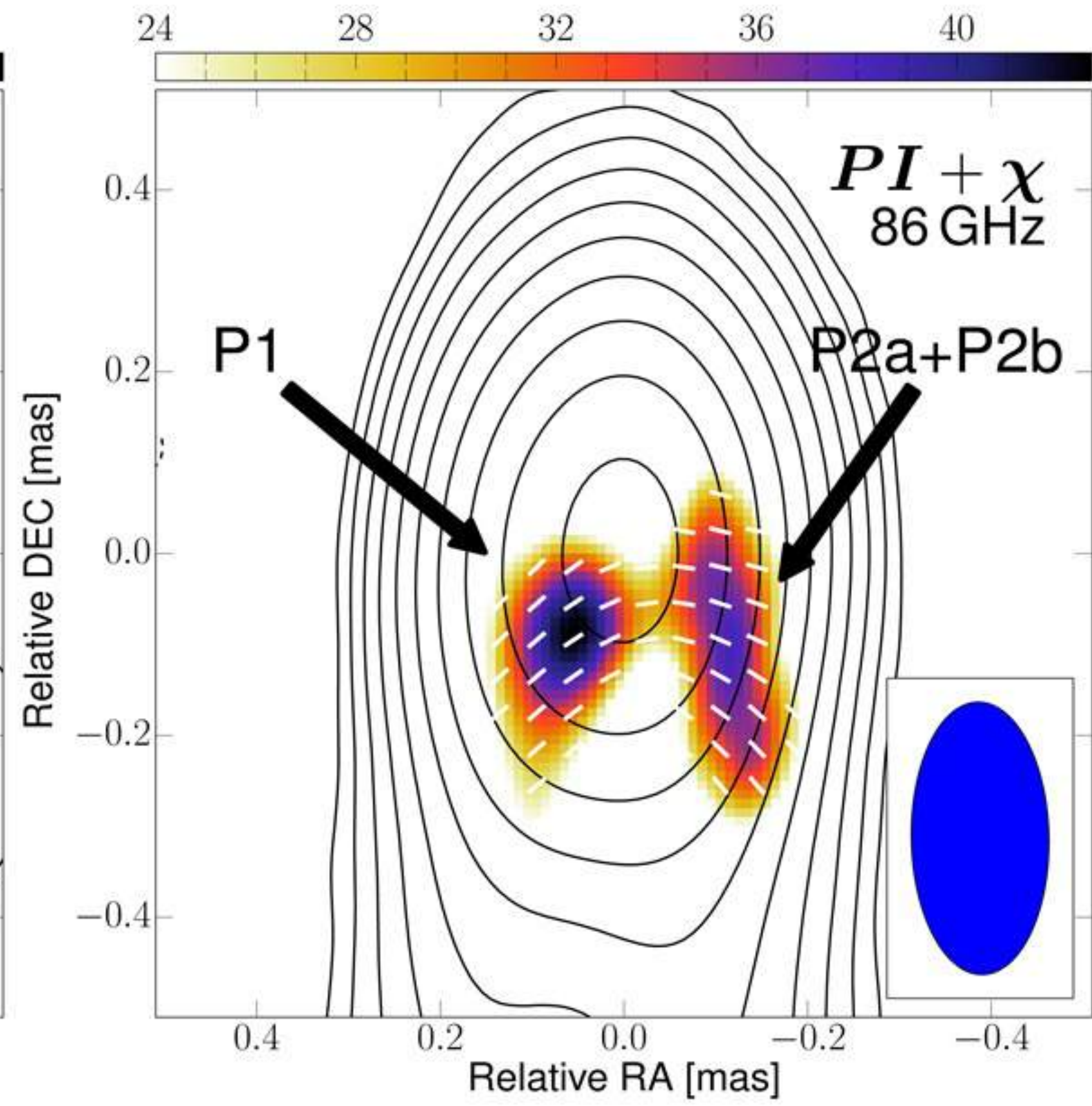
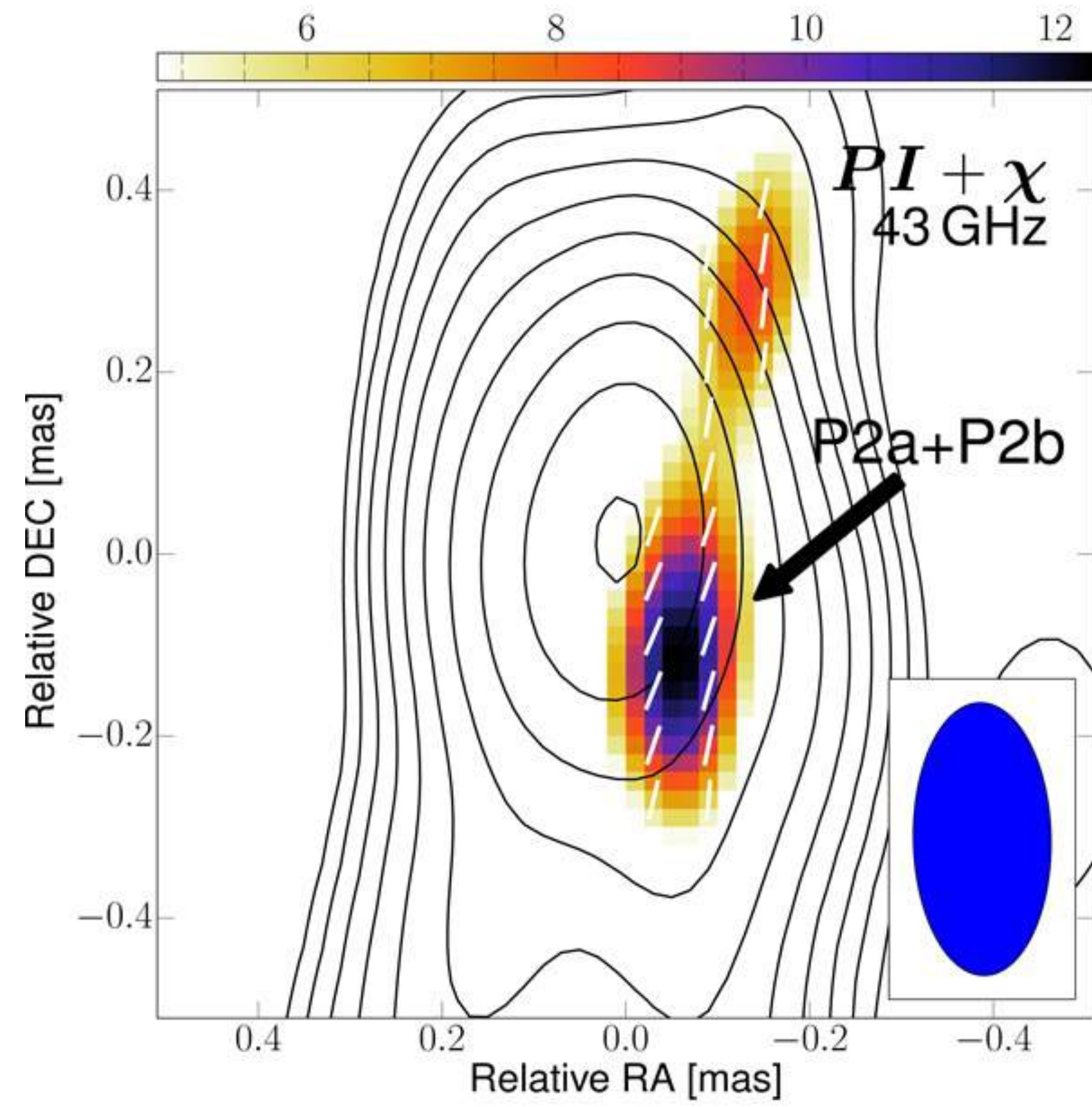
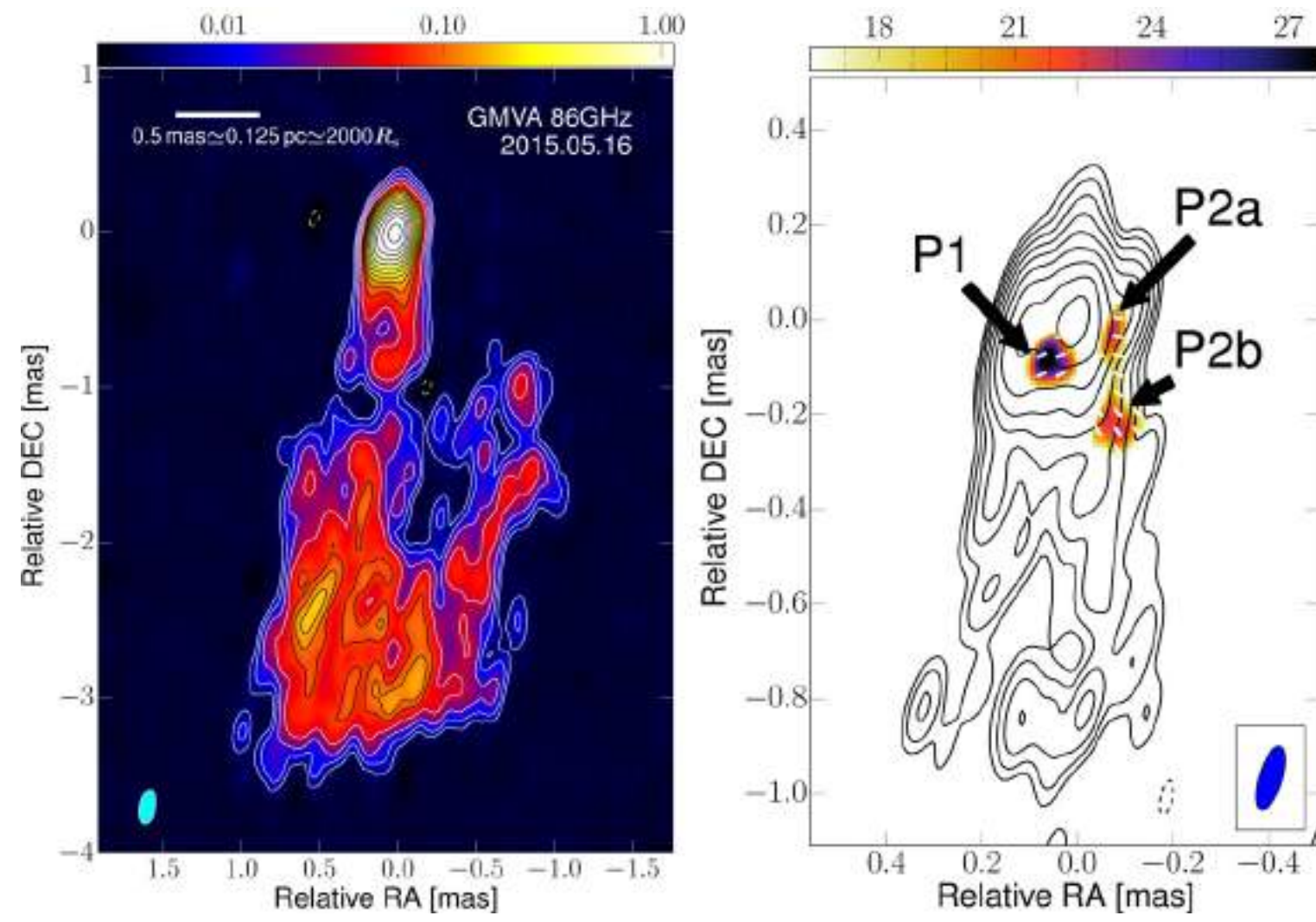
Lico et al. A&A 658, L10 (2022)

GMVA+ALMA
polarimetric imaging
Innermost B structure

Zhao et al. ApJ 932 72(2022)



Polarisation in the core of 3C 84 (NGC 1275)



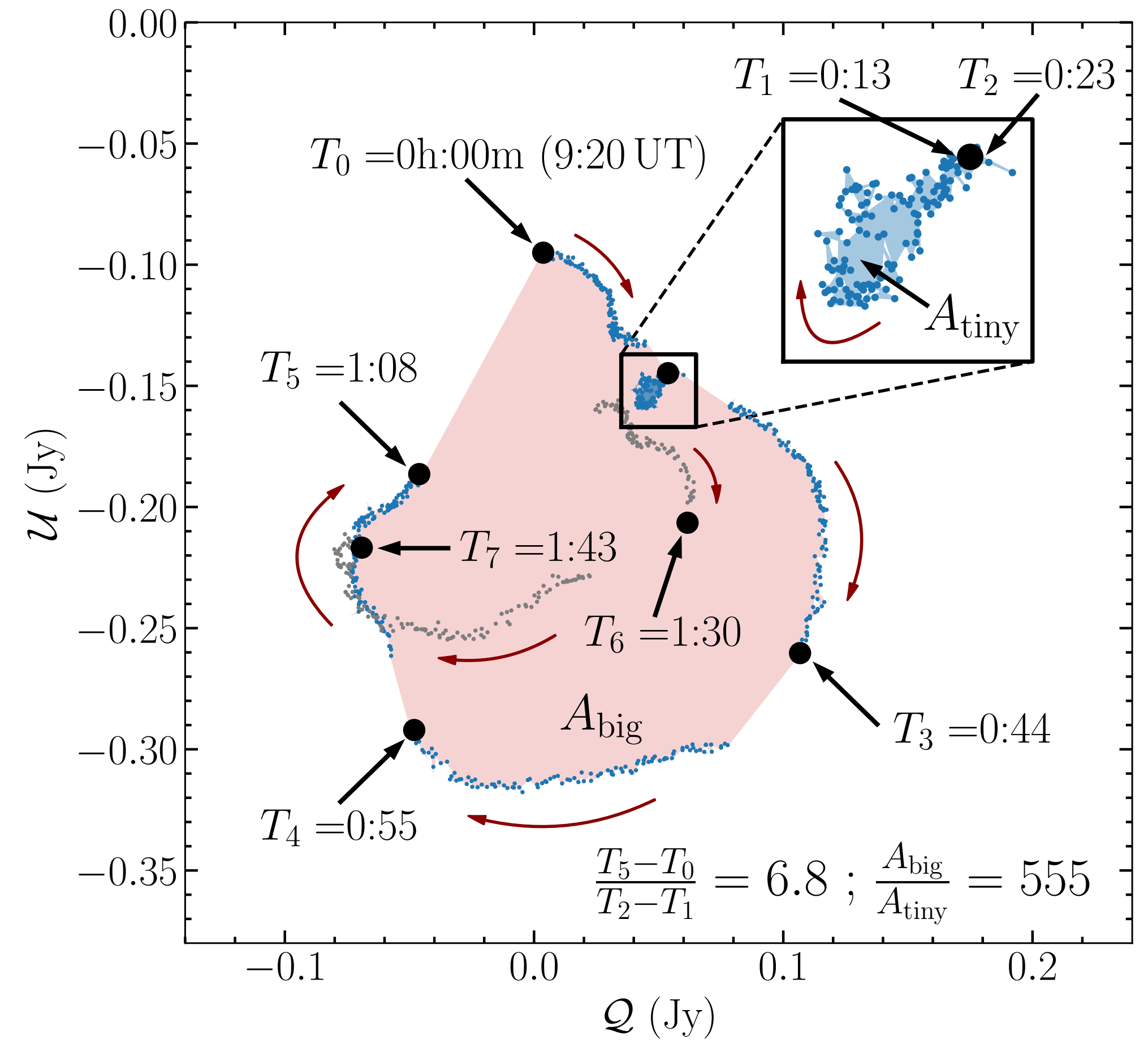
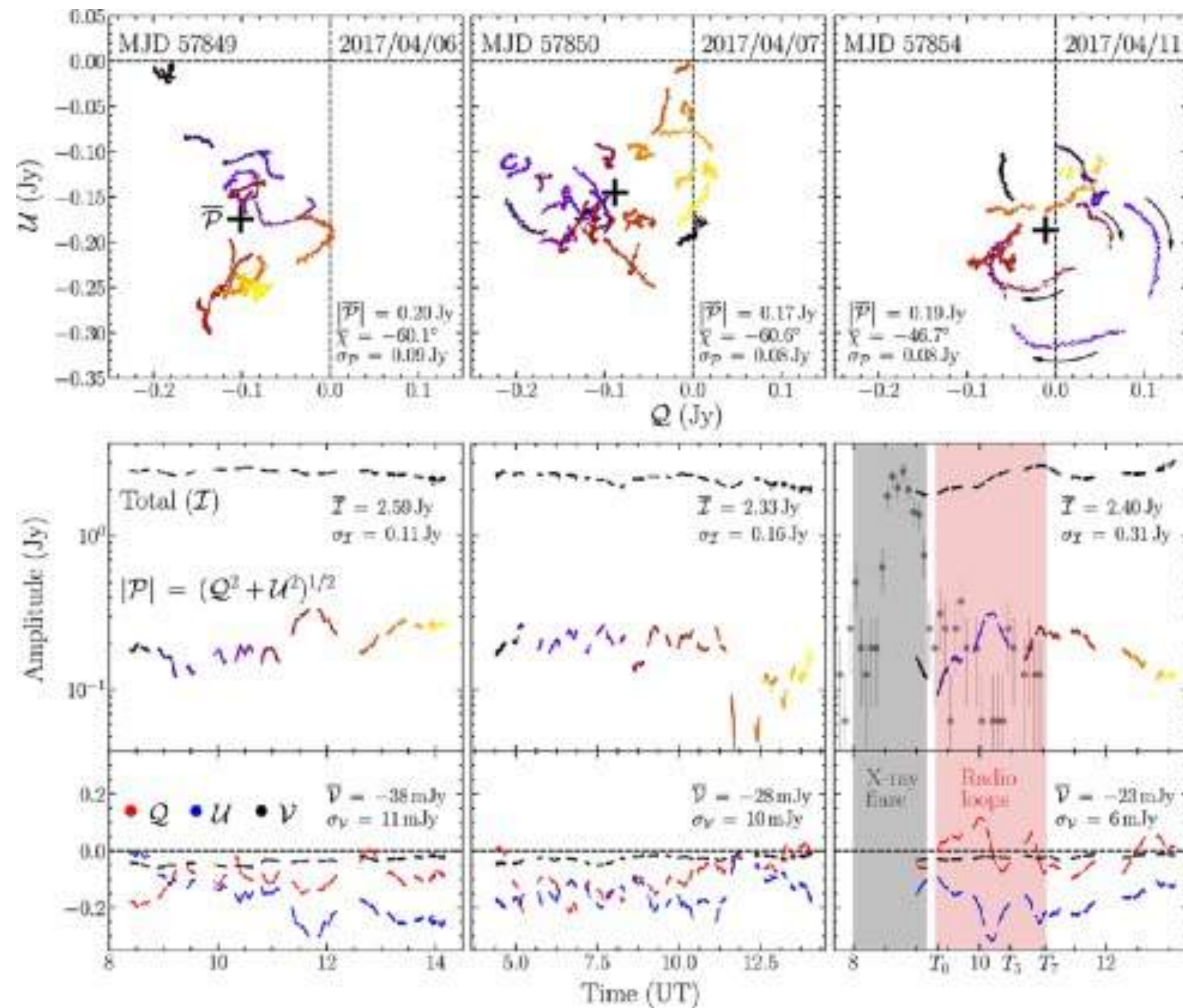
Kim et al. A&A 622, A196, 2019: Spatially resolved origin of millimeter-wave linear polarization in the nuclear region of 3C 84

(a)

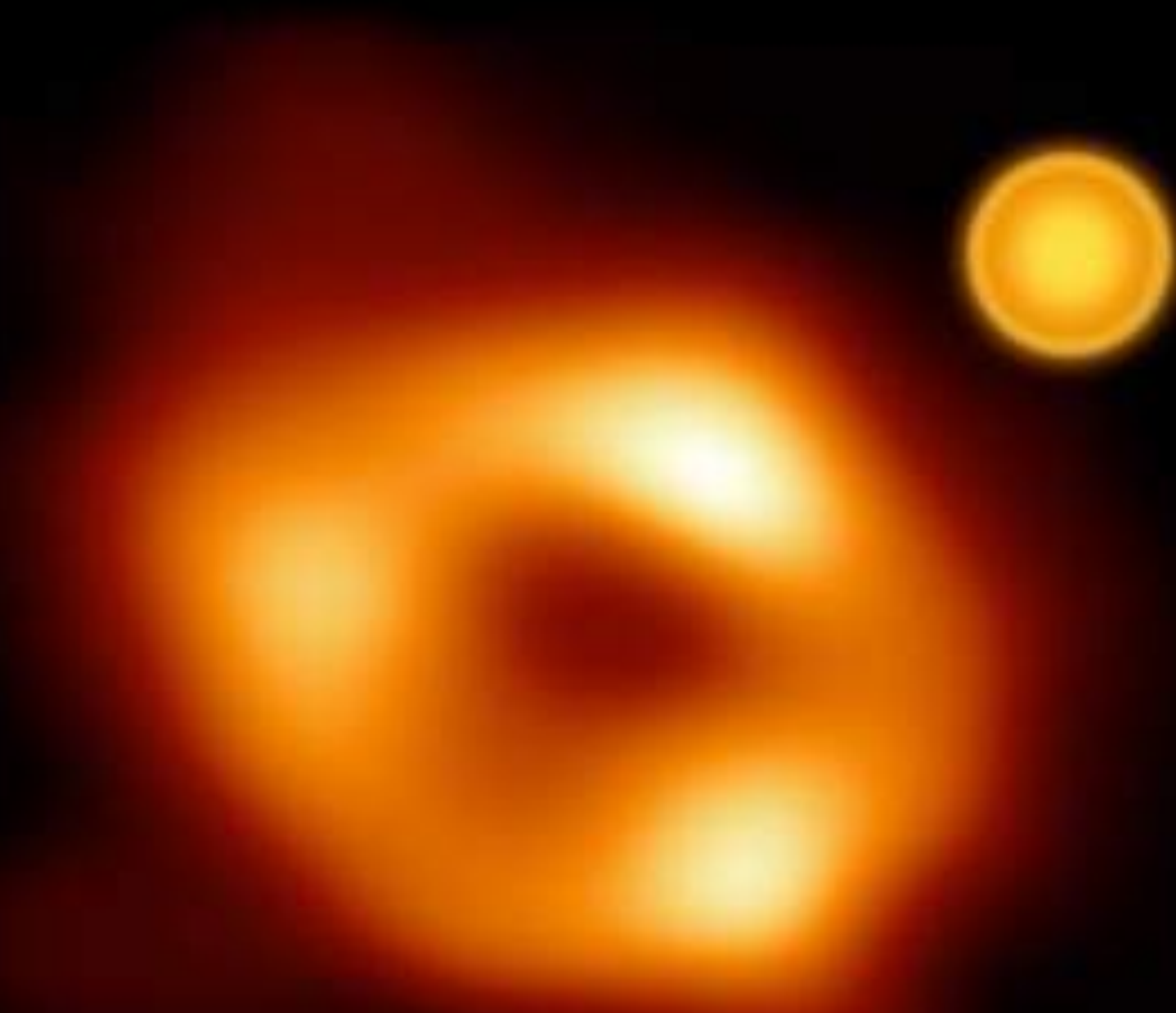
(b)

ALMA: QU -polarization loops in SgrA* indicate orbital motion around BH (low-luminosity radio core)

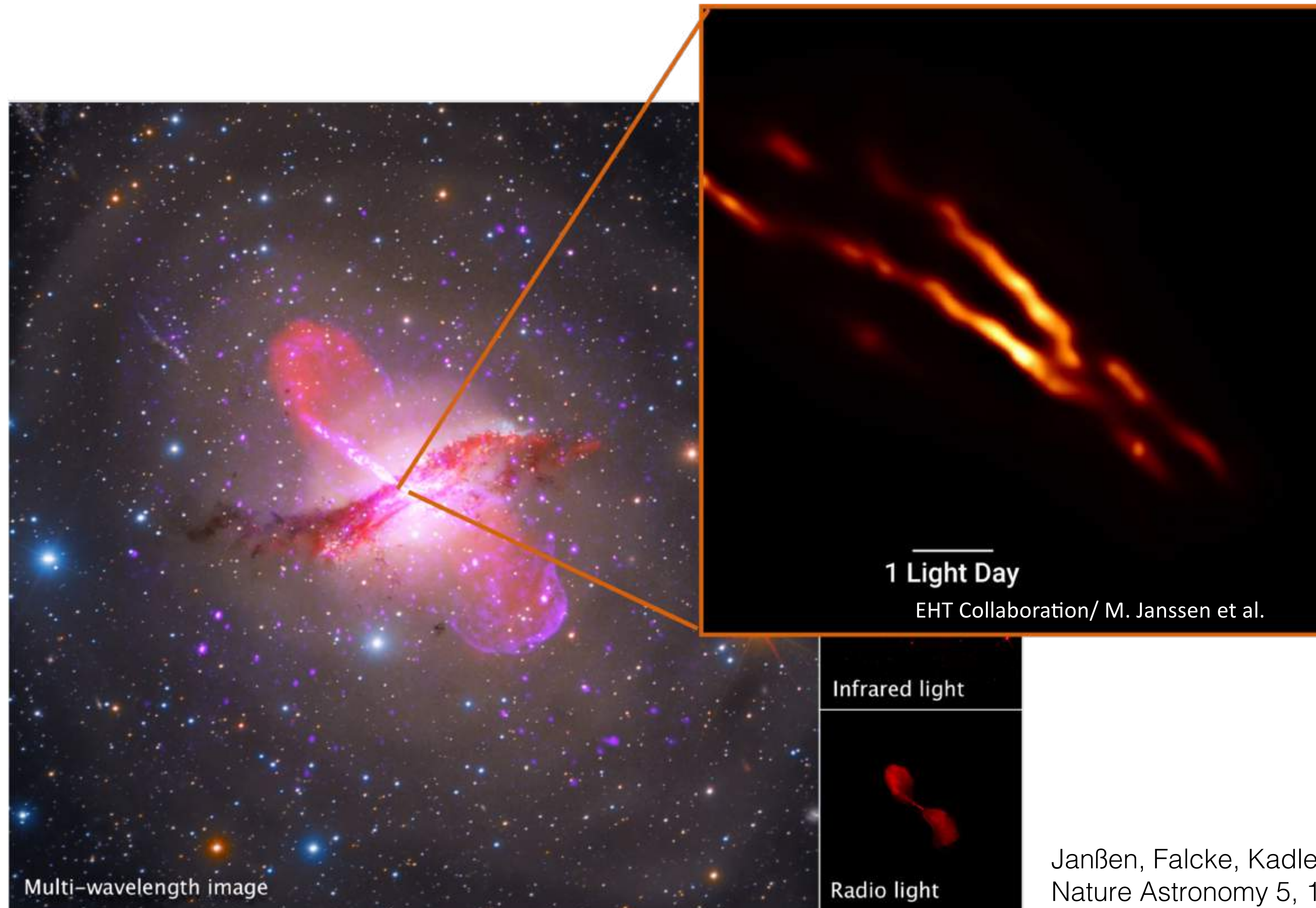
Wielgus et al. A&A 665 L6 (22sep2022)



See also, e.g., Trippe et al. [2007 MNRAS 375, 764-772](https://doi.org/10.1093/mnras/stx100)



EHT imaging: the jets in Centaurus A



- 1mm VLBI imaging with EHT reveals edge-brightened jet base
- Opt. thick radio core?
- Helical magnetic field?

Janßen, Falcke, Kadler, Ros, et al.,
Nature Astronomy 5, 1017–1028 (19jul2021)

3C274 or Messier 87

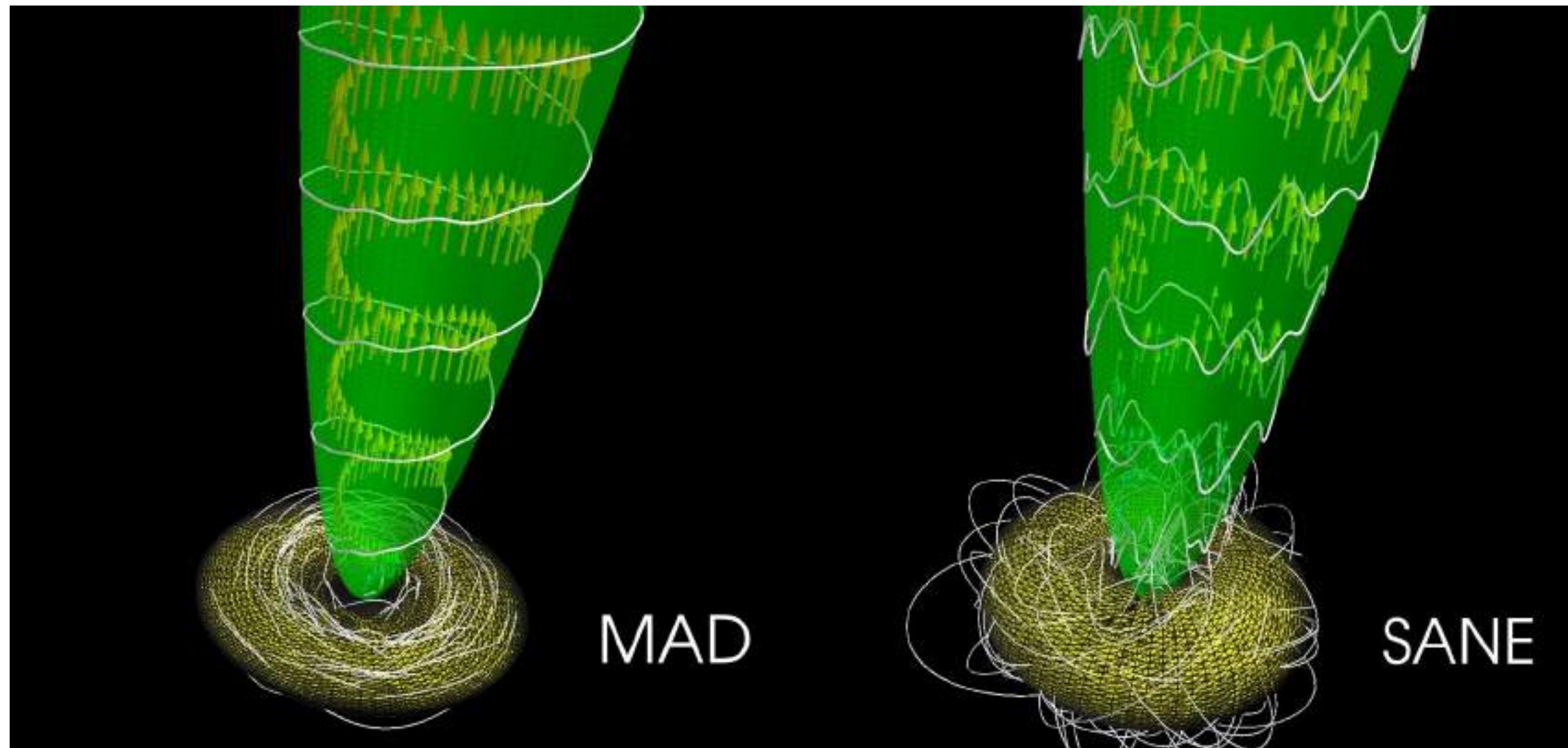


ALMA 230 GHz
1300 light years

VLBA 43 GHz
0.25 light years

EHT 230 GHz
0.0063 light years

Jets: Accretion dynamics and ejection processes

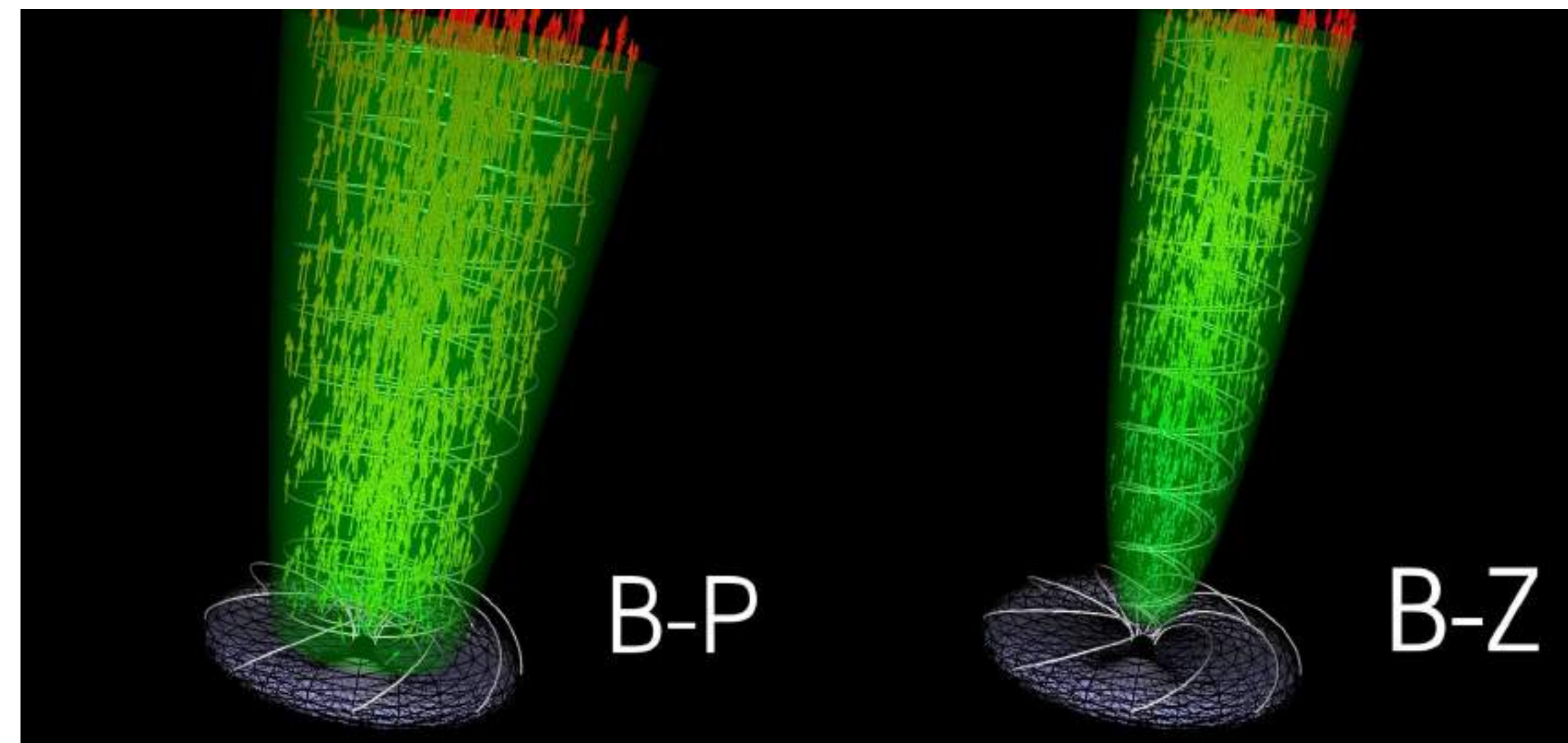


BP (Blandford-Payne): Accretion flux magnetosphere generates outflowing matter stream from disk wind (Lorentz)

BZ (Blandford-Znajek): Electro-magnetic extraction of energy from spinning BH

MAD: *Magnetically Arrested Disks*

SANE: *Standard And Normal Evolution*

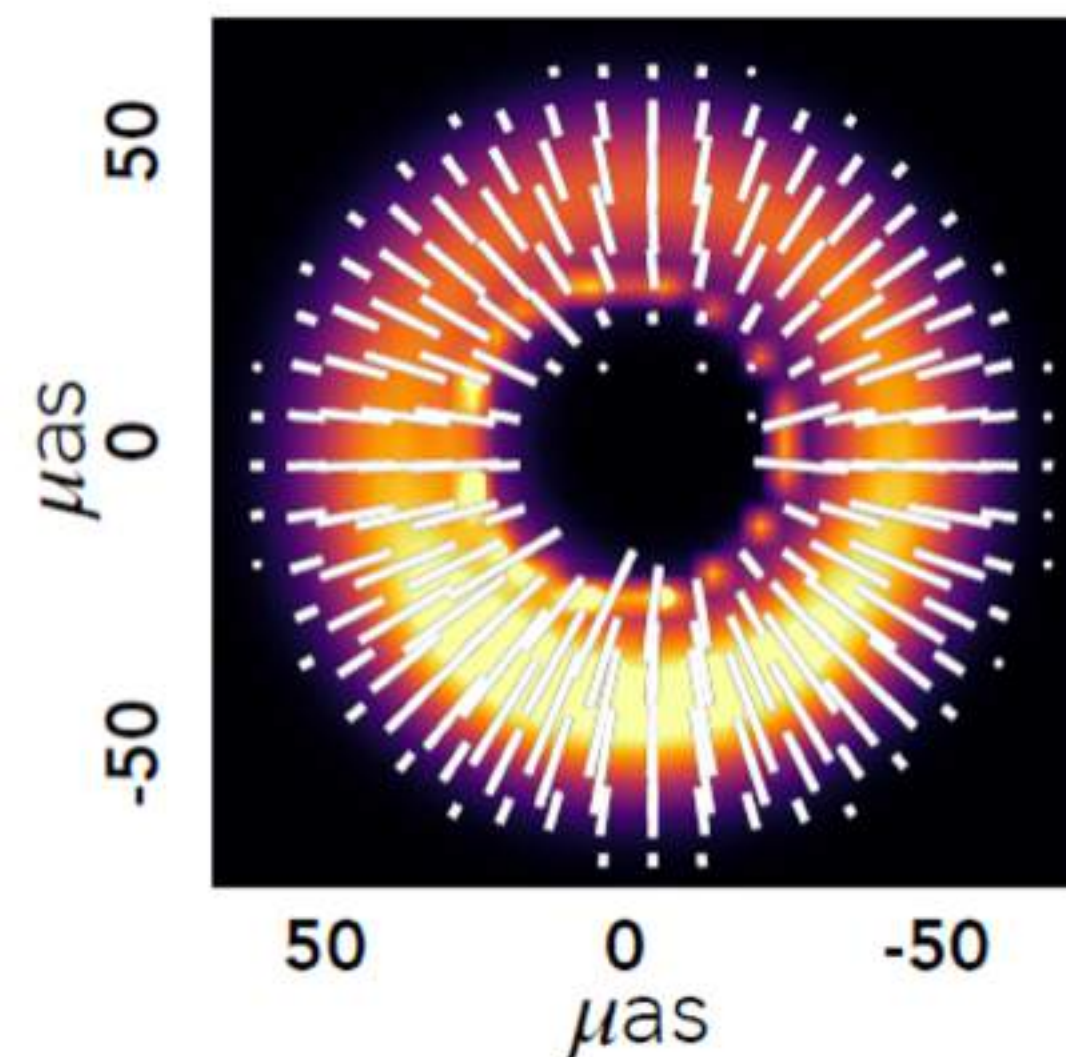


Polarisation: additional Information

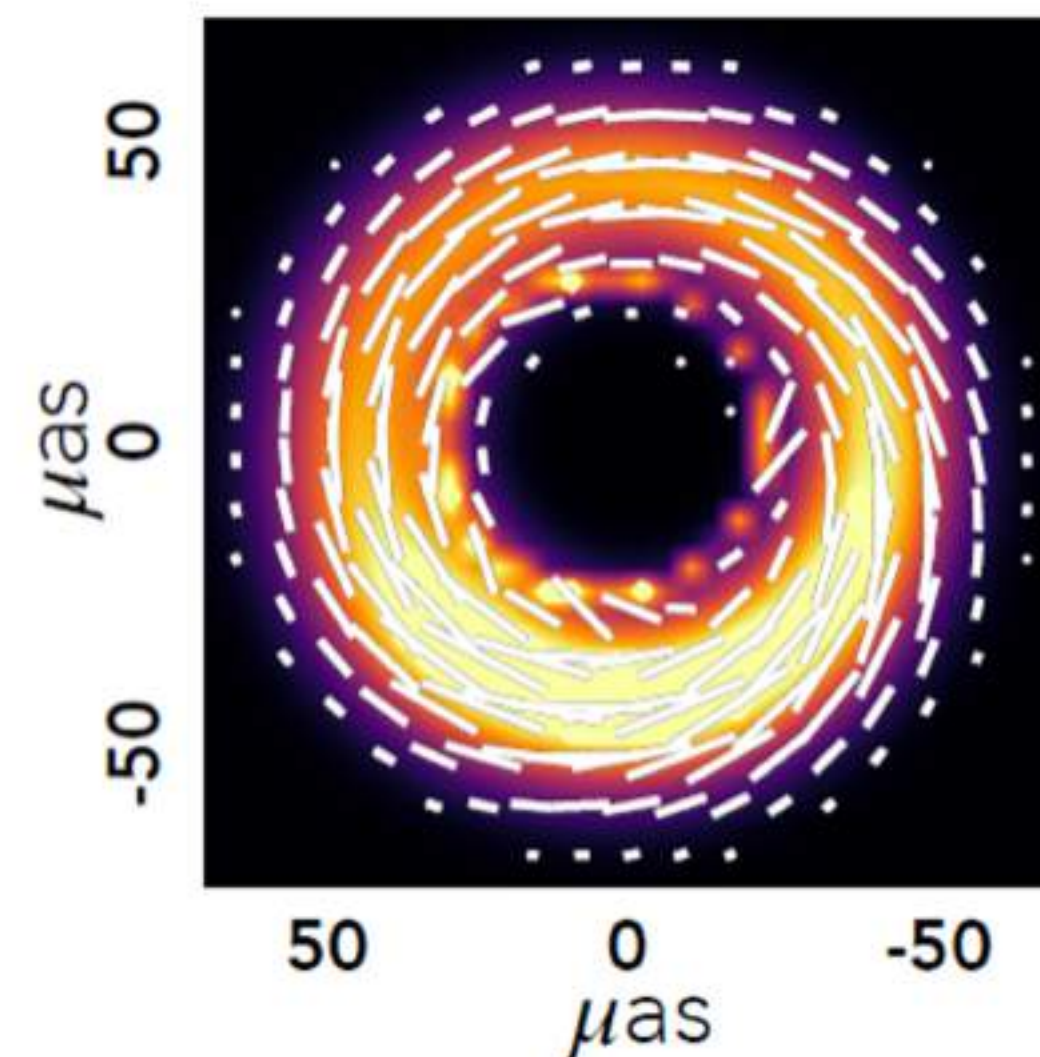


- Magnetic field geometry
- Faraday opacity
- Electron density
- Electron temperature
- Magnetic field strength
- Electron energy distribution
- Accretion rate

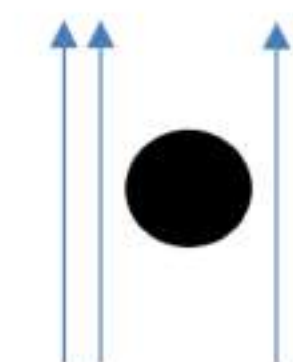
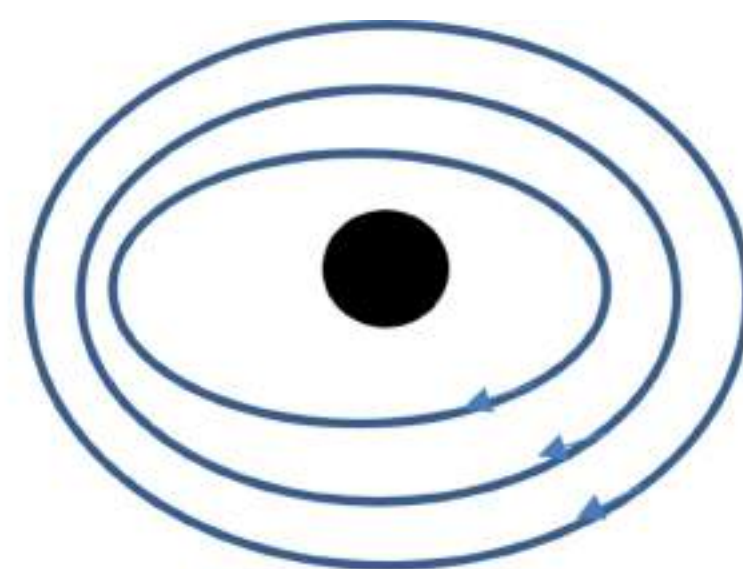
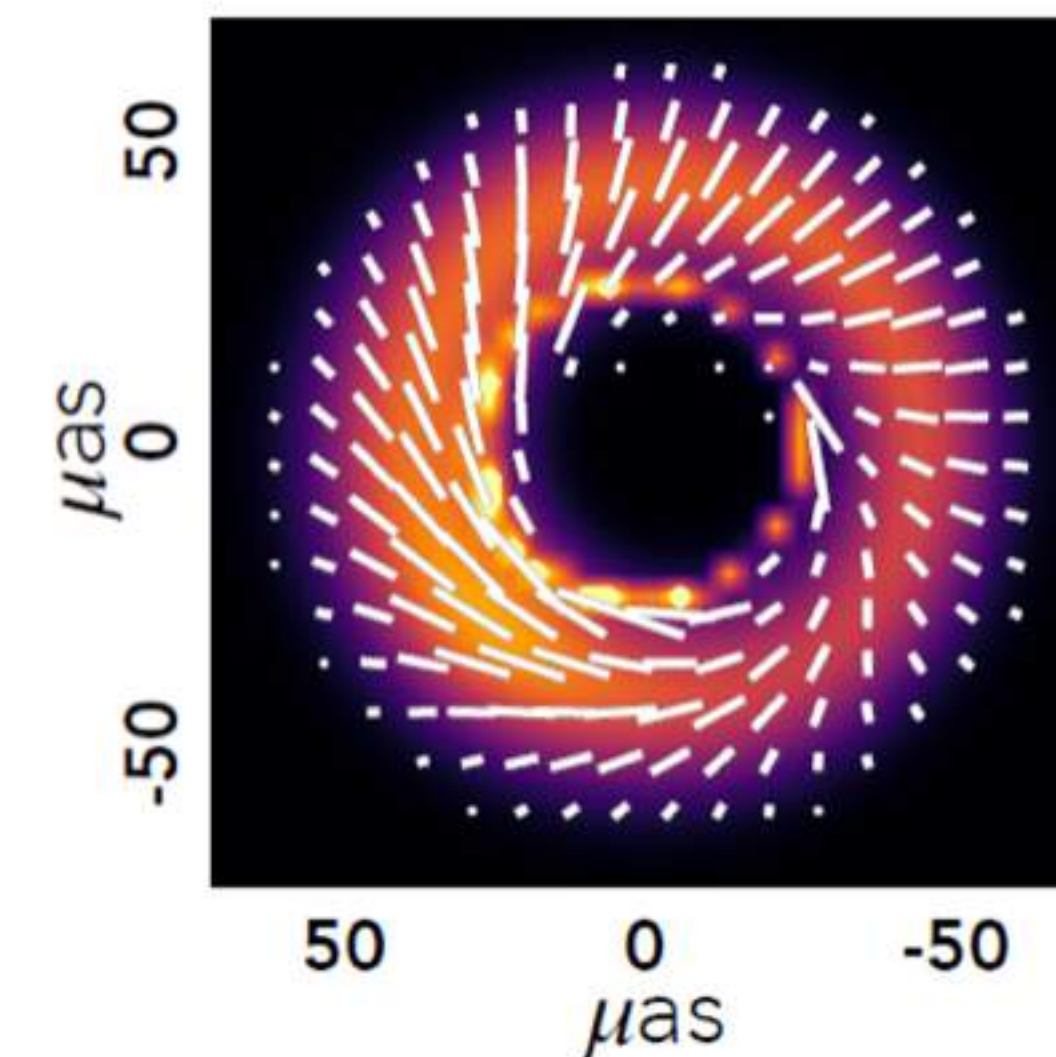
Toroidal field



Radial field



Vertical field



How to describe images? M87 polarimetric image metrics



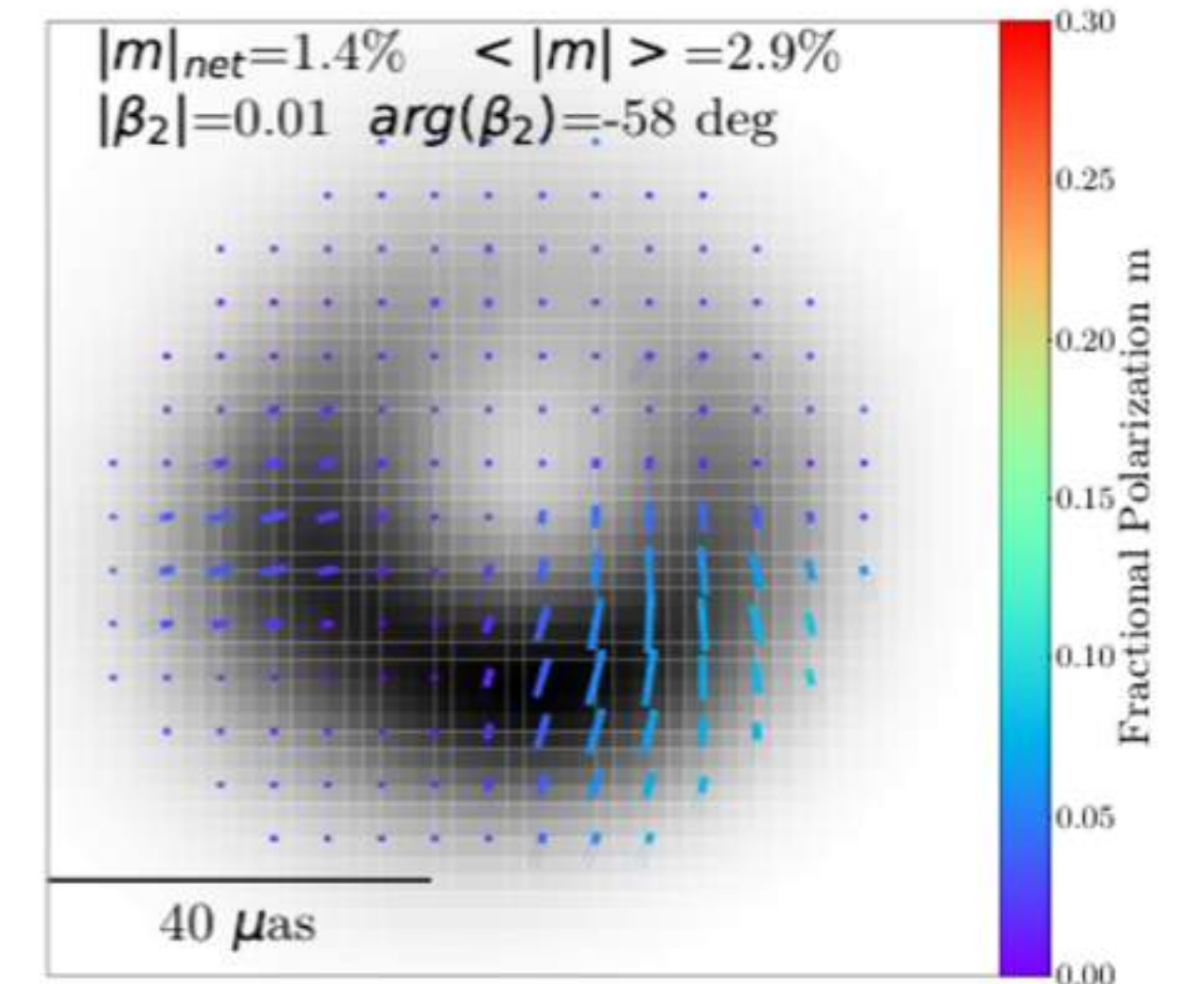
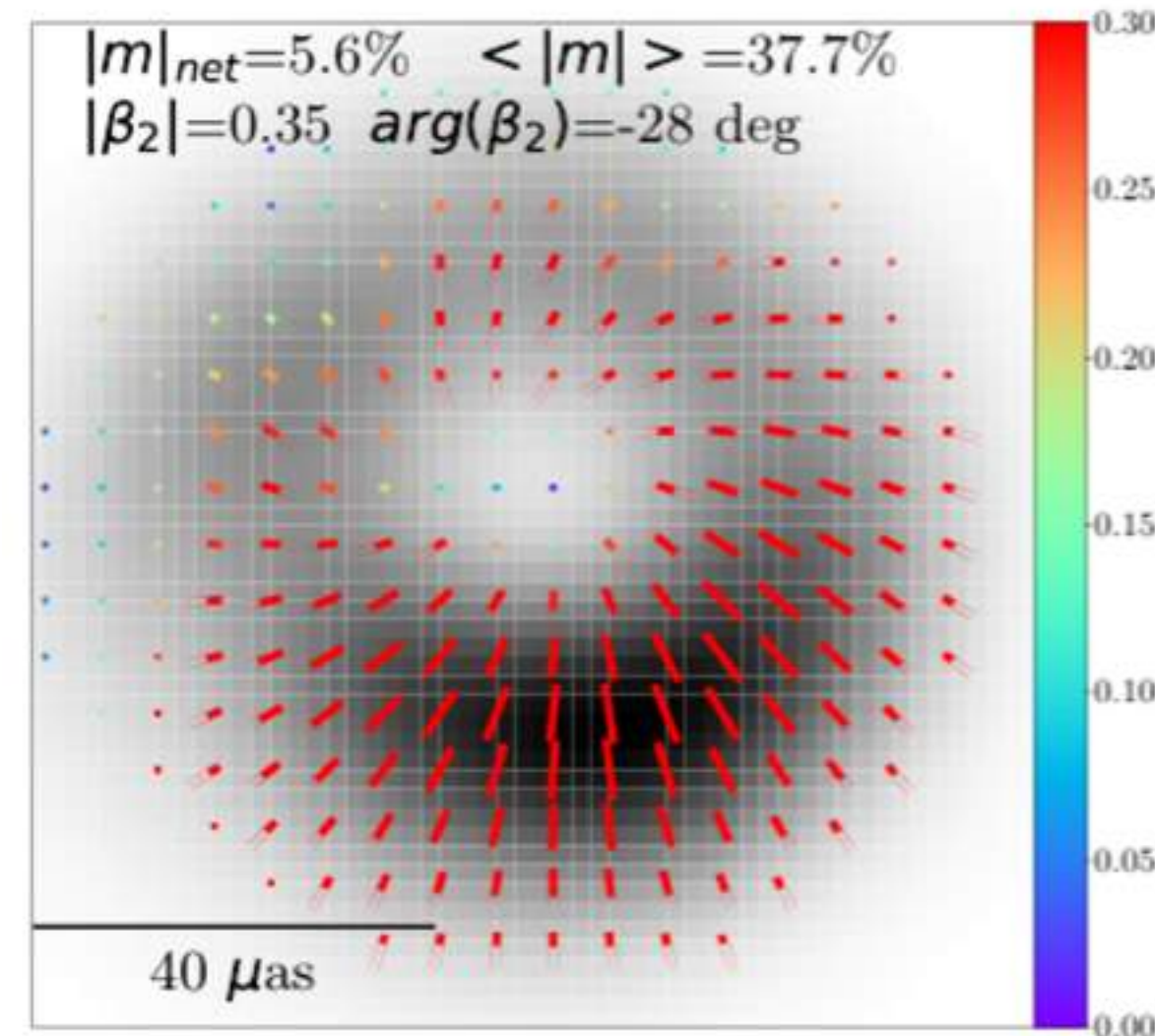
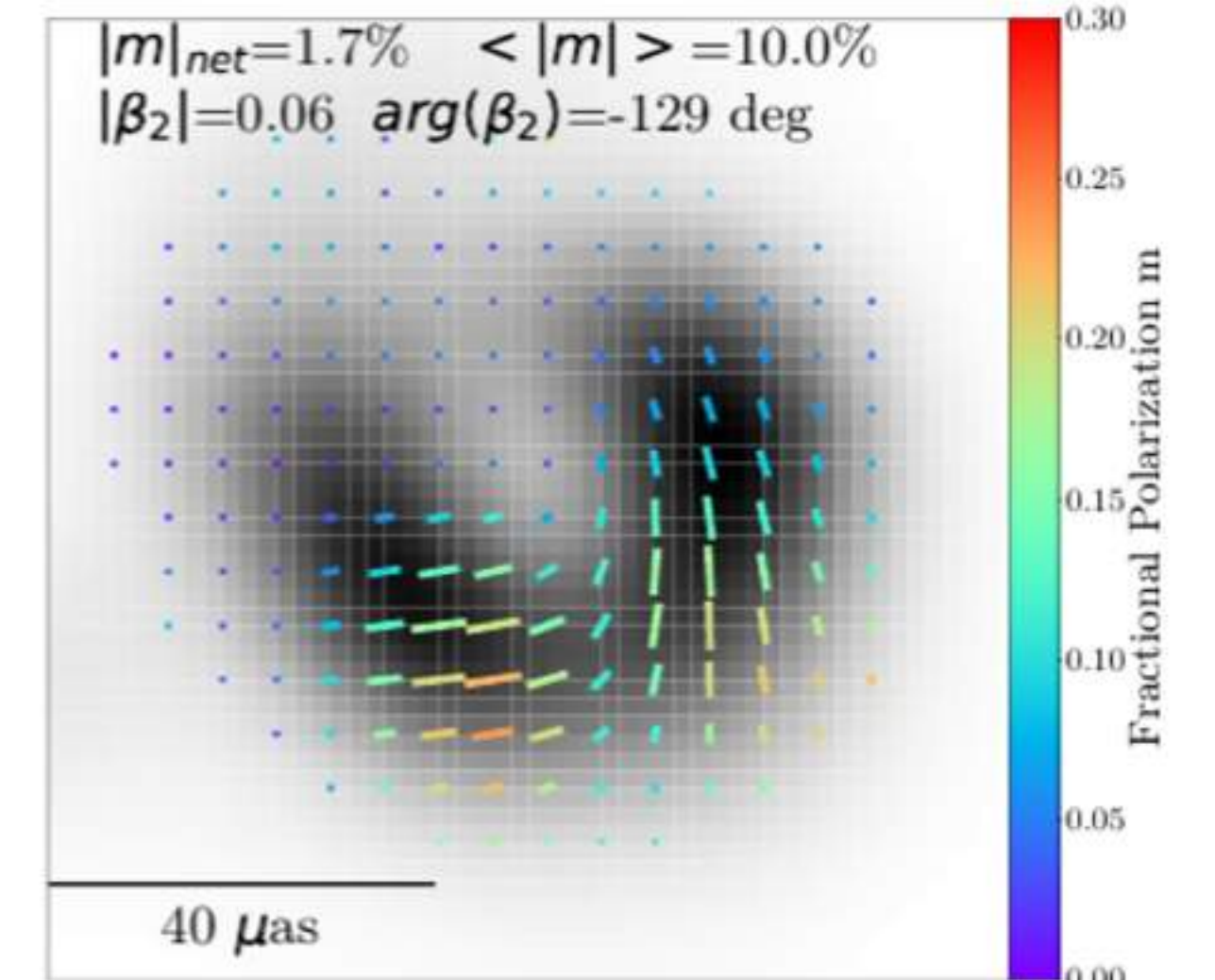
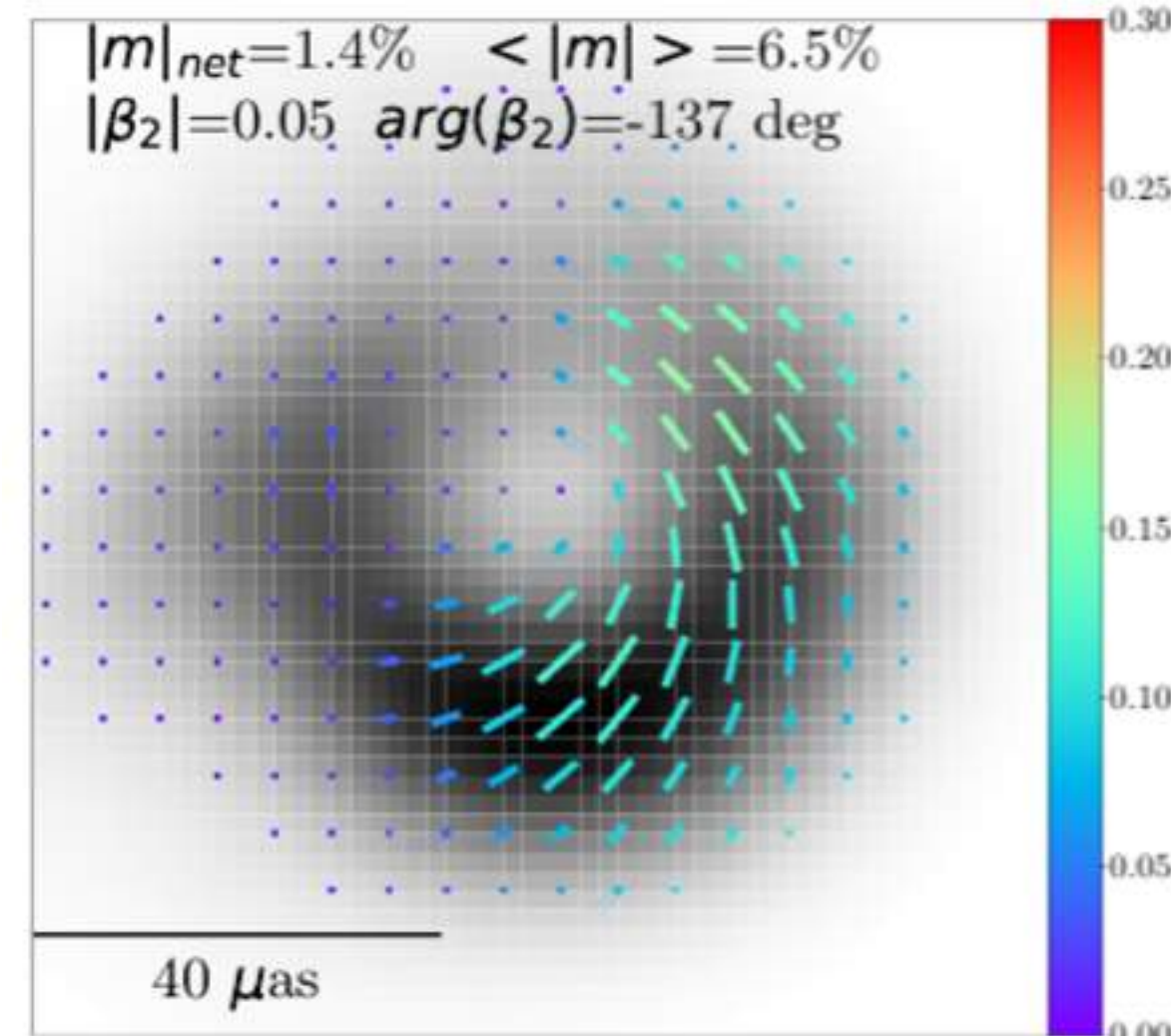
$$|m|_{\text{net}} = \frac{\sqrt{(\sum_i Q_i)^2 + (\sum_i U_i)^2}}{\sum_i I_i}$$

$$\langle |m| \rangle = \frac{\sum_i \sqrt{Q_i^2 + U_i^2}}{\sum_i I_i}$$

$$\beta_2 = \frac{1}{I_{\text{ring}}} \int_{\rho_{\text{min}}}^{\rho_{\text{max}}} \int_0^{2\pi} P(\rho, \varphi) e^{-2i\varphi} \rho d\varphi d\rho$$

Palumbo et al. (2020)

Examples of metric using GRMHD
simulated images of black holes
EHTC 2021, see Paper VIII



How to describe images?

M87 Polarimetric image metrics

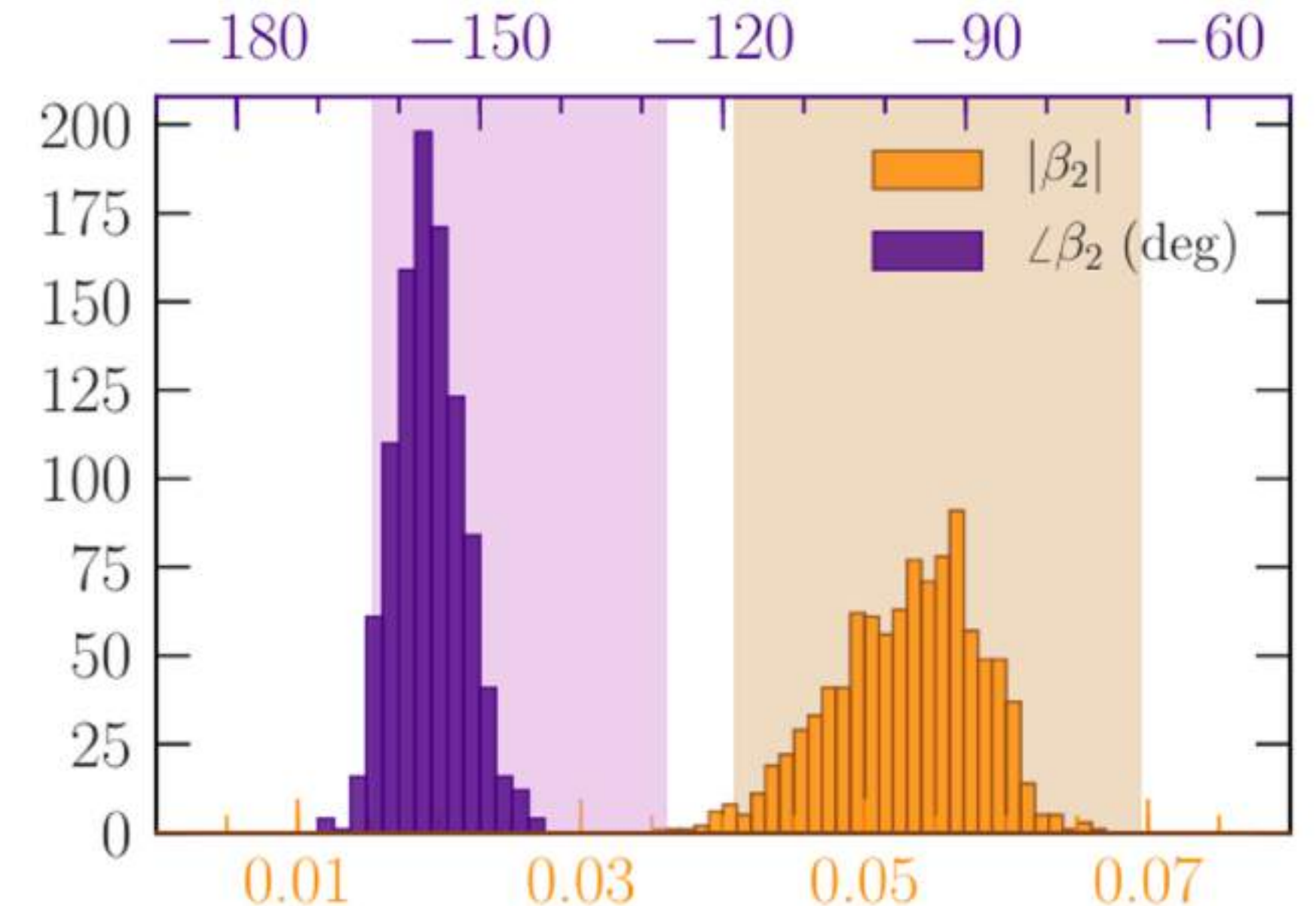
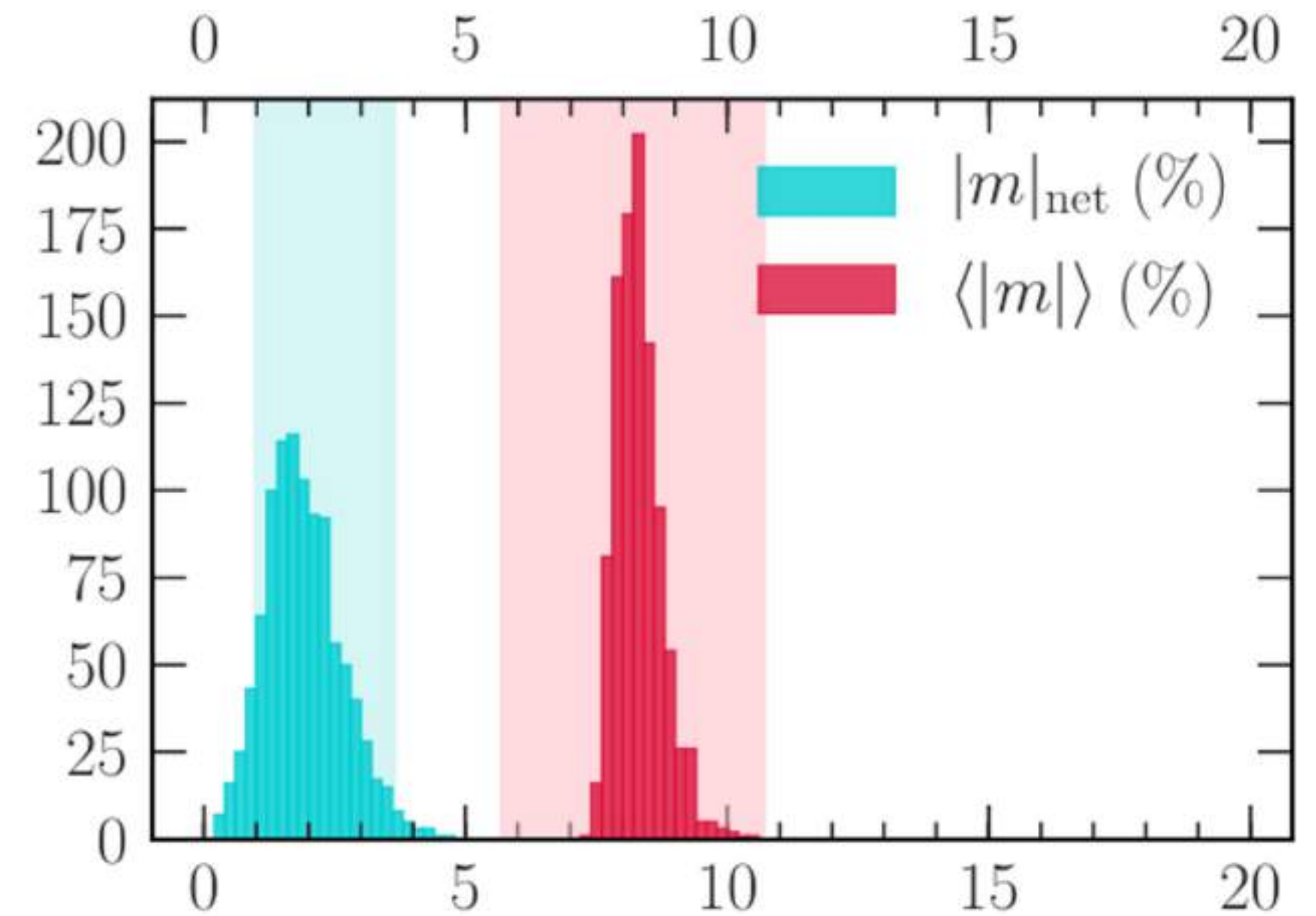
$$|m|_{\text{net}} = \frac{\sqrt{(\sum_i Q_i)^2 + (\sum_i U_i)^2}}{\sum_i I_i}$$

$$\langle |m| \rangle = \frac{\sum_i \sqrt{Q_i^2 + U_i^2}}{\sum_i I_i}$$

$$\beta_2 = \frac{1}{I_{\text{ring}}} \int_{\rho_{\text{min}}}^{\rho_{\text{max}}} \int_0^{2\pi} P(\rho, \varphi) e^{-2i\varphi} \rho d\varphi d\rho$$

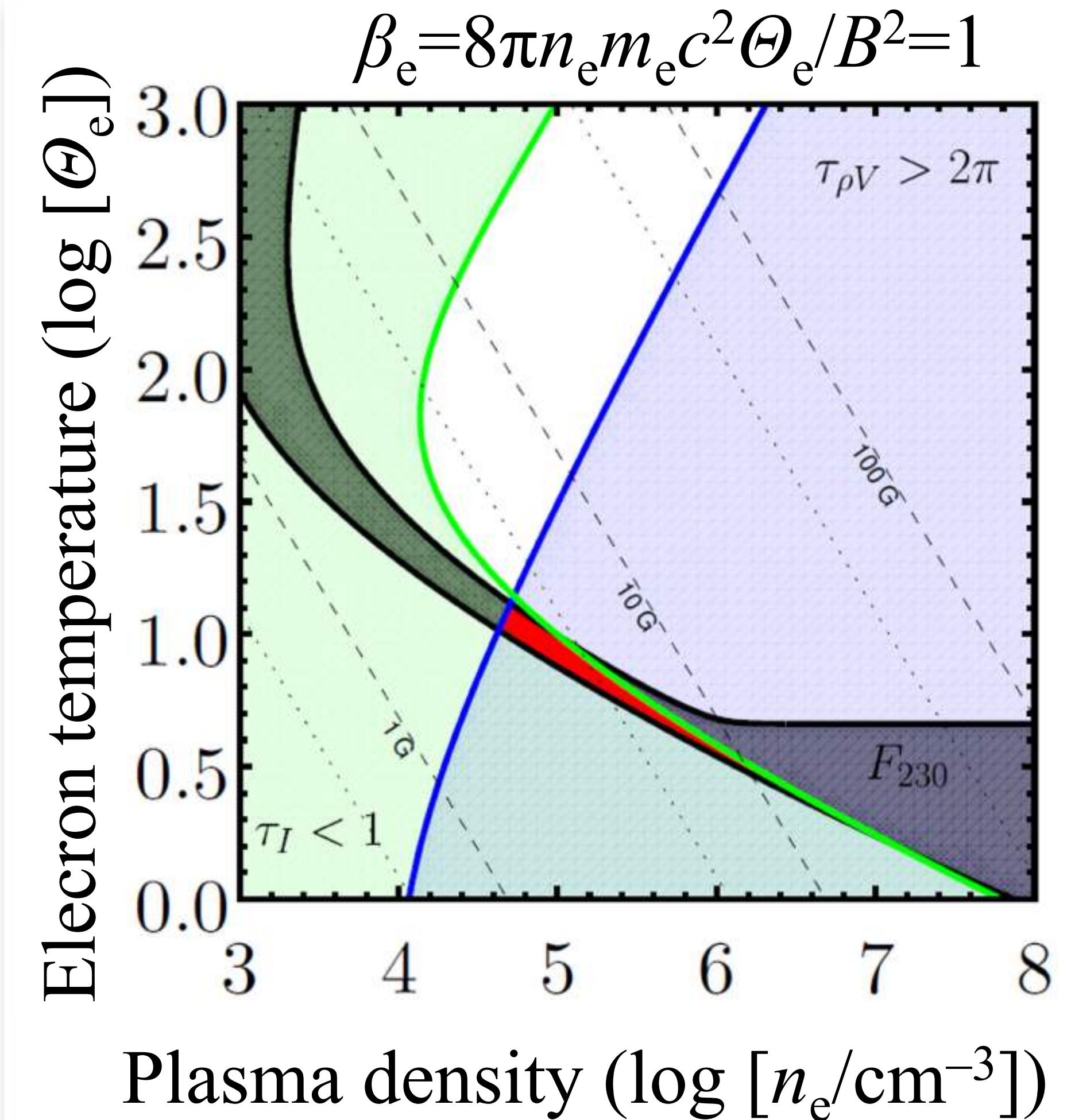
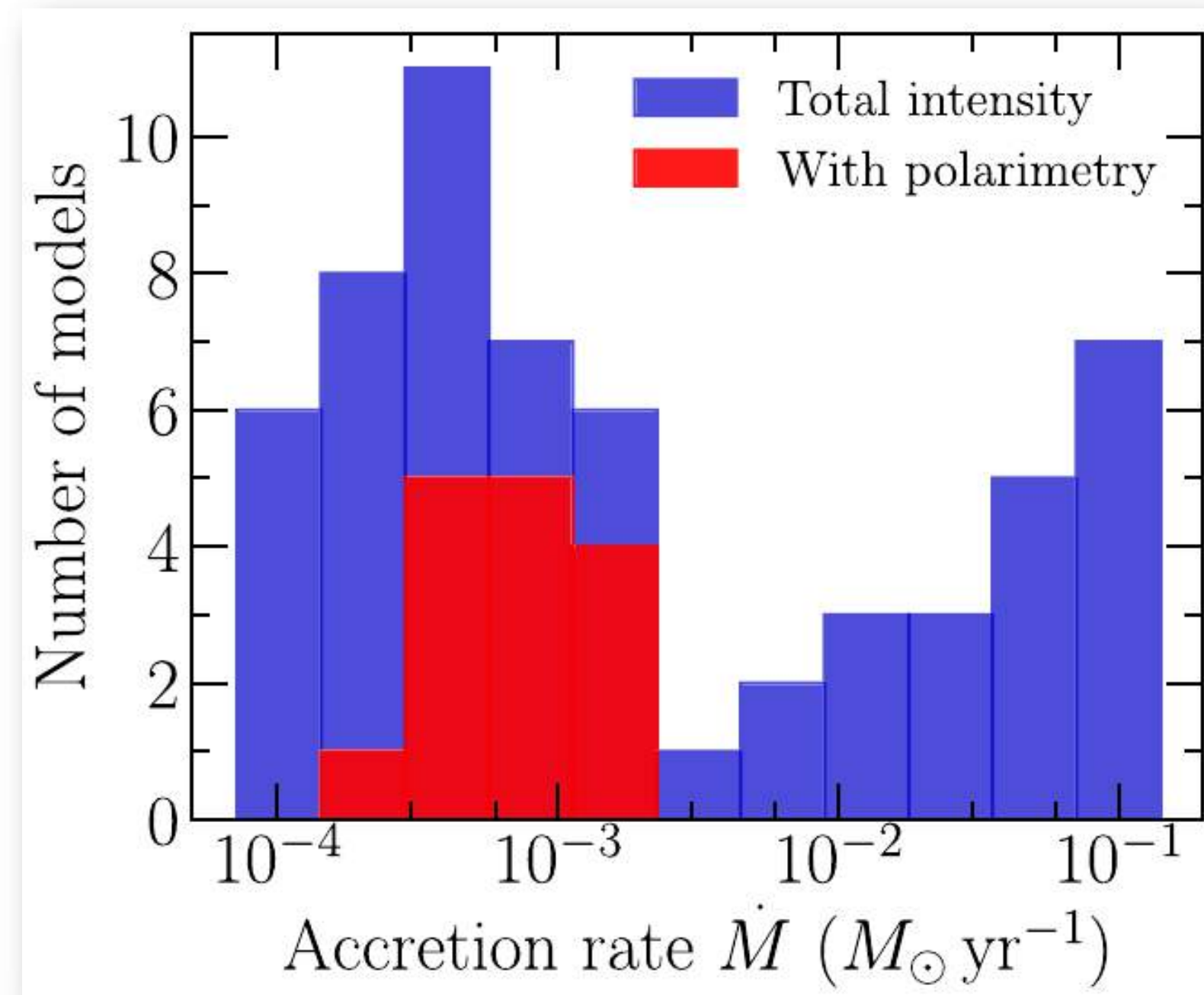
Palumbo et al. (2020)

Example distribution of metrics based on 1000 M87 April 11 images on with different D-term calibration

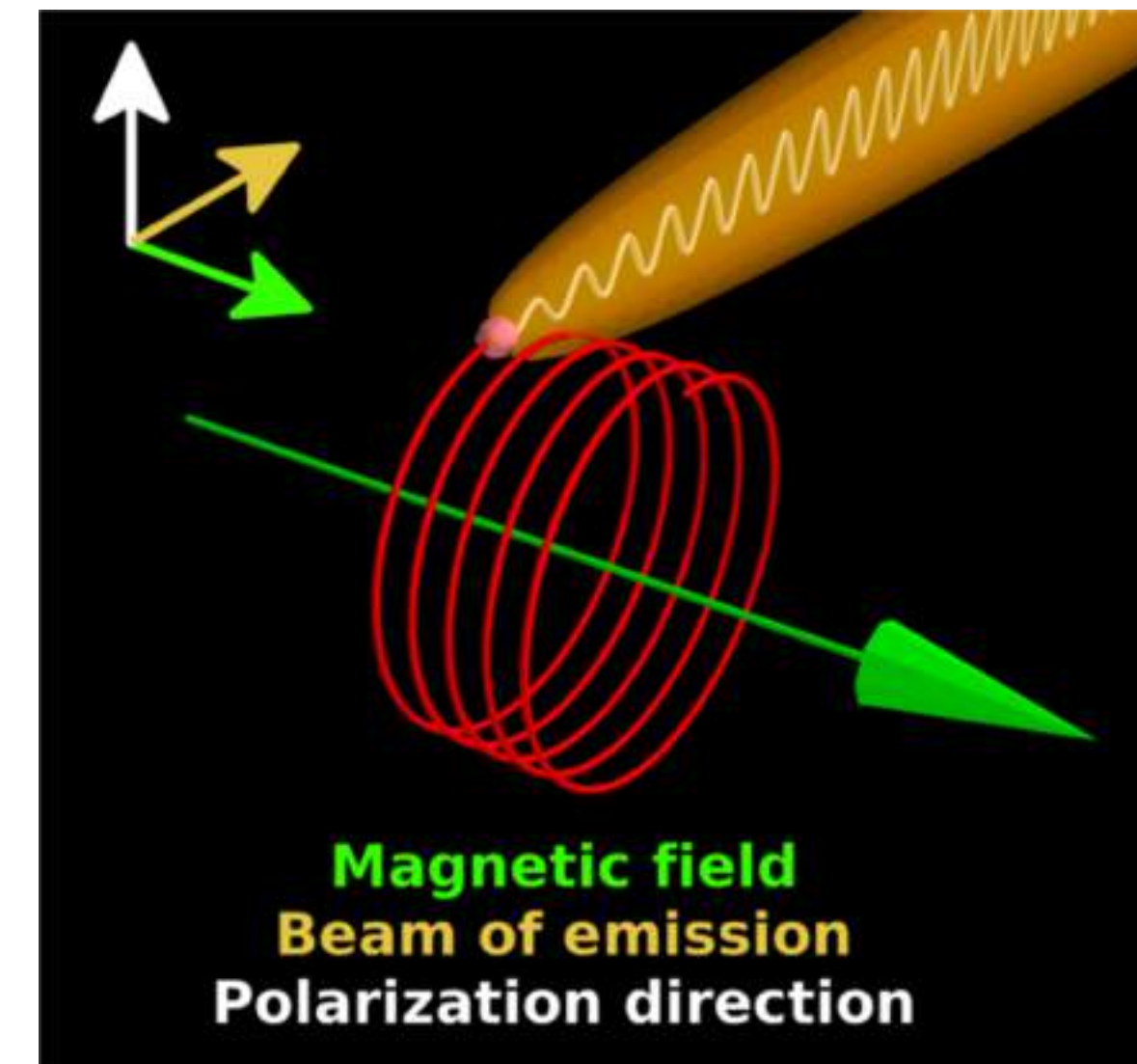
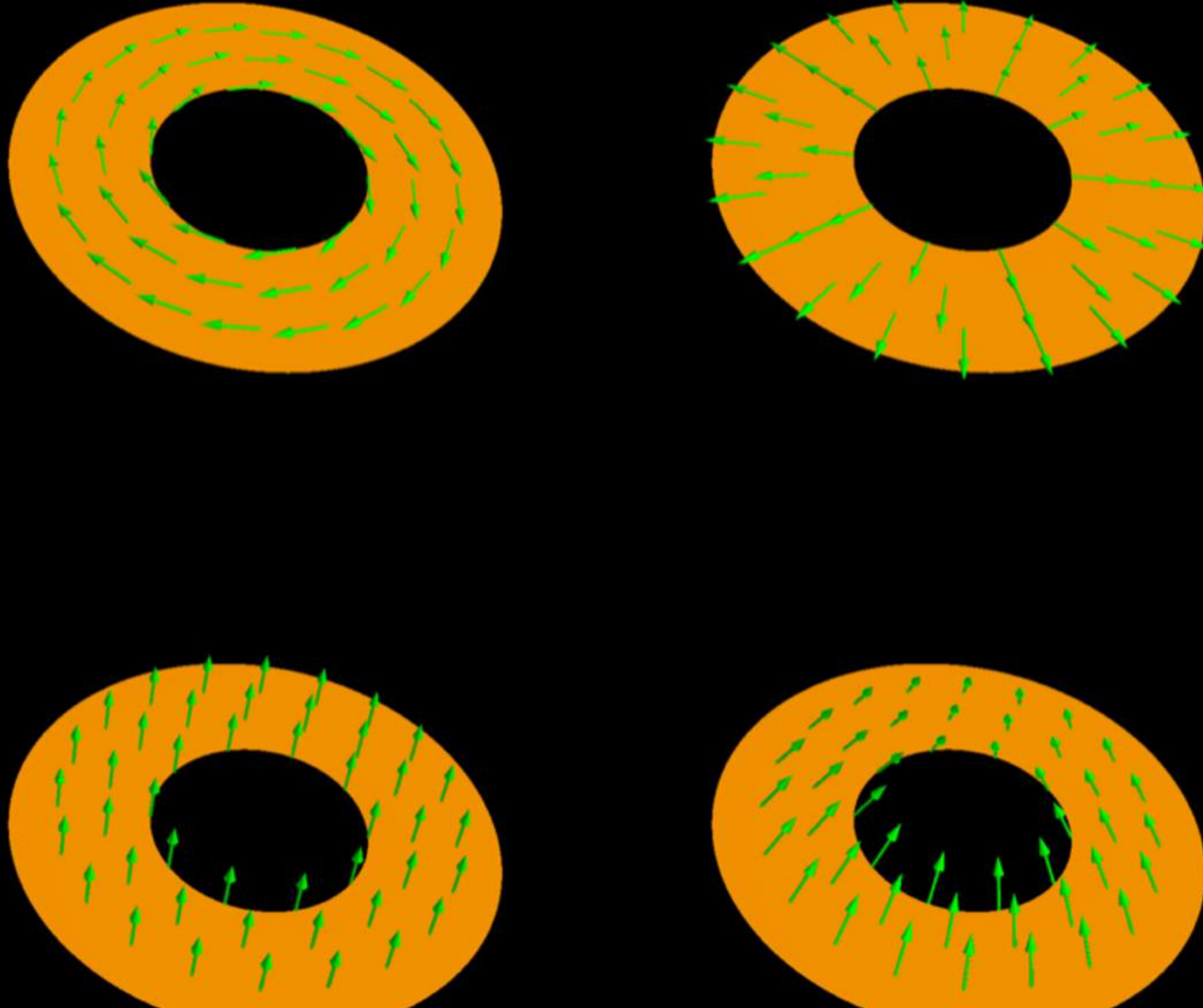


All SANE models are discarded. M87* seems to be MAD!
 Schwarzschild metric ($a = 0$) is discarded. M87* obeys the Kerr metric.

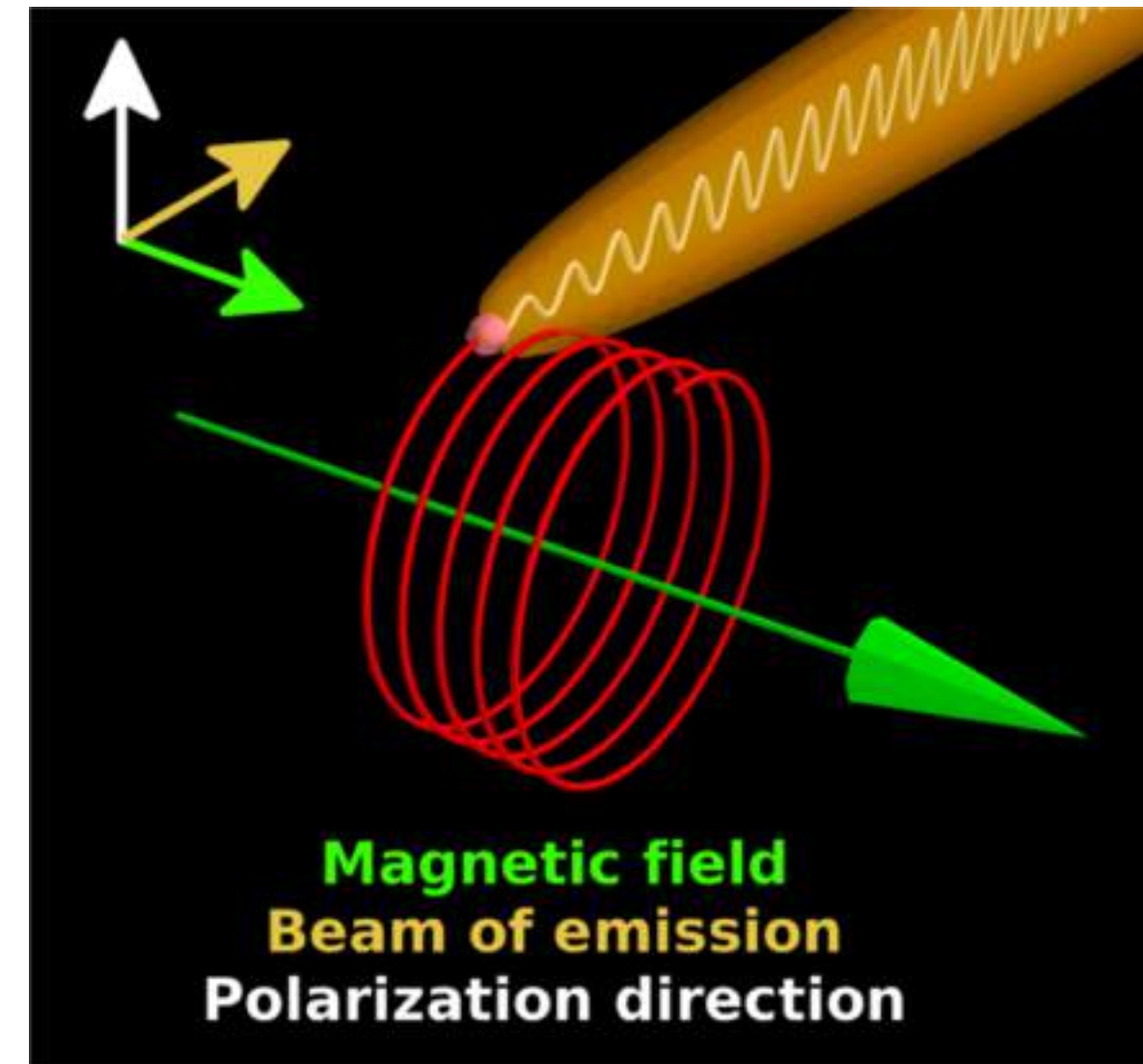
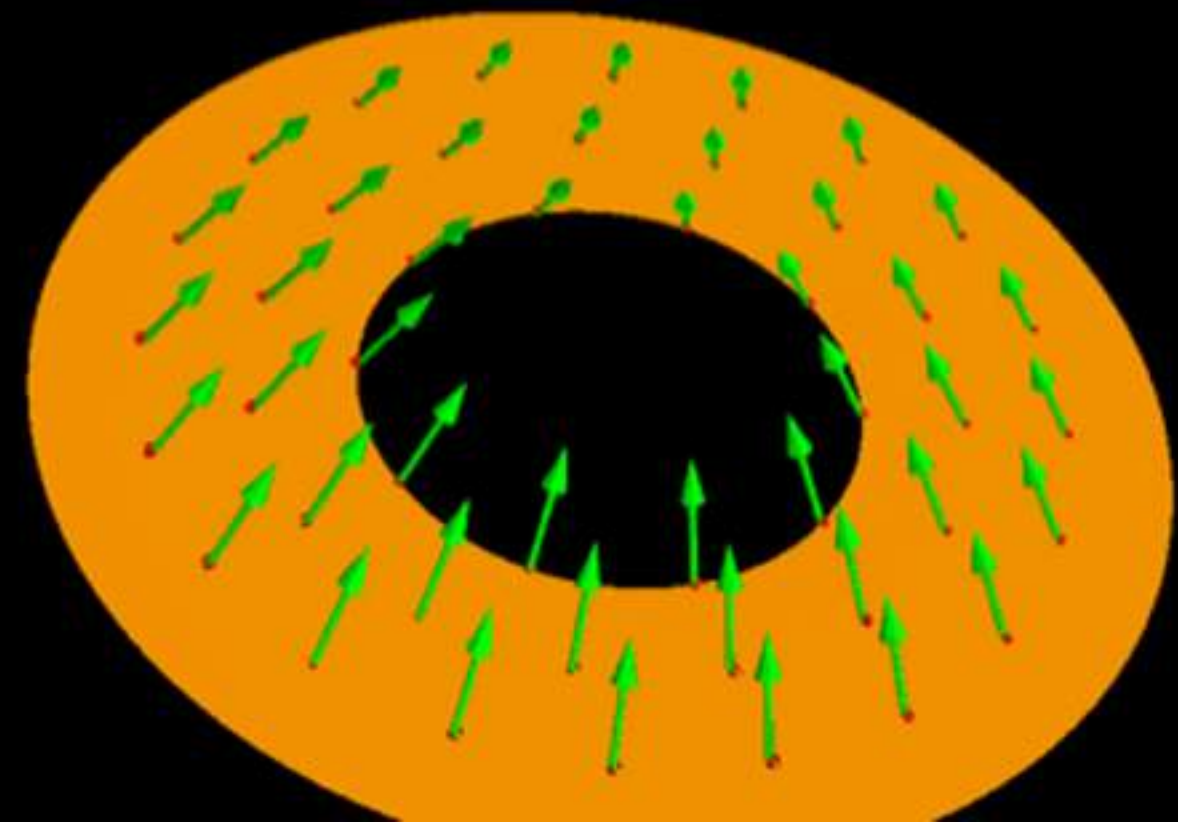
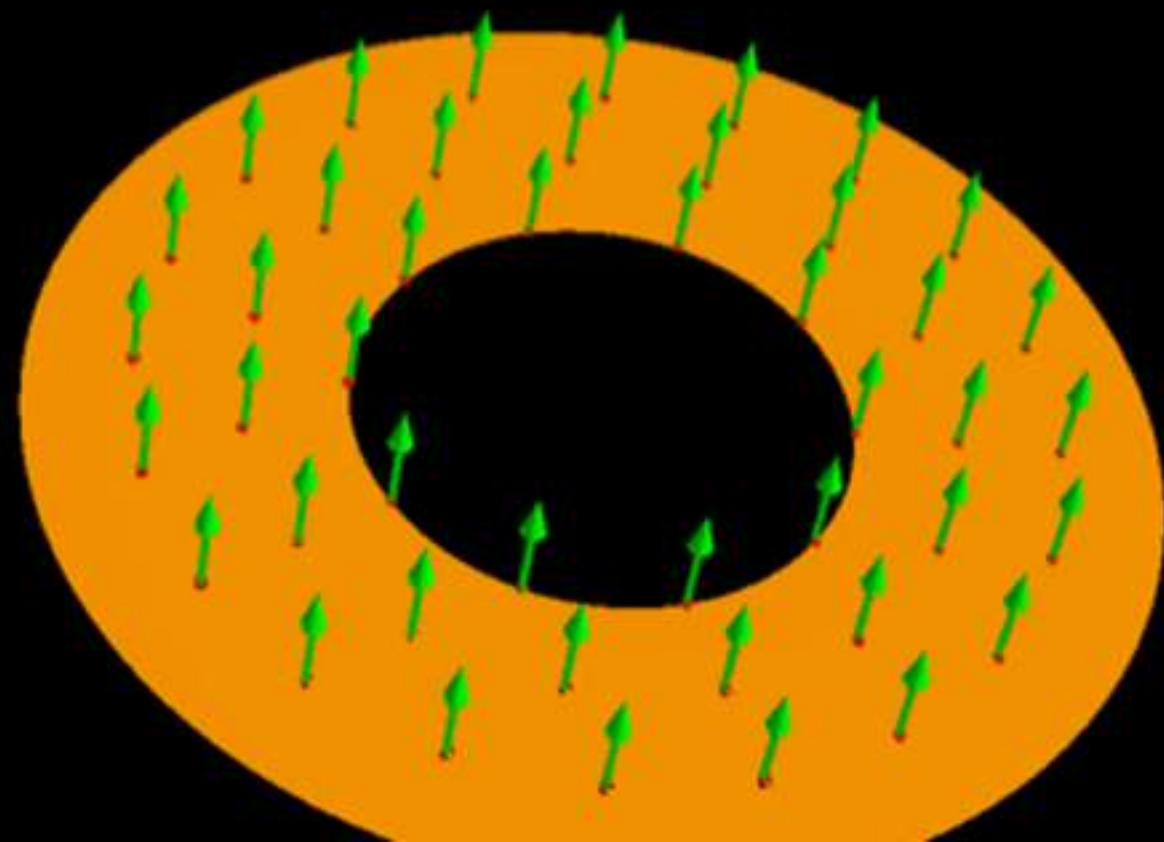
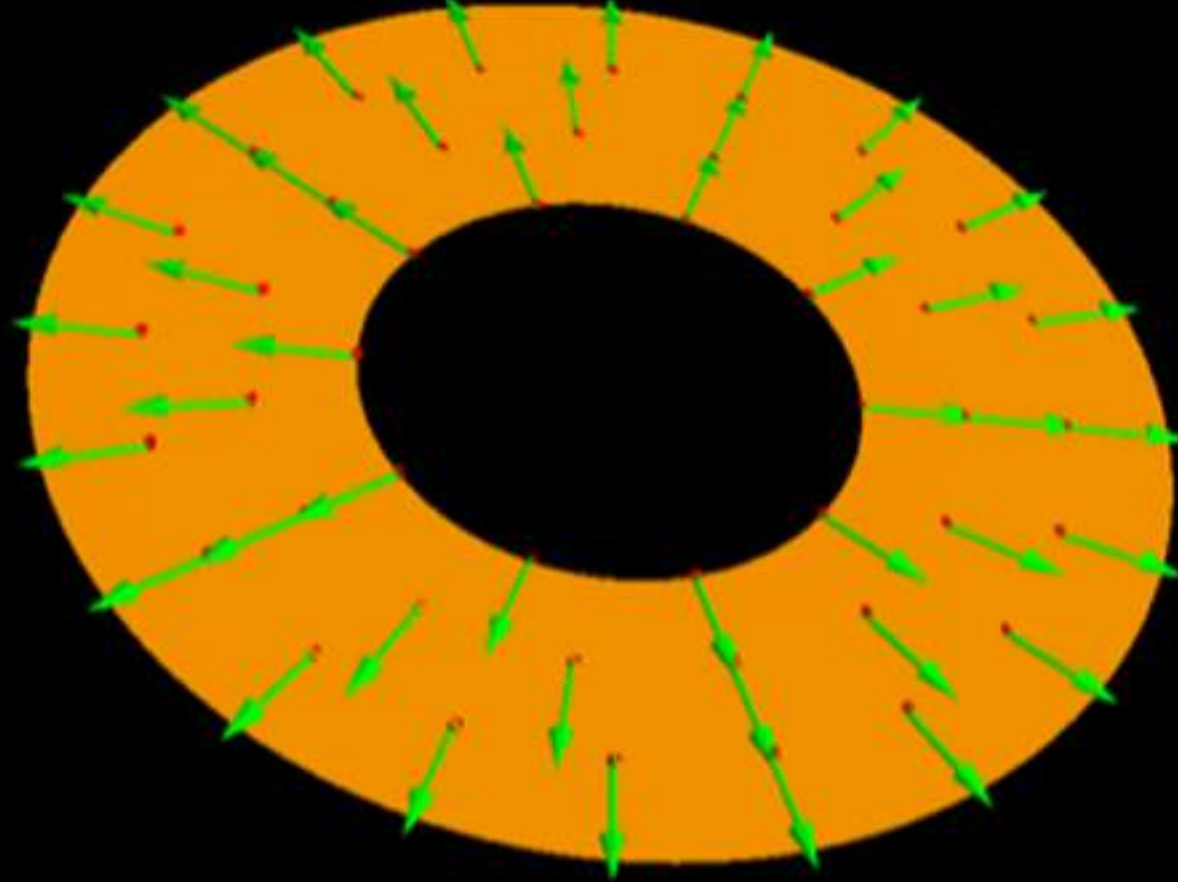
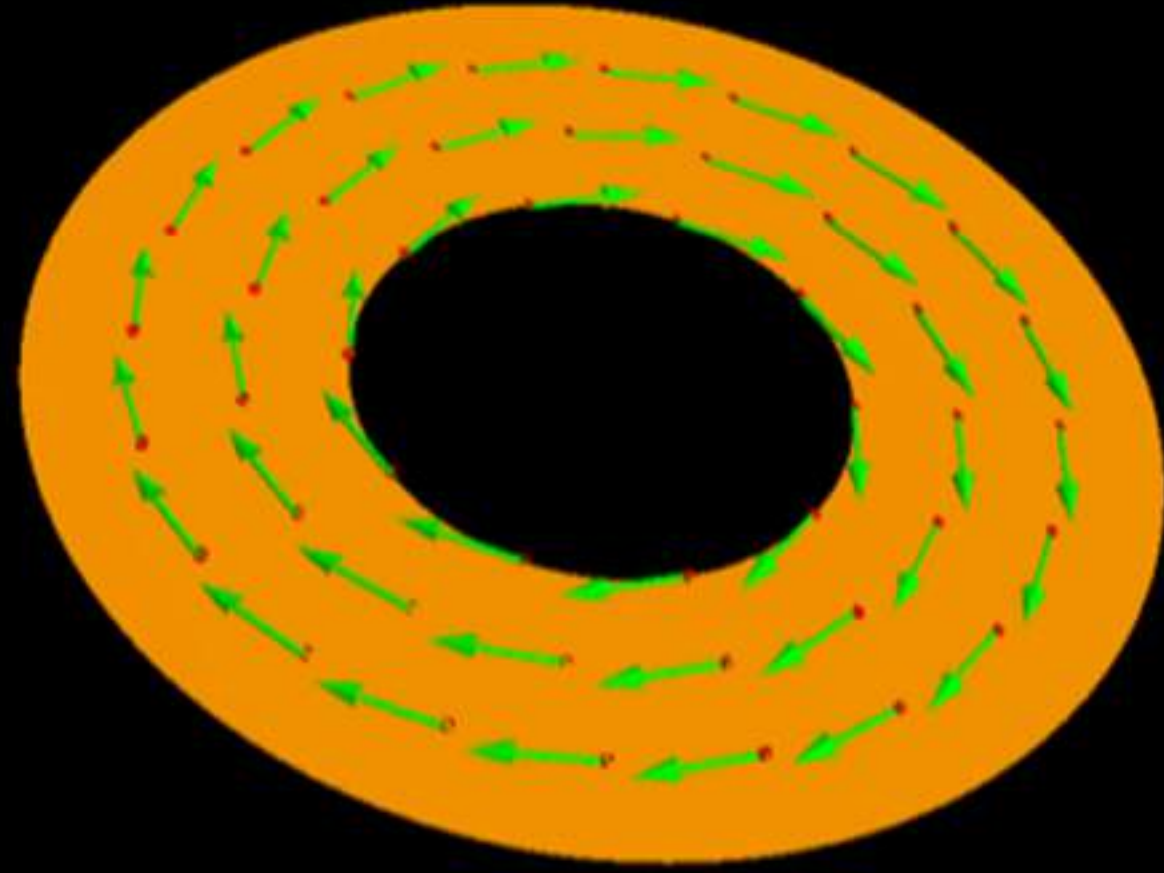
- Polarized non-thermal emission dominates the southern part of the ring.
- Magnetic field with a strong poloidal component.
- Important hints to the Blandford-Znajek mechanism.
- Accretion rate:
 $\dot{M} \sim (3 - 20) \times 10^{-4} M_{\odot} \text{yr}^{-1}$
 $(\sim 10^{-5} \dot{M}_{\text{Edd}})$
- Magnetic field:
 $|B| \sim (7 - 30) \text{ G}$.
- Plasma density:
 $n \sim 10^{4-5} \text{ cm}^{-3}$.



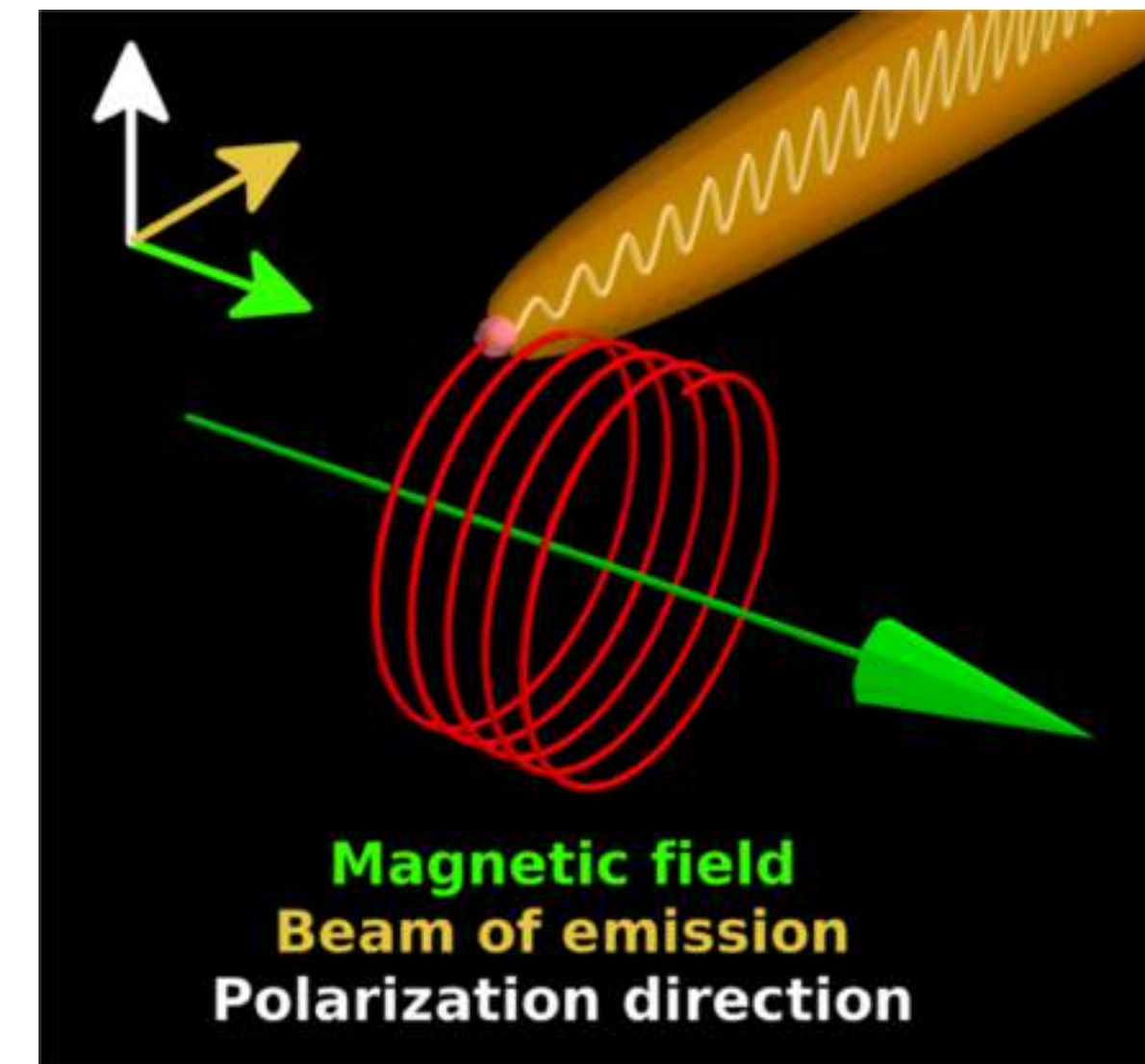
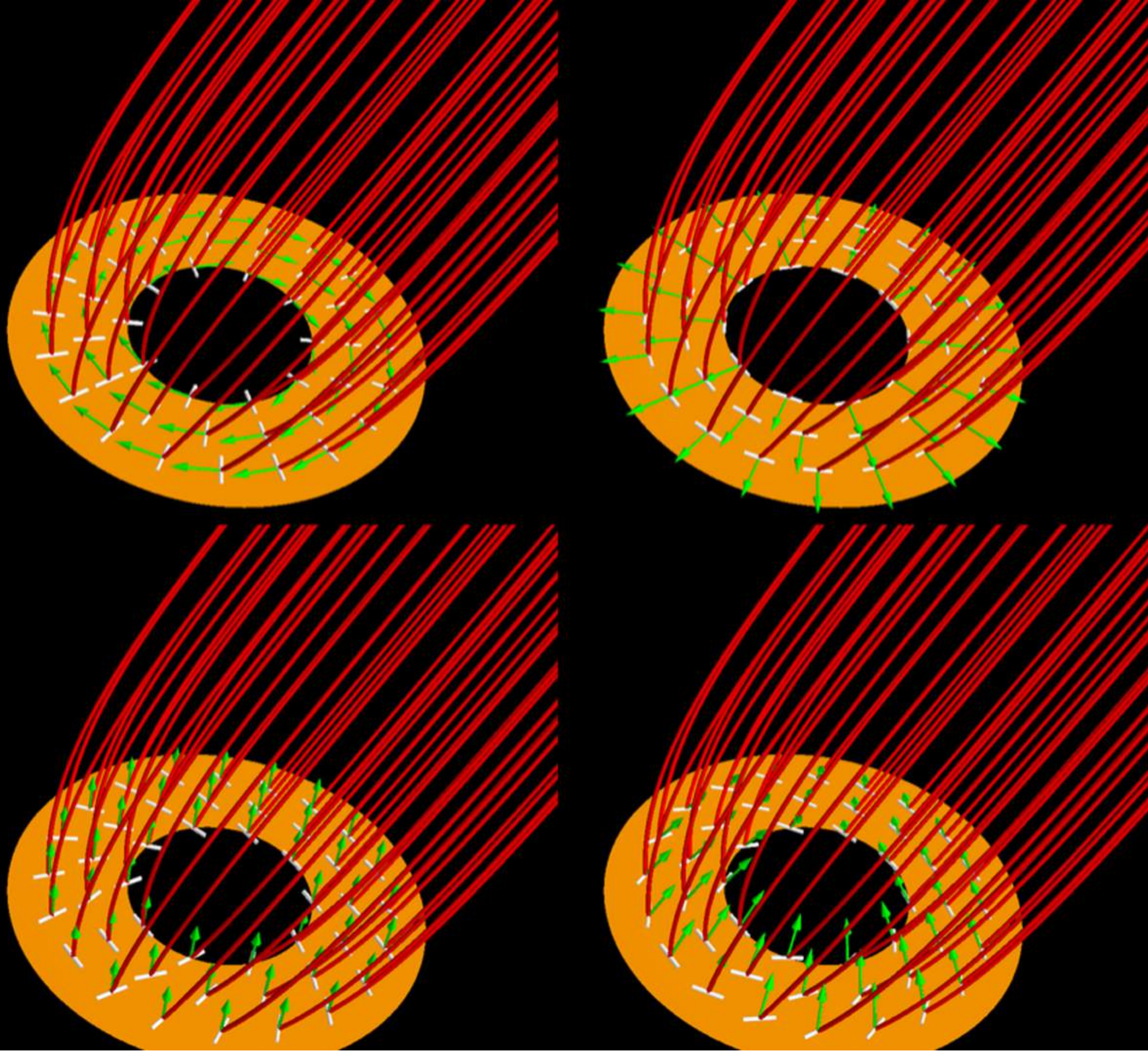
Magnetic field structure: Toy Models (with space curvature)



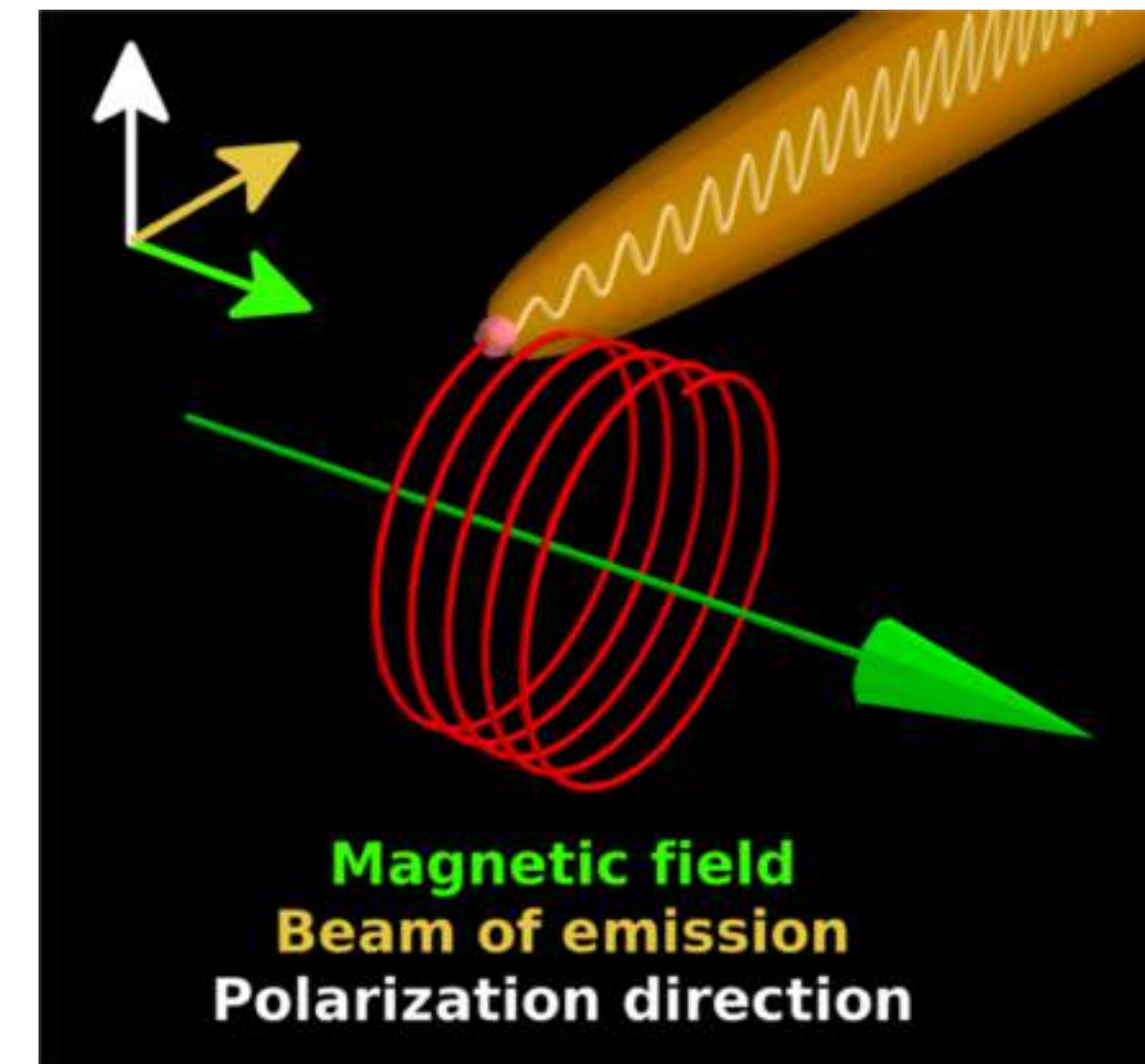
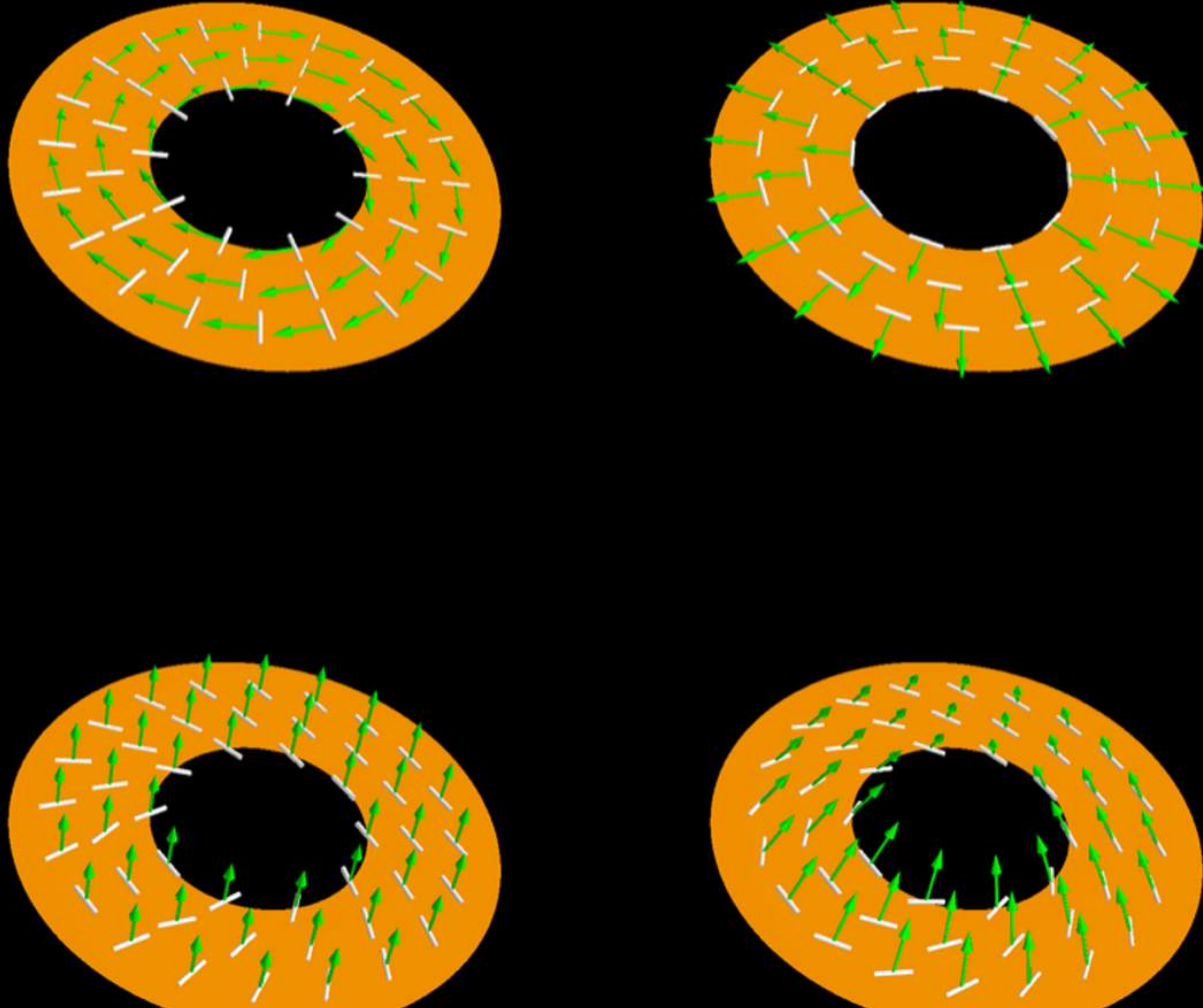
Magnetic field structure: Toy Models (with space curvature)



Magnetic field structure: Toy Models (with space curvature)



Magnetic field structure: Toy Models (with space curvature)



Technological and methodological progress

Recent boost in development of algorithms for data reduction

Example: software used in M87 polarization papers

- *Ehtim* (regularized maximum likelihood method) (Chael et al. ApJ 829 11 2016)
 - Sets Stokes $V=0$; iterative D-term fitting and polarimetric imaging
- LPCAL (AIPS + CLEAN) (Leppänen, Zensus & Diamond AJ 110, 2479 1995)
 - Classical pol-calibration routine; ignores second-order D-terms, not solving for Stokes V
- SMILI (only in total intensity) (Akiyama et al. ApJ 838, 1 2017; AJ 153, 159 2017)
- POLSOLVE (CASA) (Martí-Vidal, Mus, Janßen et al. A&A 646, A52 2021)
 - Uses CLEAN model, like LPCAL; solves for full Stokes, also includes second order D-term effects
- D-term Modeling Code (DMC) (Pesce AJ 161, 178 2021)
 - Successor of dynasty; full MCMC “imaging”, simultaneously solving for the D-terms; full Stokes solved, also RCP and LCP gains simultaneously fitted
- THEMIS (Broderick et al. ApJ 837, 139 2020)
 - Full MCMC “imaging”, similar to DMC
- rPICARD (Janssen A&A 626, A75 2019)
 - Pipeline data analysis in CASA

See also RESOLVE (Junklewitz et al. A&A 581, A15 2015) and DoG-HiT (Müller & Lobanov A&A 666, A137 19oct2022)

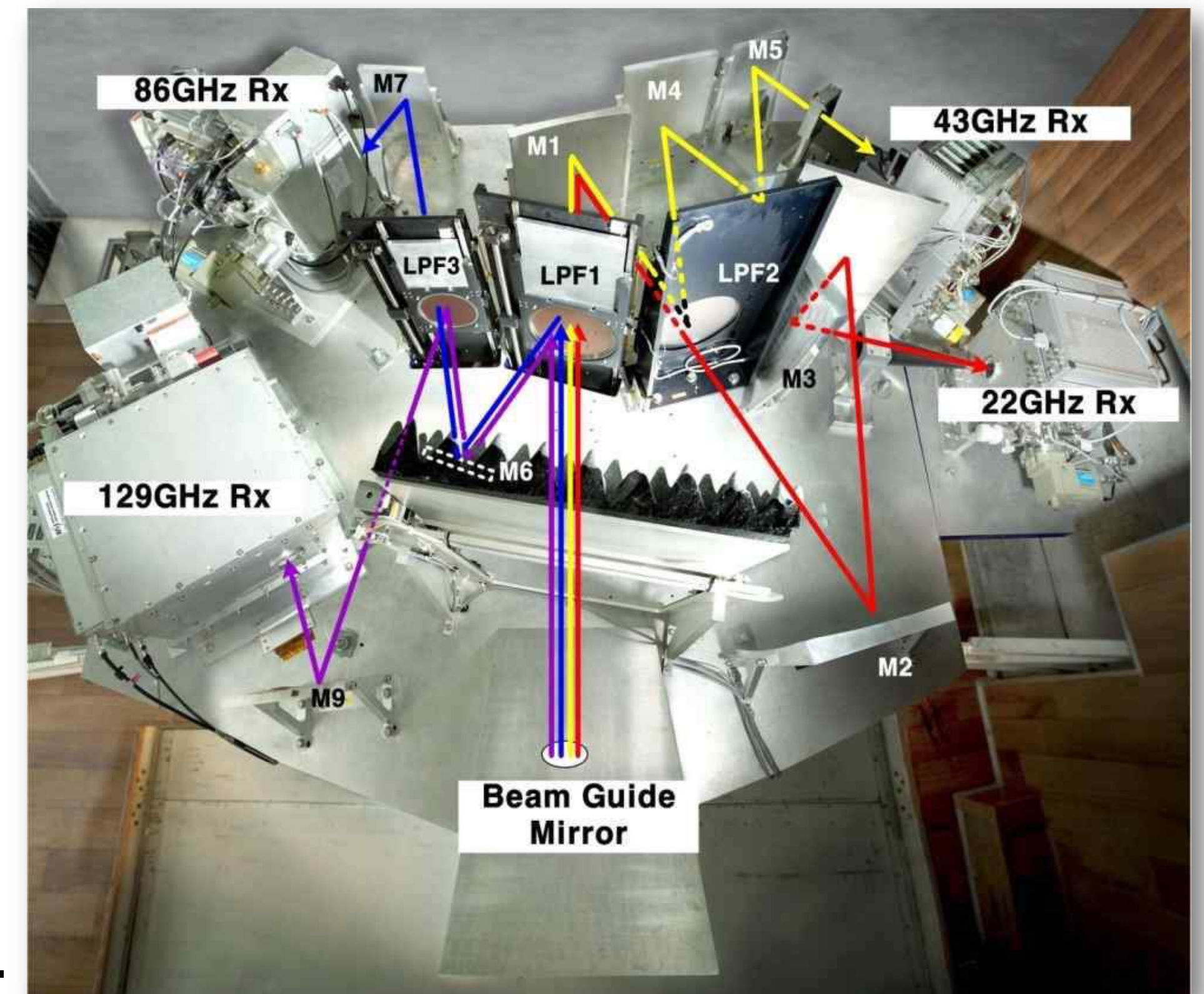
Technical development: multi-frequency receivers

BRAND (BRoad-bAND EVN)

- Prototype of continuous band 1.5-15.5 GHz under development, funded by RadioNet
- Deployable over the EVN array
- Collaboration MPIfR/INAF/ASTRON/INAF/OSO

KVN 4 or 3-freq suite box

- 22/43/86/130 GHz receiver implemented at the KVN

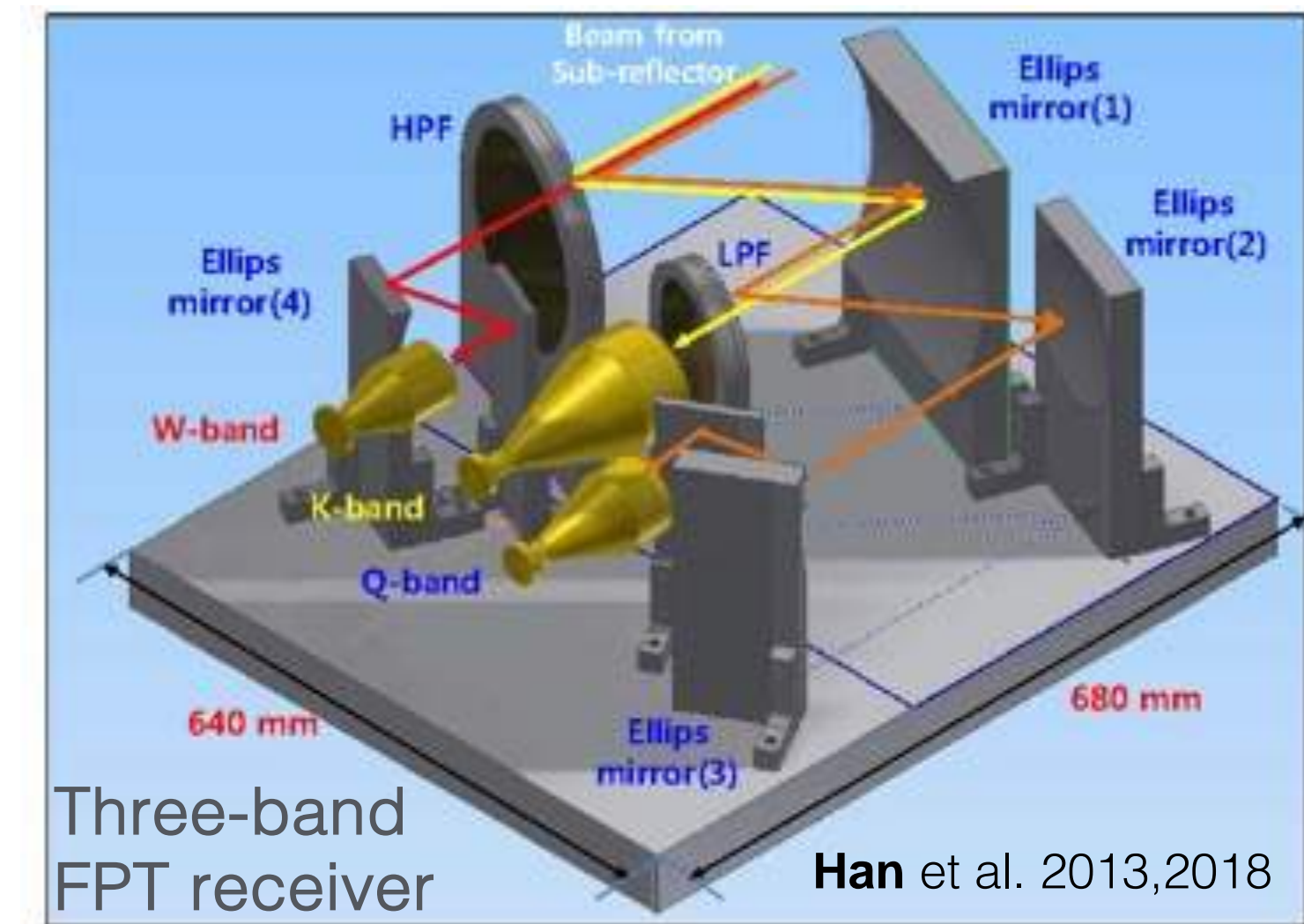


Han et al.

Next-generation mm-VLBI with FPT Receivers



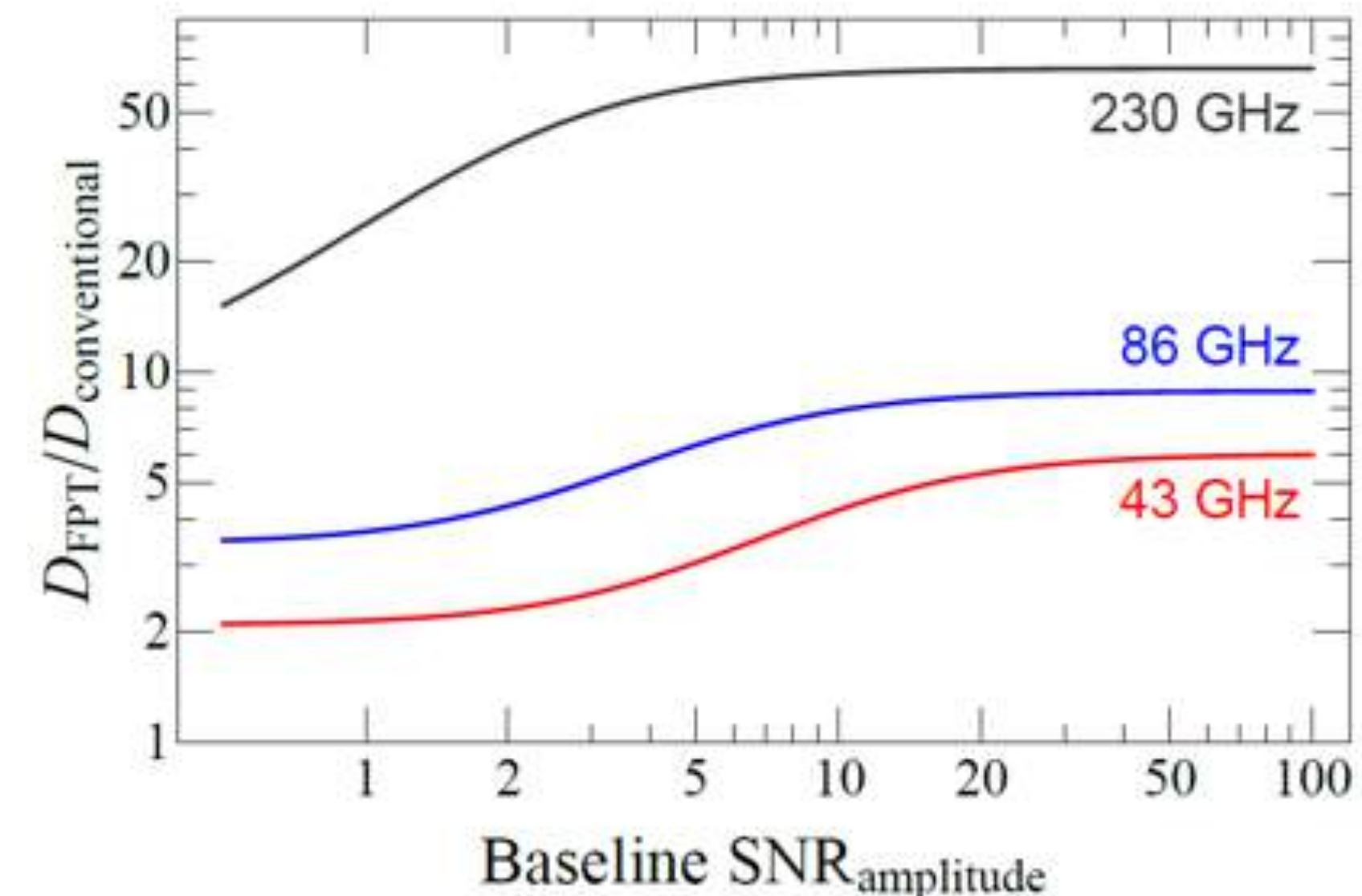
- Shared Optics Multifrequency Receivers for Frequency Phase Transfer (FPT)
 - FPT pioneered in house (Middelberg+2006), later implemented at KVN and now, gradually, also at a number of European telescopes;
 - Three-band (22/43/86 GHz) FPT receiver is **funded at Effelsberg**; to be used for astrometry measurements with KVN/Yebes/Europe for M2FINDERS and precision cosmology (10 μ as accuracy) with annual and secular parallaxes;
 - FPT @ GMVA: factor of 10+ improvement of dynamic range; matching the EHT in effective image resolution;
 - FPT @ 230 GHz: factor of 50+ boost for the EHT imaging dynamic range



Multi-frequency receivers for FPT

| Antenna | Receiver Band | | | | |
|-------------------|---------------|--------------|--------------|---------|---------|
| | 22 GHz | 43 GHz | 86 GHz | 130 GHz | 230 GHz |
| KVN: Yonsei | Yes | Yes | Yes | Yes | |
| KVN: Ulsan | Yes | Yes | Yes | Yes | |
| KVN: Tamna | Yes | Yes | Yes | Yes | |
| eKVN: Pyeongchang | planned | planned | planned | planned | planned |
| Yebes | Yes | Yes | construction | | |
| Noto | installation | installation | installation | | |
| SRT | installation | installation | installation | | |
| Medicina | planned | planned | planned | | |
| Onsala | planned | planned | planned | | |
| Metsahovi | proposed | proposed | proposed | | |
| Effelsberg | funded | funded | funded | | |

Dynamic range improvement with FPT



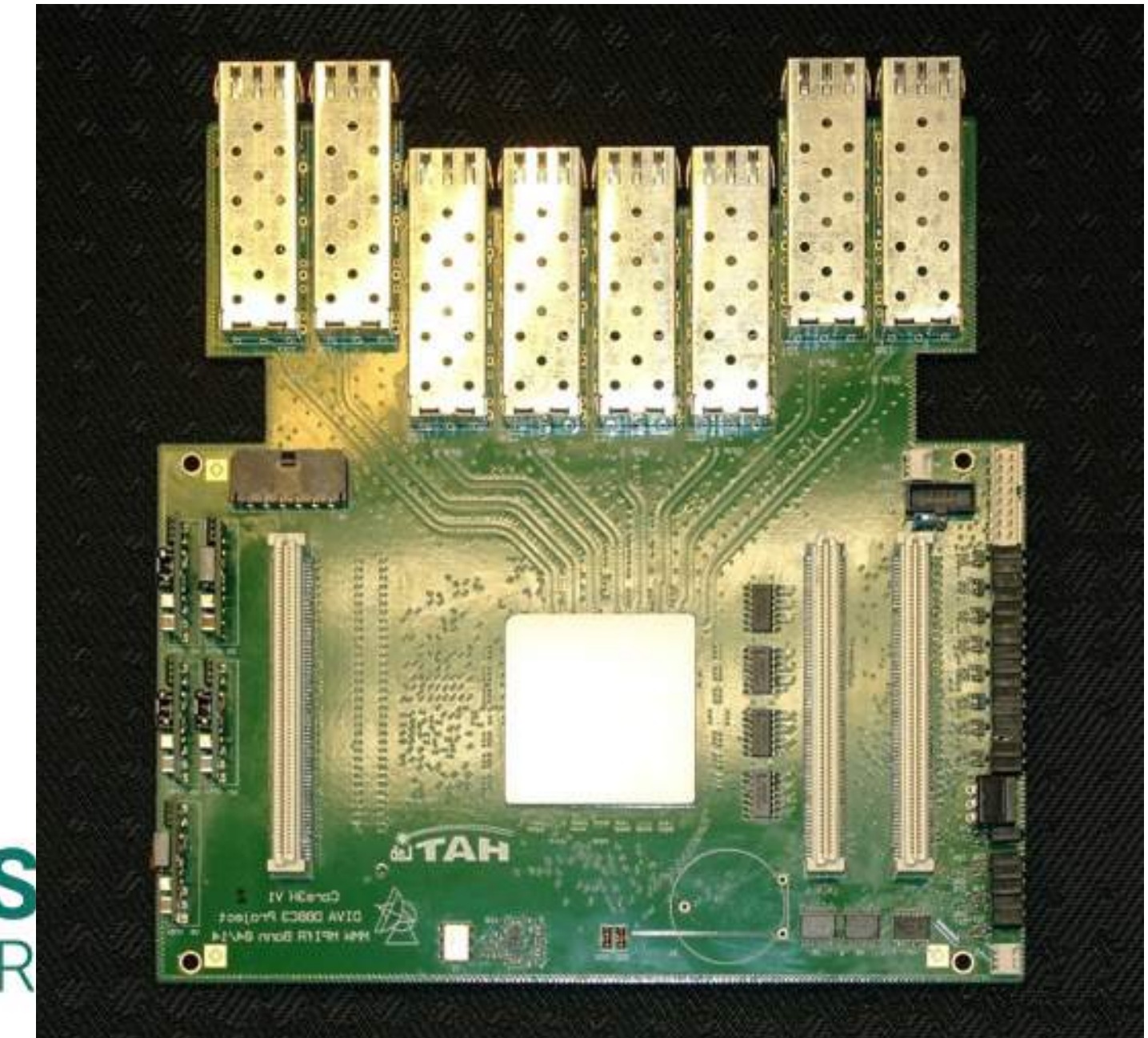
VLBI Technology Developments

- DiFX correlator (GMVA, EHT, RadioAstron, Geodesy)
 - 68 Nodes with 20 cores each = 1360 cores
 - 56 Gbps Infininband interconnect
 - RAID storage = 1.3 PB
 - Rmax: 40 TFlops
 - Data playback units: 15x Mark5, 9x Mark6
- Digital backend
 - DBBC3 (w 128 Gbps)
 - Support for mm-VLBI obs
 - APEX, IRAM, ALMA
 - ALMA phasing project

VLBI correlator cluster



DBBC3



DBBC3 CORE3H processing board

The M2FINDERS project

Multifrequency VLBI – magnetic fields around black holes



- Polarisation VLBI progress
 - Imaging P^1 and Faraday RM^2 to derive 3D structure of B
 - Turnover frequency mapping to determine the B strength³
 - Using core shift to derive the magnetic field strength and its evolution along the jet⁴
 - Improvements in calibration at mm-wavelengths⁵
- Turnover frequency imaging and core-shift boosted by the source-frequency phase referencing technique⁶ implemented at multi-band receiver systems⁷
- New methods for imaging are underway⁸
- Combination of numerical⁹ and analytical¹⁰ methods to study relativistic plasma jets and their B ¹¹

1: Leppänen et al. 1995, Ros et al. 2000, Gómez et al. 2016; 2: Gabuzda et al. 2015, 2017; 3: Lobanov 1998a, Sokolovsky et al. 2011; 4: Lobanov 1998b, Plavin et al. 2019; 5: Martí-Vidal 2015b, EHTC 2021, 6: Rioja et al. 2015, Jung et al. 2015, Park et al. 2015, Zhao et al. 2019; 7: KVN: Han et al. 2017); 8: (Mertens & Lobanov 2015, 2016, Mertens et al. 2016; 9: e.g., Perucho et al. 2006, 2012, Fromm et al. 2016, 2019, Porth et al. 2017, MacDonald & Marscher 2018; 10: (e.g., Zensus et al. 1995, Lobanov & Zensus 1999, 2001; 11: e.g., Hirovani 2005, Kovalev et al. 2008, O'Sullivan & Gabuzda 2009, Sokolovsky et al. 2011, Pushkarev et al. 2012, Fromm et al. 2013, Zamaninasab et al. 2014, Plavin et al. 2019

M2finders Advanced Grant

Mapping Magnetic Fields with INterferometry Down to Event hoRizon Scales

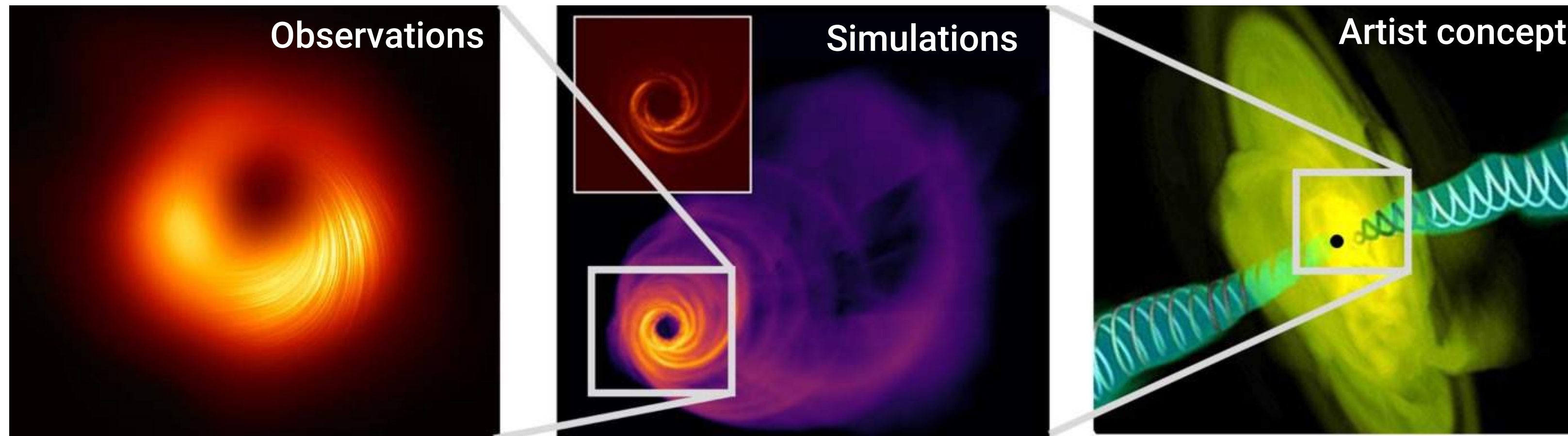
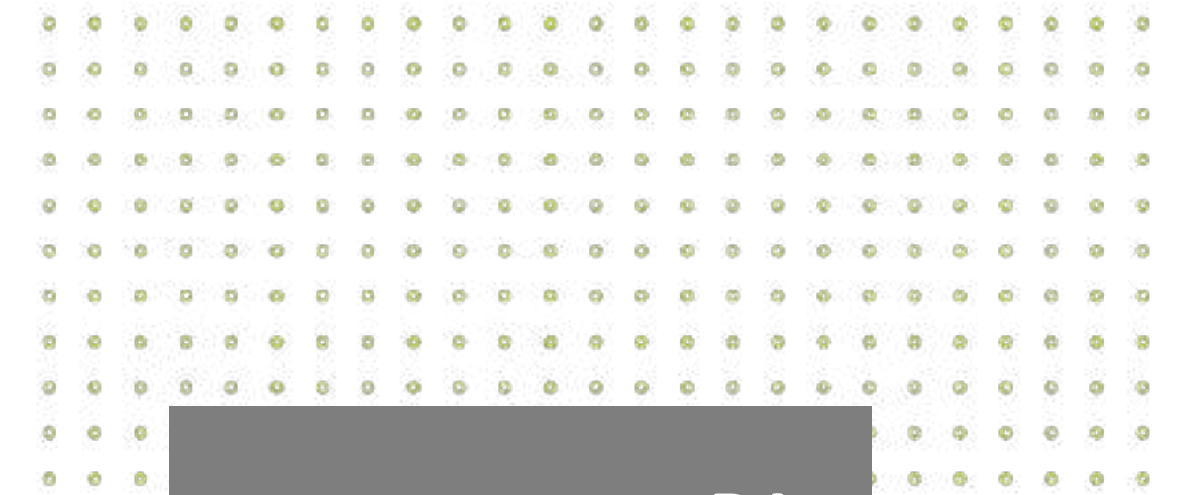


Image: Eduardo Ros © EHT Collaboration, Nakamura et al. 2020, Tchekhovskoy 2015

- Three working packages to probe magnetic fields near black holes
 - Mapping magnetic fields through polarisation and astrometric VLBI
 - Developing VLBI interferometry techniques
 - Deriving robust magnetic field properties near the event horizon
 - 2,5 M€ funded from the European Research Council

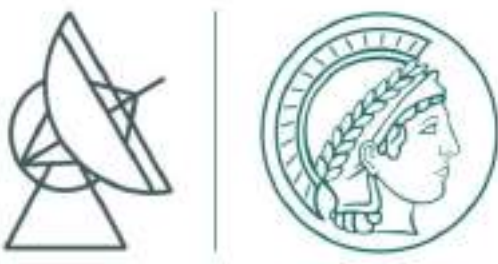
Project started in November 2021



P.I.
J.A. Zensus



M2FINDERS goals



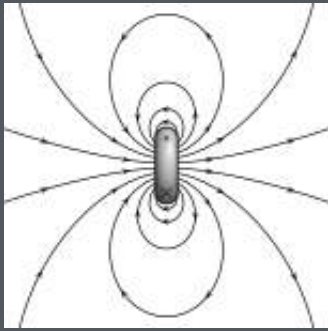
- Measuring magnetic fields in the region $< 1000 r_g$ to address questions:
 1. What is the maximum strength and 3D structure of B in the region within $1000 r_g$ of the BH?
 2. Is there a $B \gg 10^4$ G in the vicinity of the central BH in AGN?
 3. How fast B decrease with the distance from the BH?
 4. Is there evidence for dipole morphology of B ?
 5. How does B affect the generation and transport of energy in the vicinity of BH?



M2FINDERS work packages



WP1



Magnetic field measurements

Task 1

Obtain multi-freq. polarimetric images from VLBI observations of a sample of AGN jets.


Task 2

Use the Task 1 images to derive maps of the synchrotron turnover freq.

Task 3

Measure the freq.-dependent location of the jet base (core-shift).

WP2



Interferometric techniques

Task 4

Optimize the VLBI polarization calibration, to achieve the required accuracy of polarimetric measurements in Task 1.


Task 5

Expand the wavelet-based approach to deconvolution, to minimize the image noise in Tasks 1 & 2

Task 6

Implement and commission the source freq. phase referencing technique at the Eff, to improve the accuracy of Task3

WP3



Physical modelling

Task 7

Develop technique for the turnover freq. imaging using dual freq. observations.

Task 8

Develop a method for combining the polarisation and turnover freq. images for obtaining maps of the 3D distribution of B.

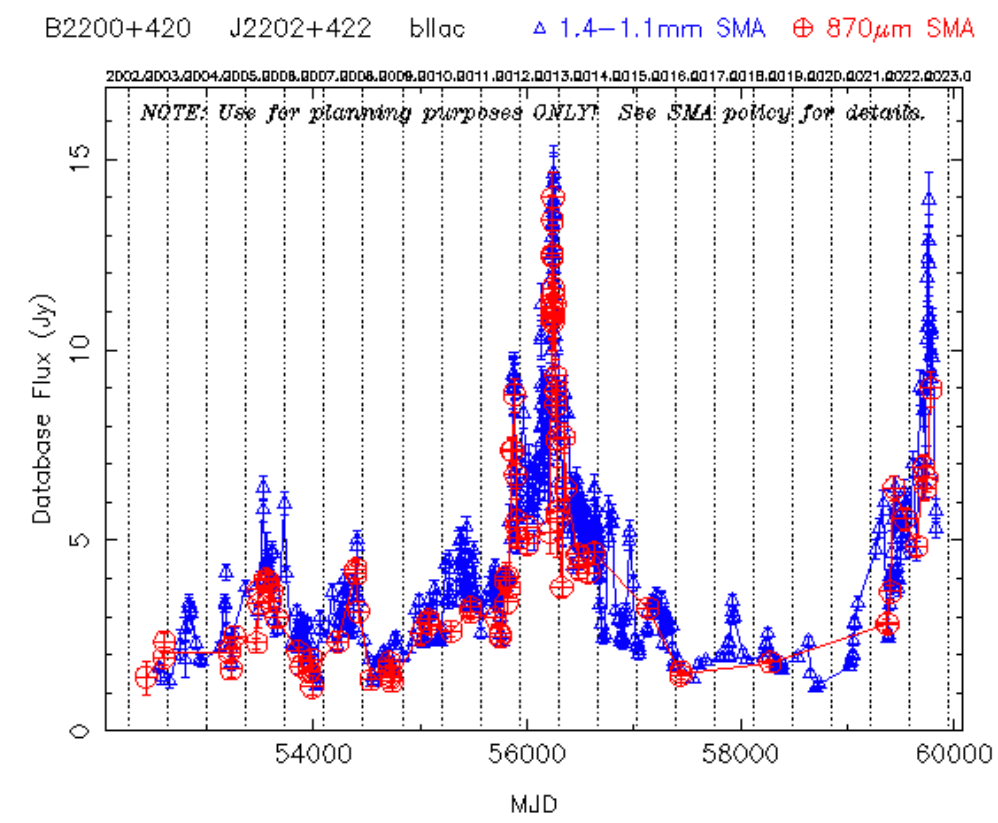
Task 9

Expand the method for estimating the B-strength from the core shift (take into account the collimation and acceleration of the flow.

WP1

New observations underway

- Defined M2FINDERS sample of objects



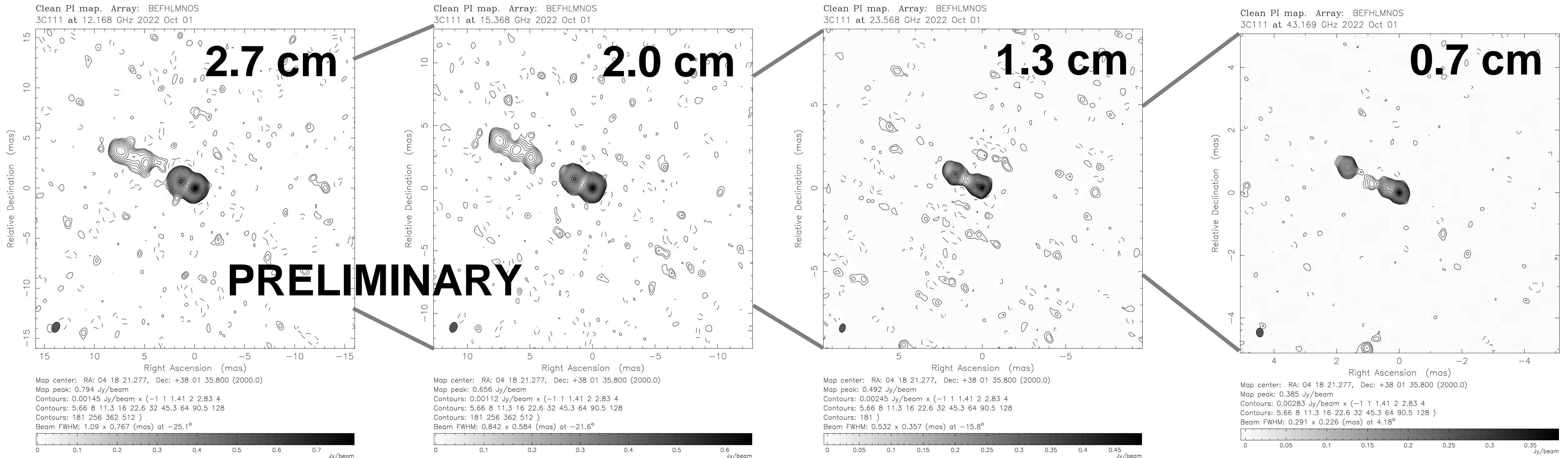
Now flaring!!

| Code | Array | Date | λ [mm] | NGC 1052 | 3C 111 | 3C 120 | 3C 371 | Cyg A | 3C 273 | 3C 345 | BL Lac | Cen A |
|------------------|---------|---------|----------------|----------|--------|--------|--------|-------|--------|--------|--------|-------|
| BL298A/B | VLBA+Eb | 01oct22 | 20/17/13/7 | ✓ | ✓ | ✓ | ✓ | ✓ | | | | |
| MB019A/B | GMVA | 06oct22 | 3 | | ✓ | ✓ | ✓ | ✓ | | ✓ | ✓ | |
| 01740 | EHT | 12apr23 | 1.3 | | | | | | | | ✓ | |
| MB019C/ MJ004 | GMVA | 04may23 | 3 | ✓ | | | | | ✓ | ✓ | | ✓ |

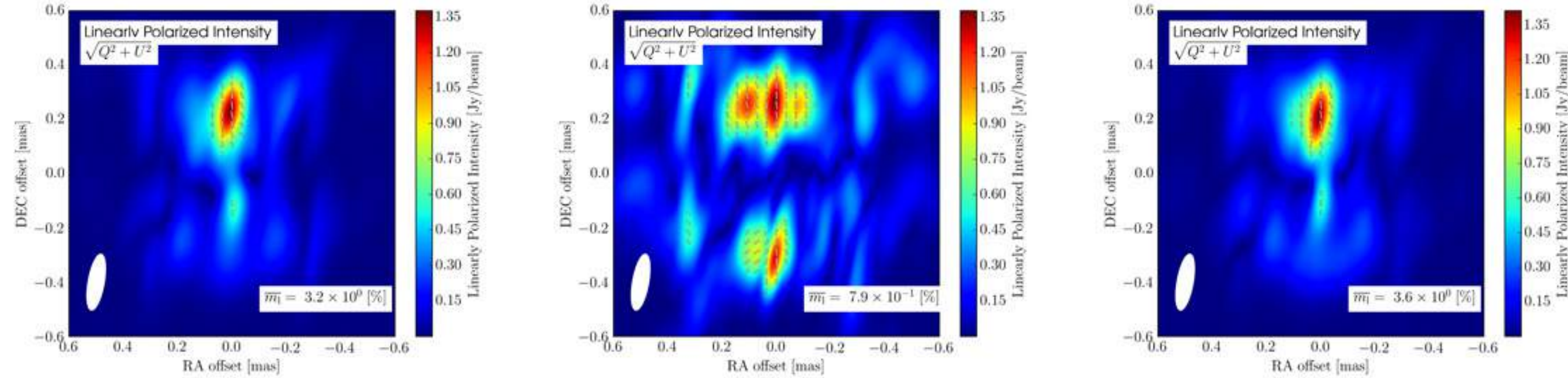
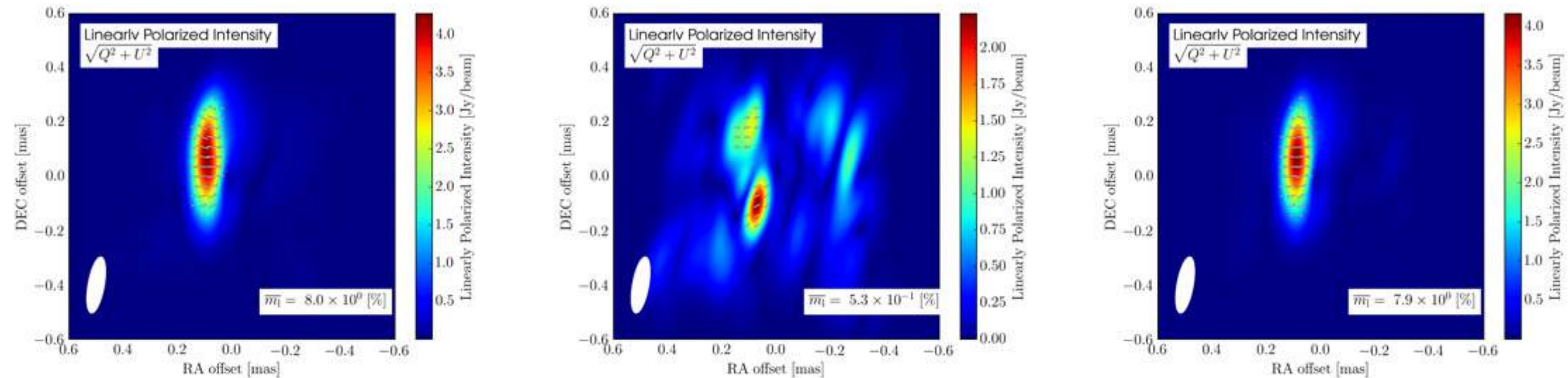
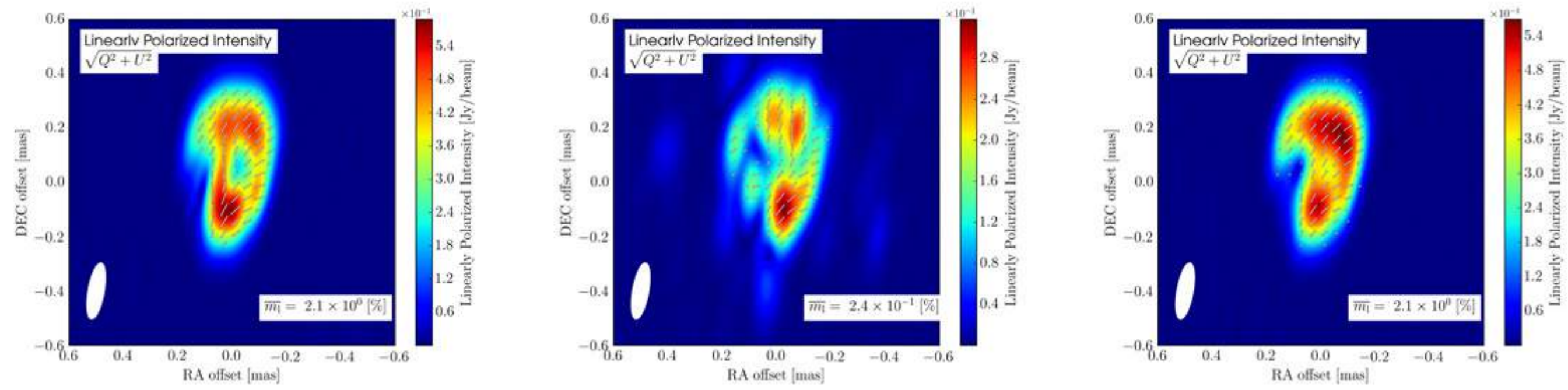
- Also KVN+Yebes Frequency-Phase-Transfer observations on sources with expected large core-shift
 - 0014+813, 0954+65, 3C 309.1, NGC 6251, 2007+77, 2023+76

New observations underway

| Code | Array | Date | λ [mm] | NGC 1052 | 3C 111 | 3C 120 | 3C 371 | Cyg A | 3C 273 | 3C 345 | BL Lac | Cen A |
|------------------|---------|---------|----------------|----------|--------|--------|--------|-------|--------|--------|--------|-------|
| BL298A/B | VLBA+Eb | 01oct22 | 27/20/13/7 | ✓ | ✓ | ✓ | ✓ | ✓ | | | | |
| MB019A/B | GMVA | 06oct22 | 3 | | ✓ | ✓ | ✓ | ✓ | | ✓ | ✓ | |
| 01740 | EHT | 12apr23 | 1.3 | | | | | | | | ✓ | |
| MB019C/ MJ004 | GMVA | 04may23 | 3 | ✓ | | | | | ✓ | ✓ | | ✓ |



WP3 Polarimetric study of B morphology (ray-tracing)



(1) $n_e(\gamma) \propto \rho$

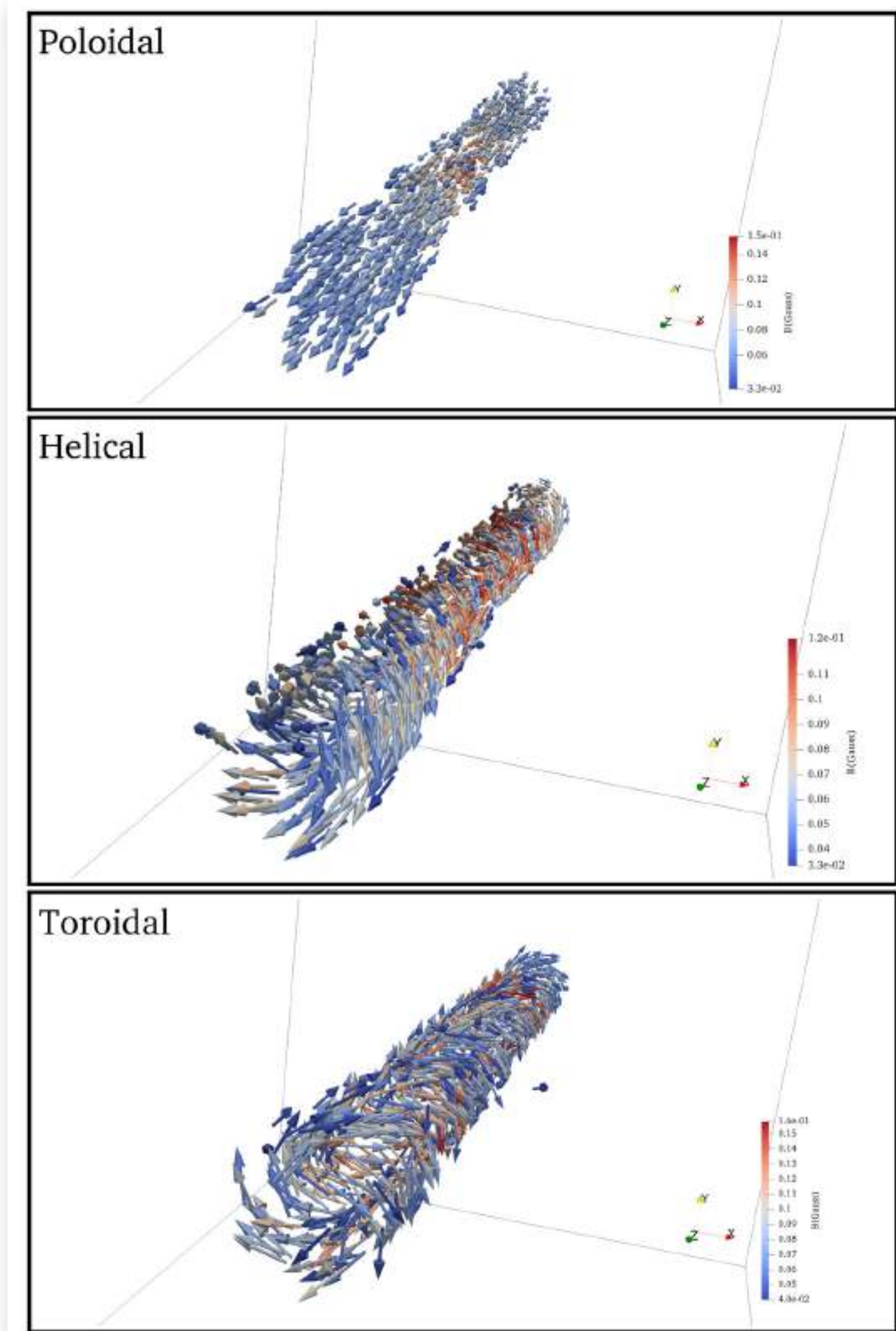
(2) $n_e(\gamma) \propto p$

(3) $n_e(\gamma) \propto B^2$

(i) Poloidal

(ii) Helical

(iii) Toroidal



Conclusions: the M2FINDERS project



- AGN power comes from rotating SMBH, involving accretion discs, relativistic plasma jets, and magnetic fields.
- Measurements of magnetic field near the event horizon yield fundamental information on BH physics and the formation of relativistic jets.
- M2FINDERS meets technical and astronomical challenges to map magnetic fields at distances smaller than $1000 r_g$, combining:
 - multi-frequency polarimetric VLBI imaging,
 - opacity measurements,
 - novel methods for image analysis,
 - and modeling of relativistic flows
- Observational program is underway.

Bardzo dziękuję!
Danke!

M2FINDERS

Max Planck Institute for Radio Astronomy (MPIfR)

Auf dem Hügel 69, 53121 Bonn, FRG

Email: m2finders@mpifr.de

Internet: www.mpifr-bonn.mpg.de/m2finders



European Research Council
Established by the European Commission

MAX-PLANCK-INSTITUT
FÜR RADIOASTRONOMIE



The M2FINDERS project has received funding from the European Research Council (ERC) under the European Union's Horizon 2020 research and innovation programme (grant agreement No 101018682).

Eduardo Ros, MPIfR, 7 November 2022